General Disclaimer

One or more of the Following Statements may affect this Document

- This document has been reproduced from the best copy furnished by the organizational source. It is being released in the interest of making available as much information as possible.

- This document may contain data, which exceeds the sheet parameters. It was furnished in this condition by the organizational source and is the best copy available.

- This document may contain tone-on-tone or color graphs, charts and/or pictures, which have been reproduced in black and white.

- This document is paginated as submitted by the original source.

- Portions of this document are not fully legible due to the historical nature of some of the material. However, it is the best reproduction available from the original submission.

PHASE ONE DESIGN REPORT
FOR
HIGH SENSITIVITY INFRARED 10.6 MICRON HETERODYNE HgCdTe RECEIVER DEVELOPMENT

September 1969

Contract No. : NAS5-11665

AIL Report 8783-1

Prepared by

AIL, a division of CUTLER-HAMMER
Melville, New York 11746

for

Goddard Space Flight Center
Greenbelt, Maryland 20771

PHASE ONE DESIGN REPORT
FOR
HIGH SENSITIVITY INFRARED 10.6 MICRON HETERODYNE
HgCdTe RECEIVER DEVELOPMENT

September 1969

Contract No.: NAS5-11665

Goddard Space Flight Center
Contracting Officer: Wayman Wilkins
Technical Monitor: John McElroy

Prepared by

AIL, a division of CUTLER-HAMMER
Melville, New York 11746

Project Manager: B. Peyton

for

Goddard Space Flight Center
Greenbelt, Maryland 20771

ACKNOWLEDGMENTS

The following staff members of AIL, F. Arams, E. Sard, D. Breitzer, and F. Pace, have made significant contributions to various phases of the analysis in this report. R. Lange, also of AIL, contributed in some of the reported measurements.

We wish to express our appreciation for helpful discussion and comments provided by Mr. John McElroy of Optical Systems Branch, Advanced Development Division of Goddard Space Flight Center.

ABSTRACT

This report gives results of a study on the design of an infrared 10.6 micron quantum-noise-limited heterodyne receiver employing HgCdTe mixer elements, and operating near 100 K. Mixer parameters such as conversion gain, local oscillator power, DC bias power, resistance, frequency response and conductance ratio are investigated for operating temperature from 80 to 120 K. Operational receiver parameters such as Noise Equivalent Power, total power dissipation, error-sensing techniques and required IF amplifier characteristic are also considered.

Heterodyne operation in photoconductive HgCdTe is analyzed on several levels of complexity. Both n- and p-type photoconductive HgCdTe are considered.

Engineering expressions for heterodyne operation in photovoltaic HgCdTe are presented. Supporting experimental results have been obtained. A measured NEP of 2.2×10^{-19} watt/Hz was obtained for a total power dissipation of less than 2 mw at a temperature of 77 K. The measured frequency response of the PV mixer was flat to 40 MHz.

Some supporting measurements are given for a p-type photoconductive HgCdTe mixer element with a 4-nsec response time.

TABLE OF CONTENTS

LIST OF ILLUSTRATIONS

I. INTRODUCTION

A. SCOPE

This Design Report on Phase 1 of Contract NAS5-11665 presents an analysis of a 10.6 micron quantum-noise-limited, heterodyne infrared mixer subsystem employing mercury cadmium telluride (HgCdTe) mixer elements and operating in the 100 K temperature region. An information bandwidth of 5 MHz and an intermediate frequency centered at 20 MHz are considered. Parameters to be analyzed include local oscillator (LO) power, DC bias power, mixer impedance and dimensions, operating temperature, receiver sensitivity, frequency response, error sensor techniques and performance, IF preamplifier interface, and others. A laboratory breadboard model will be delivered in Phase 2.

This report is divided into three main parts:

- Mixing in photoconductive HgCdTe
- Mixing in photovoltaic HgCdTe
- Receiver subsystem design

These three sections are further explained in the following paragraphs.

B. MIXING IN PHOTOCONDUCTIVE HgCdTe

For maximum usefulness, mixing in photoconductive HgCdTe is analyzed on several levels of complexity since useful conclusions can often be drawn from simpler equations involving some assumptions. Therefore, the analysis of mixing in photoconductive HgCdTe is presented in the following sequence:

1. General expressions for heterodyne receivers. Here, it is assumed that
   - The mixer dark conductance is very small (as in impurity-activated mixer elements, such as Ge:Cu),
   - The carrier lifetime is constant; that is, independent of LO (and bias) power.
   - The lifetimes, conversion gains, and IF noise factors required for optimum receiver sensitivity are calculated.

2. Expressions for finite dark conductance, as in both p-type and n-type PC-HgCdTe. The lifetime τ is still taken as almost constant. Derivations are given for optimum DC power to LO power ratio, and optimum mixer conductance ratio, to achieve the maximum mixer conversion gain as a function of total power dissipation in the mixer.

3. Expressions for finite dark conductance and τ varying with LO power. The concepts of heterodyne (small signal) and LO lifetimes are introduced.

4. Analysis from physical principles of behavior of heterodyne and LO lifetime as a function of LO power in PC-HgCdTe. Two operating regions are distinguished:

   - Large LO power (large modulation case, $g_o/g_D >> 1$)
   - Small LO power (small modulation case, $g_o/g_D \lesssim 1$)

5. Parametric analysis of mixing in Auger lifetime limited n-type PC-HgCdTe and specific mixer design for the 80 to 120 K operating range.

6. Results on p-type photoconductive HgCdTe.

C. MIXING IN PHOTOVOLTAIC HgCdTe

This section contains:

1. Analysis of photovoltaic mixing. Engineering expressions for noise equivalent power, conversion gain, cutoff frequency, etc., are derived and discussed.

2. Experimental results are presented on NEP, conversion gain, LO and DC power requirements, frequency response, etc. which are very encouraging for the proposed LCE application.

D. RECEIVER SUBSYSTEM DESIGN

This section discusses:

1. Mixer element configurations for signal detection and error sensing; comparison of nutating single-element and quadrant-array receivers.
2. Design of IF electronics.

This report benefited materially from the First and Second Summary Design Reports, ATS-F Laser Communication Experiment Infrared Mixer and Radiation Cooler Subsystem, by J. McElroy, S. Cohen, H. Walker, S. Flagiello, and J. McDay, Goddard Space Flight Center, Greenbelt, Maryland. Tabulated data on n-type PC-HgCdTe found in the GSFC reports were used in connection with Section VI of this report.

II. GENERAL ANALYSIS OF PHOTOCONDUCTIVE MIXING

This section presents a generalized engineering analysis of infrared heterodyne operation in photoconductive HgCdTe mixer elements and is expanded in later sections.

A. GENERAL EXPRESSIONS FOR HETERODYNE RECEIVERS

An engineering analysis developed under GSFC sponsorship at AIL on photoconductive mixing in Ge:Cu has previously been reported (reference 1). Explicit engineering equations were developed which define mixer conversion gain, receiver NEP and IF frequency response in terms of LO power, DC bias power, IF amplifier noise temperature, mixer resistance, and mixer material parameters.

A simplified expression for the mixer conversion gain is:

$$G = \frac{\eta q\, \mu V^2}{2h\nu_s L^2} \cdot \frac{\tau}{1 + \omega^2 \tau^2} \qquad (1)$$

where

η = infrared quantum efficiency,

q = electronic charge,

μ = mobility of principal carriers,

V = mixer bias voltage,

τ = lifetime of principal carriers,

h = Planck's constant,

ν_s = signal frequency,

L = photomixer interelectrode spacing,

ω = angular IF difference frequency.

The 3-db IF frequency response of the HgCdTe mixer is

$$f_{3db} = \frac{1}{2\pi\tau} \tag{2}$$

The frequency at which mixer response is down by 0.5 db is

$$f_{0.5db} \approx \frac{0.56}{2\pi\tau} \tag{3}$$

The receiver NEP (S/N = 1) is* (reference 1)

$$NEP = \frac{2h\nu_s B}{\eta} + \frac{k\,(T_m + T'_{IF})B}{G} \tag{4}$$

where

T_m = mixer temperature,

T'_{IF} = effective input temperature of IF amplifier

B = IF bandwidth.

The first term on the right in equation 4 represents the quantum noise contribution. The second term represents the Johnson noise due to the mixer element (T_m) and the IF amplifier noise (T'_{IF}) for a given source conductance, all divided by the mixer conversion gain G. For quantum-noise-limited operation, the mixer must be designed and operated to minimize the second term with respect to the quantum noise term over the range of radiation cooler temperatures to be encountered.

From equation 4, the minimum achievable noise equivalent power (NEP) for photoconductors is

$$P_{MIN} = \frac{2h\nu_s B}{\eta} \tag{5}$$

---

* Equation 4 holds approximately, even when finite dark conductance and lifetime varying with LO power are considered (equation 75), such as in the Auger lifetime limited case.

For a quantum efficiency of 0.5, the minimum achievable photoconductive NEP at 10.6 μ is thus calculated to be

$$P_{MIN} = 7.5 \times 10^{-20} \text{ watt/Hz} \tag{6}$$

B. MIXER CONVERSION GAIN

Given particular values for mixer lifetime, carrier mobility, operating temperature, mixer area and thickness (volume), quantum efficiency, and DC bias voltage, it is instructive to use equation 1 to calculate the mixer conversion gain for a specified IF frequency. It is often convenient to use an alternative expression for conversion gain which can be derived from equation 1.

$$G = \frac{P_{DC}}{2P_{LO}} \quad \frac{1}{(1 + \omega^2\tau^2)} \tag{7}$$

This expression, for the simplified analysis, yields a convenient measure of conversion gain in terms of measurable parameters, since it depends only on the ratio of DC bias and applied LO power for the case $\omega\tau \ll 1$.

C. LIFETIME AND FREQUENCY RESPONSE CONSIDERATIONS

The simplified gain analysis of Section II-A shows that the gain as a function of lifetime τ is proportional to the quantity $[\tau/(1 + \omega^2\tau^2)]$. The mixer conversion gain will usually be less than unity but nevertheless should be maximized to minimize second stage and thermal contributions to the receiver NEP (equation 4). For the case where the mixer bias voltage is fixed, and the carrier mobility is independent of applied LO power and carrier lifetime, the available mixer gain varies directly with the factor $\tau/(1 + \omega^2\tau^2)$. Figure 1 is a plot of the function $\tau/(1 + \omega_o^2\tau^2)$ versus τ for $\omega_o/2\pi$ equal to 20 MHz appropriate to the LCE. It can be seen (and verified analytically by equating the derivative to zero and solving for τ) that the function maximizes at $\tau \approx 7.95$ nsec, corresponding to $\omega_c\tau = 1$. Solely on the basis of Figure 1, $\tau = 8$ nsec is the appropriate value for the LCE. This conclusion would remain substantially unchanged for the more complete gain analysis in Section V, except that the small signal lifetime τ_{het} is considered.

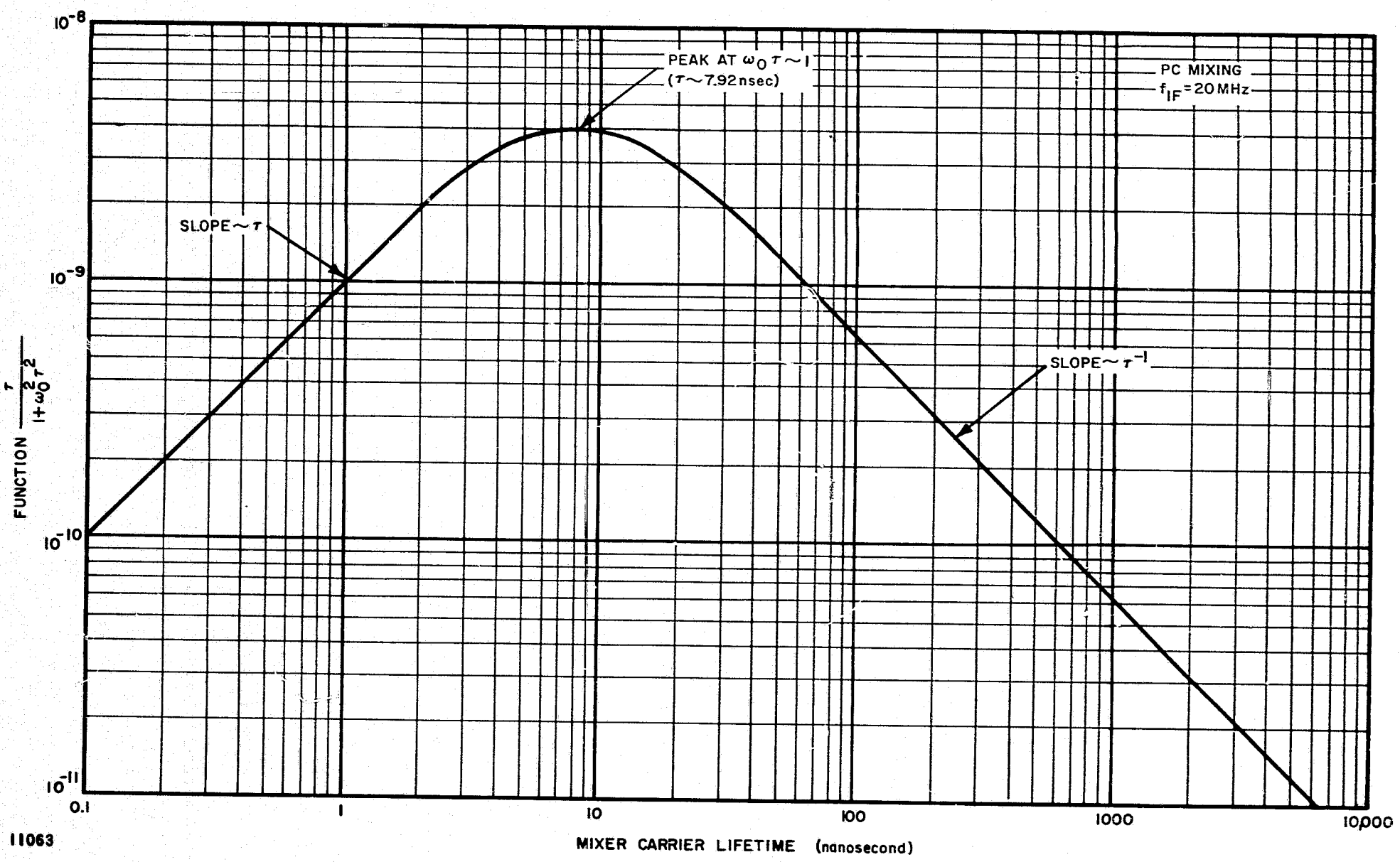

FIGURE 1. DEPENDENCE OF FUNCTION $\tau/1 + \omega_0^2\tau^2$ IN PHOTOCONDUCTIVE CONVERSION GAIN EQUATION ON CARRIER LIFETIME

Figure 2 is a plot of the amplitude and phase of the simplified gain expression (equation 7) versus frequency for the value of τ = 7.95 nsec corresponding to $\omega_o\tau = 1$. It is seen that the tentative choice of $\tau \approx 8$ nsec deviates appreciably from the desired characteristics of linear phase and flat amplitude in the 20-MHz region. These concomitant characteristics are required to approach the condition of constant group delay required for good quality video transmission. A possible solution for the proposed LCE application is to use an equalizer network to approach the ideal transmission conditions suitable for video signals. The large amount of phase and amplitude compensation required of the equalizer can be expected to make the system sensitive to radiation cooler temperature changes and aging of the LO laser.

Figure 2 also includes a plot for a compromise value of lifetime, τ = 3 nsec, corresponding to $\omega_o\tau = 0.378$. The amplitude flatness and phase linearity in the 20-MHz region is appreciably improved at the cost of only a very small decrease in the gain function ($\sim$ 0.6 db) of Figure 1. If desired, a less critical equalizer can be used to further improve the transmission characteristics.

We thus conclude that for an IF of 20 MHz, a HgCdTe mixer having approximately a 3-nsec small-signal lifetime offers the best overall approach to meeting the LCE requirements for constant DC bias voltage operation.

D. SENSITIVITY (NOISE EQUIVALENT POWER)

The receiver sensitivity for a photoconductive HgCdTe mixer-IF amplifier combination is determined by:

- The mixer quantum efficiency η
- The mixer conversion gain G
- The effective input noise temperature of the IF amplifier T'_{IF}
- The IF bandwidth B

The quantum efficiency of photoconductive HgCdTe mixers has been fully discussed in the Second GSFC Study Report and is taken to have a value of η = 0.5 for a mixer element thickness D = 12 microns. All calculations are carried out and referenced to a 1-Hz bandwidth in order to normalize receiver bandwidth. The mixer temperature is taken to vary from 80 to 120 K, and a receiver sensitivity objective of NEP = 10^{-19} w/Hz is utilized. The mixer conversion gain required to obtain an NEP of 10^{-19} w/Hz is plotted in Figure 3 as a function of IF amplifier noise factor for mixer temperatures of 80, 100, and 120 K using the standard definition:

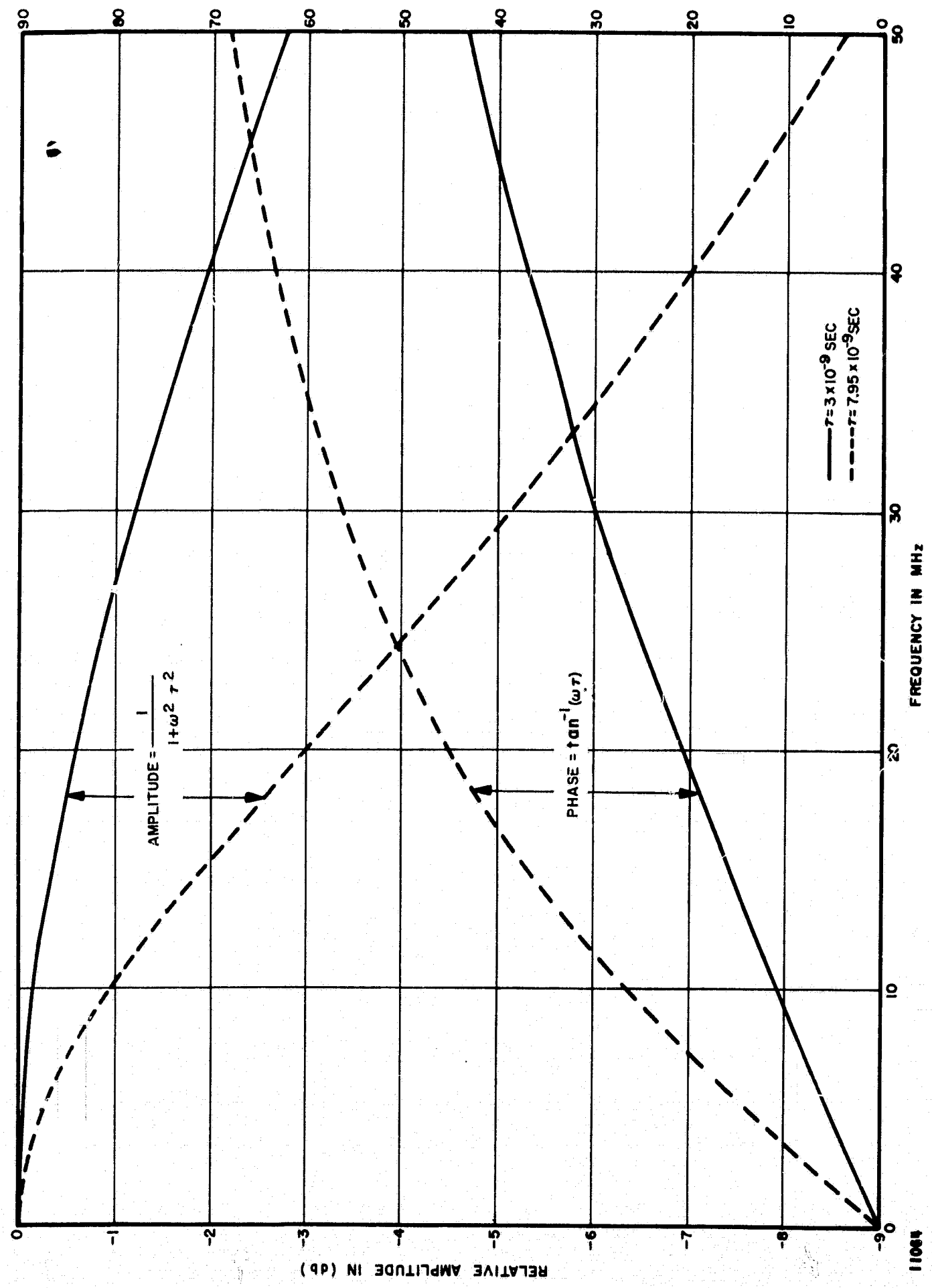

FIGURE 2. AMPLITUDE AND PHASE OF MIXER OUTPUT AS A FUNCTION OF FREQUENCY

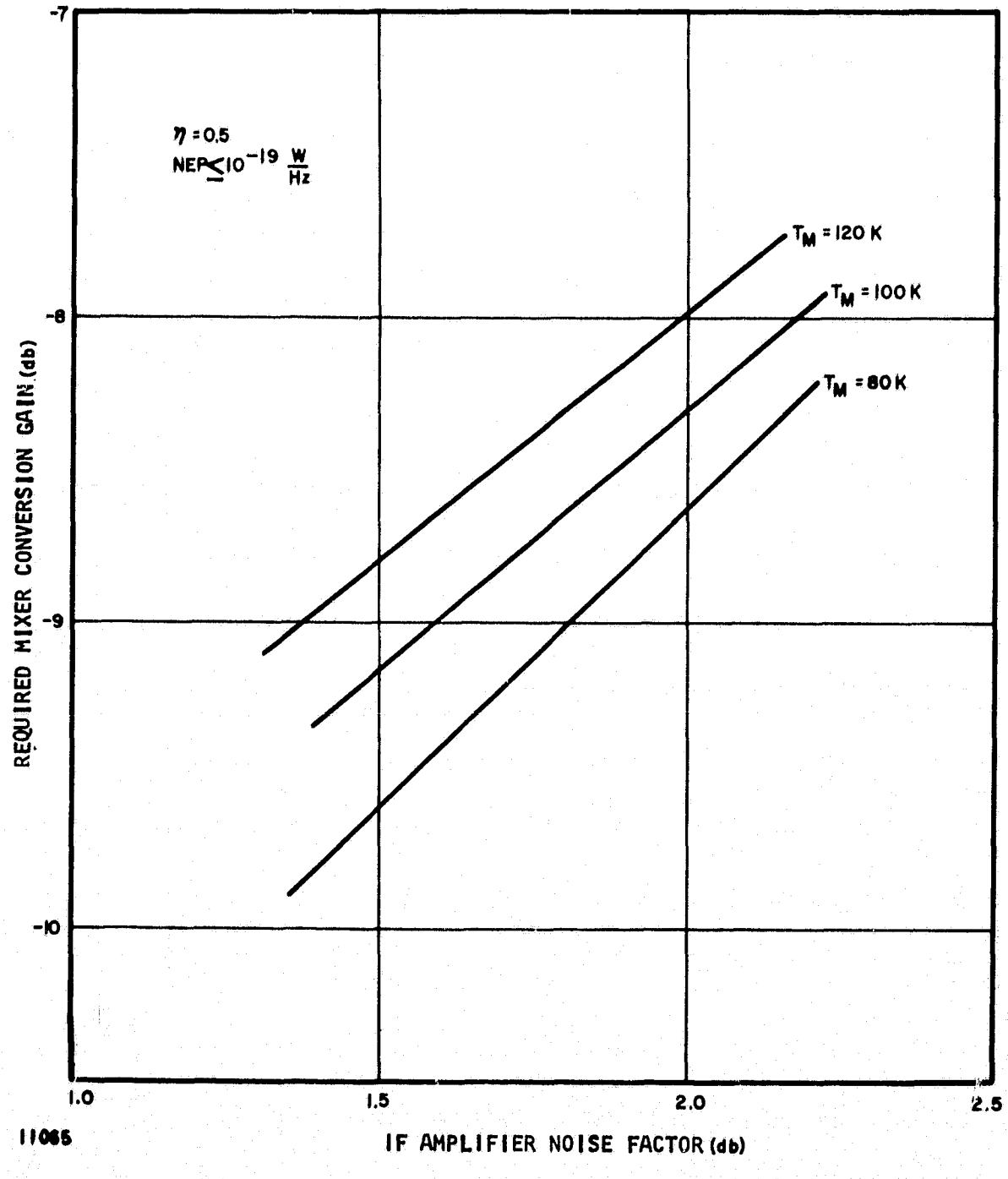

FIGURE 3. REQUIRED CONVERSION GAIN FOR VARIOUS IF AMPLIFIER NOISE FACTORS TO OBTAIN AN NEP OF 10^{-19} W/Hz USING EQUATION 4

$$T_{IF} = (F_{IF} - 1)\, T_o \qquad (8)$$

where

T_{IF} = IF amplifier noise temperature in K,

F_{IF} = IF amplifier noise factor,

T_o = reference temperature ≡ 290 K.

Low-noise low-power-drain IF amplifiers operating at megacycle frequencies and using space-approved components are achievable with noise factors in the 1.4 to 2.0 db range.

As Figure 3 shows, for F_{IF} = 1.5 db, and T_m = 100 K, a conversion gain of -9.15 db is required. For F_{IF} = 2.0 db and T_m = 100 K, the conversion gain requirement increases to -8.35 db. Thus, to obtain the same NEP, the required conversion gain must increase by 0.8 db for a 0.5-db degradation in IF noise factor. Effort to minimize F_{IF} will result in improved infrared receiver operation by improving NEP, and/or reducing conversion gain requirements, which in turn reduce the power dissipated in the mixer.

The calculated variation of receiver NEP as a function of F_{IF} with T_m = 100 K and conversion gain as the parameter is shown in Figure 4. As can be seen, when F_{IF} = 1.5 db the receiver NEP varies from 1.05 x 10^{-19} to only 1.7 x10^{-19} w/Hz as the mixer conversion gain decreases from -10 to -15 db.

E. IF ELECTRONICS DESIGN

This section discusses the effect of source conductance on the noise factor of the IF amplifier following the mixer. The design procedure to minimize noise factor degradation due to source conductance variations is discussed and measured data is presented.

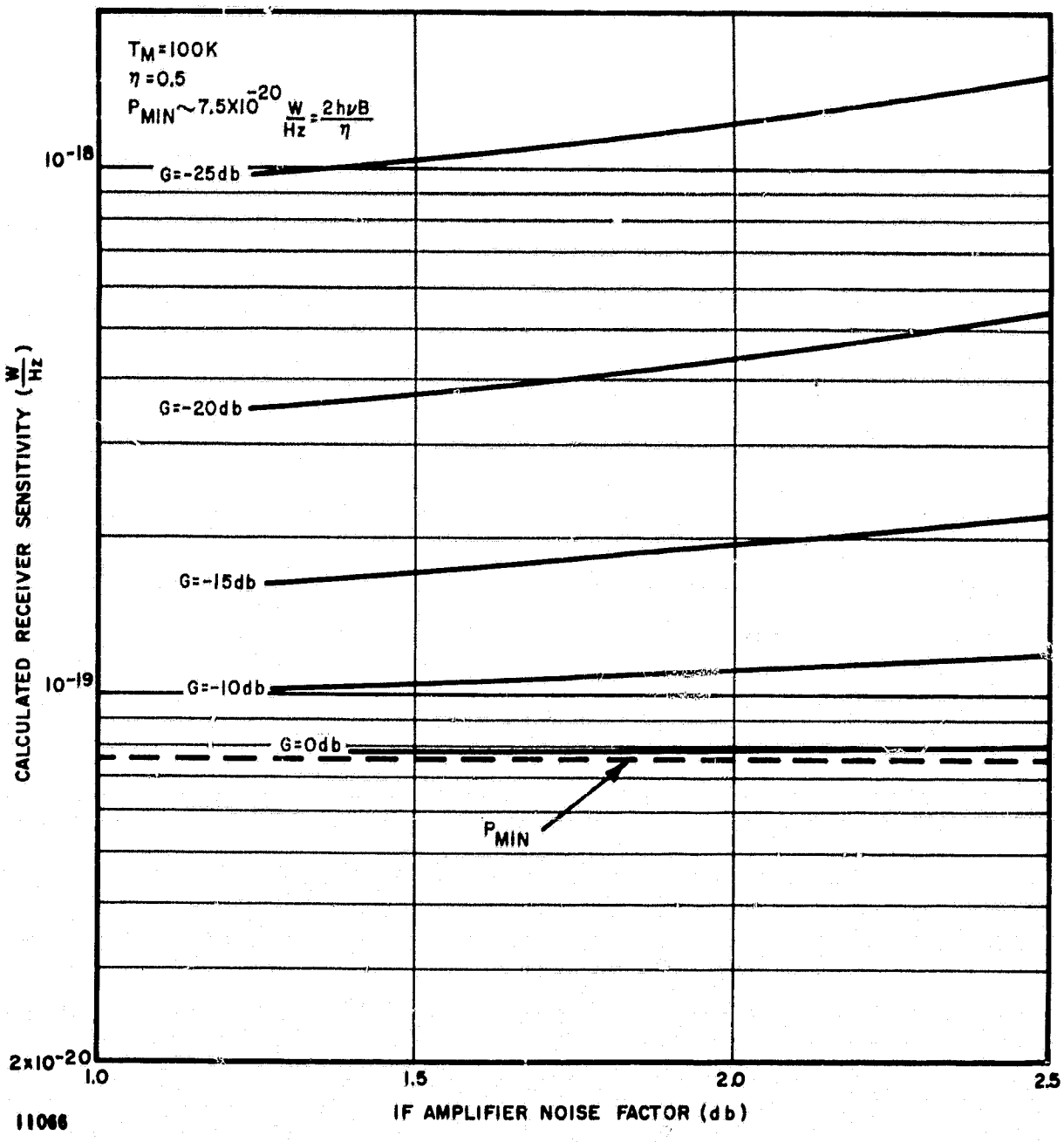

FIGURE 4. RECEIVER NEP VS IF AMPLIFIER NOISE FACTOR FOR VARIOUS VALUES OF MIXER CONVERSION GAIN USING EQUATION 4

1. ANALYSIS

The theoretical behavior of noise factor (F) in transistorized IF amplifiers as a function of frequency is illustrated in Figure 5A (reference 2). It can be seen that within a wide frequency range there is a plateau of minimum F. Figure 5B is a plot for a typical transistor (2N3570) illustrating this broad plateau from 1 to 100 MHz. This plateau is not too dependent upon source resistance as shown by data on another transistor (2N4252) given in Figure 5C where a 2 to 1 change in source impedance hardly affects the broad plateau.

The theoretical equation for the F of a transistor amplifier is (references 2, 3, and 4)

$$F = 1 + \frac{r_b'}{R_g} + \frac{r_e}{2R_g} + \frac{(R_g + r_e + r_b')^2}{2R_g r_e h_{fb}} \left\{ \left[1 + (f/f_a)^2 \right] \left[\frac{h_{FB}}{h_{fb}} \left(1 + \frac{I_{CBO}}{I_c} \right) \right] - h_{fb} \right\} \quad (9)$$

where

F = noise factor

f_a = common-base alpha cutoff frequency

h_{FB} = DC common-base short-circuit current gain

h_{fb} = AC common-base short-circuit current gain

I_c = collector current

I_{CBO} = collector cutoff current (emitter open)

r_b' = bulk resistance of base region

r_e = emitter resistance

R_g = generator resistance

The variation of F with frequency arises because of the term f/f_a. That is, for the application of interest it is only important to establish f_{CH}, the high

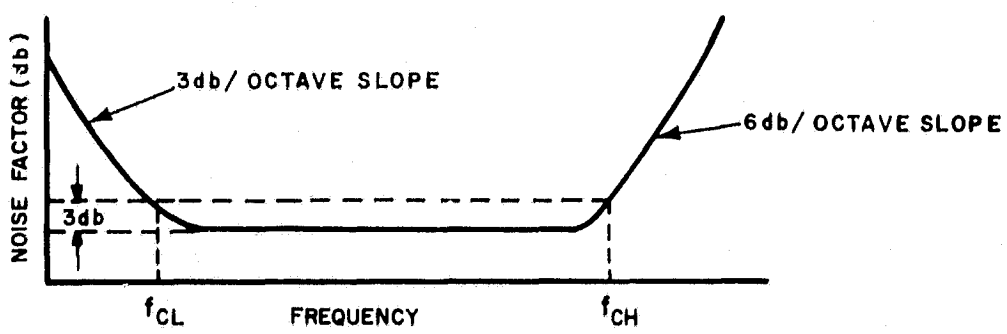

A. THEORETICAL BEHAVIOR OF NOISE FACTOR VERSUS FREQUENCY.

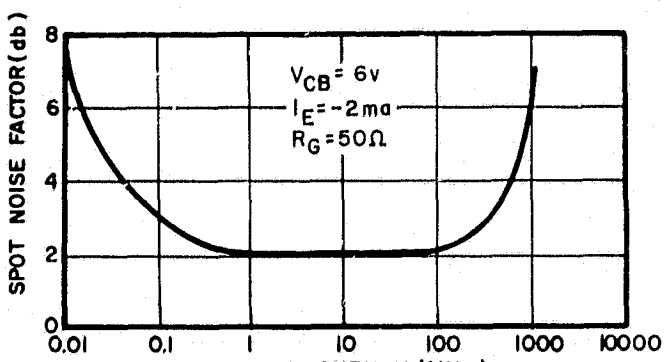

B. NOISE FACTOR VERSUS FREQUENCY FOR 2N3570 TRANSISTOR

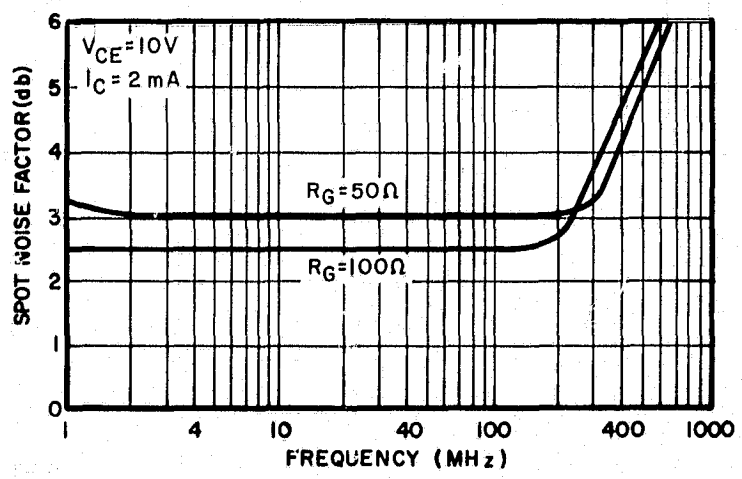

C. NOISE FACTOR VERSUS FREQUENCY FOR 2N4252 TRANSISTOR

11067

FIGURE 5. VARIATION OF AMPLIFIER NOISE FACTOR WITH IF FREQUENCY

frequency noise corner above the highest desired frequency of operation. This, in turn, means selecting a transistor with a high cutoff frequency compared to the operating frequency of approximately 20 MHz.

The F behavior versus source (or mixer) resistance depends somewhat upon the frequency of operation and the emitter current. Figure 6A shows such a measured plot (reference 4) where a variation of R_g from 1 to 10 kilohms produces about a 0.5-db change in F. This kind of insensitivity to R_g is possible if the frequency of operation is very small compared to the transistor cutoff frequency.

To examine this NF versus source resistance behavior in more detail, we can normalize equation 9 and obtain

$$\frac{F}{F_{min}} = 1 + \frac{\frac{1}{2}\left[\frac{R_g}{R_{g(F\ opt)}} + \frac{R_{g(F\ opt)}}{R_g}\right] - 1}{1 + K} \tag{10}$$

where

$$F_{min} = 1 + \frac{K_1}{R_g} + \frac{(K_2 + R_g)^2 K_3}{R_g}$$

$$K = \frac{K_2 + \frac{1}{2K_3}}{R_{g(F\ opt)}}$$

$$K_1 = r_b' + \frac{r_e}{2}$$

$$K_2 = r_b' + r_e$$

$$K_3 = \frac{(1 - a_o)\left[1 + \left(\frac{f}{\sqrt{1 - a_o f_a}}\right)^2\right]}{2 a_o r_e}$$

where a_o = the low frequency common-base current gain.

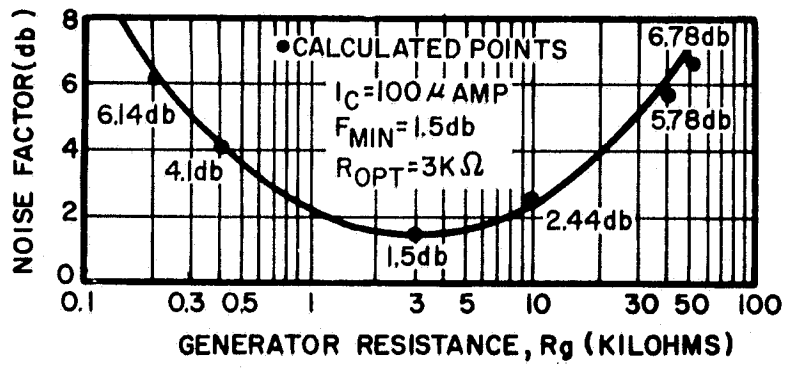

A. MEASURED VARIATION OF NF WITH SOURCE RESISTANCE FOR 2N930 TRANSISTOR.

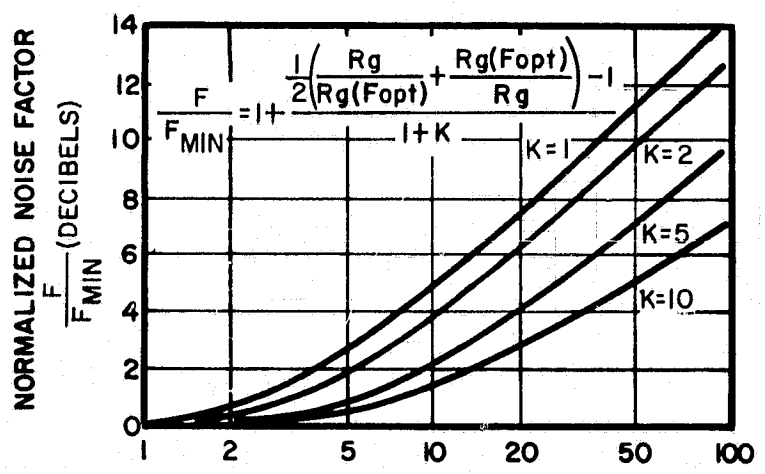

B. CALCULATED VARIATION OF IF NOISE FACTOR WITH SOURCE RESISTANCE.

11068

FIGURE 6. VARIATION OF IF NOISE FACTOR WITH SOURCE RESISTANCE

Equation 10 is plotted in Figure 6B for different values of K. Note that the larger values of K arise principally because of having an operating frequency f that is small compared to the transistor cutoff frequency f_a.

The mixer output impedance will be transformed to provide the optimum source resistance R_g to the IF amplifier for an average value of mixer resistance. For a transistor with K = 1, and a mixer output resistance variation of 1.33 to 1, the maximum F variation (for K = 1) is less than 0.3 db. For a mixer resistance variation of 2.0 to 1, the increase in F is less than 0.5 db for K = 1. However, since transistors with cutoff frequencies in excess of 1 GHz can be used, and the signal frequency is about 20 MHz, the curves for K = 10 would be more appropriate. In this case, the increase in F would be less than 0.2 db for an approximate 4 to 1 change in R_g.

2. MEASUREMENTS

Measurements have been made on a low-noise transistorized IF amplifier potentially suitable for the proposed application. The small-index frequency modulation used in the CO_2 laser requires a channel bandwidth approximately twice the 5-MHz video bandwidth. Test results for a source resistance of 50 ohms were:

Frequency (MHz)	Noise Factor (db)	Gain (db)
15	1.53	30
20	1.50	30
25	1.54	30

With the anticipated mixer resistance change of less than 2 to 1 caused by changes in mixer temperature, the expected change in F is almost negligible. Noise factor measurements with a 30-ohm source resistance on the above amplifier have confirmed this.

In order to minimize phase distortion of the video information, the IF amplifier bandwidth can be made larger than required. The equivalent IF noise bandwidth of the video channel is then determined by a single-pole filter with a 3-db bandwidth near 10 MHz centered at 20 MHz. Figure 7 shows the measured data on such a filter, compared to computed values. Such a filter could also prove very useful in minimizing crosstalk and radio frequency interference from the laser transmitter and modulator, as well as other sources.

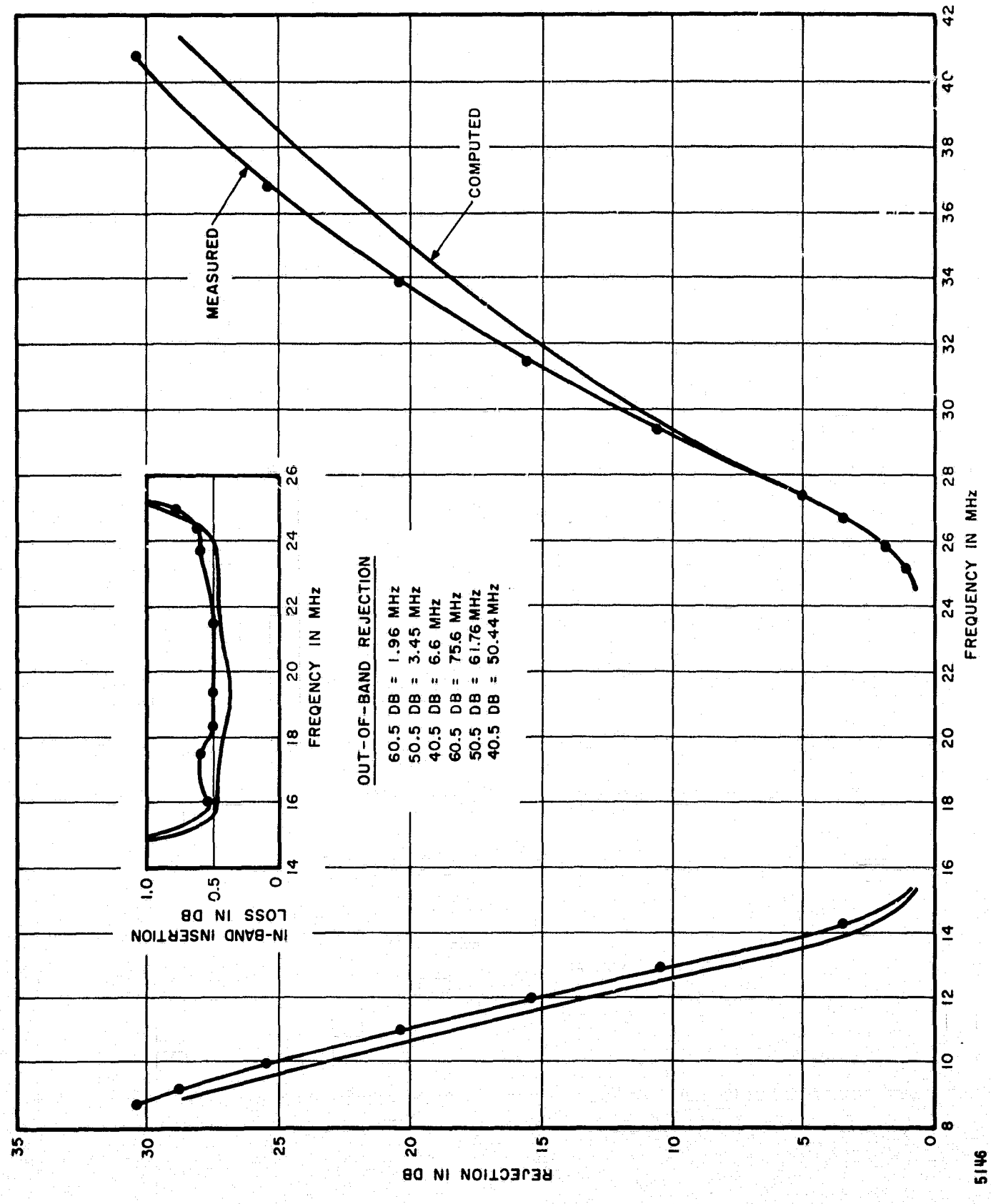

FIGURE 7. COMPARISON OF MEASURED AND COMPUTED ATTENUATION VS FREQUENCY OF SINGLE-POLE 15 TO 25 MHz FILTER

III. ANALYSIS OF MIXING IN PC-HgCdTe WITH FINITE DARK CONDUCTANCE

The expressions for photoconductive heterodyne operation in Section II are extended in this section for finite dark conductance ($g_D/g_o \neq 0$) as is the case for both n- and p-type photoconductive HgCdTe. The resultant expressions yield quantitative data on the increase in mixer conductance due to LO-generated carriers which is required to obtain sufficient conversion gain for quantum-noise-limited heterodyne operation.

The optimum ratio of DC bias power to LO power for various values of total power dissipated in the mixer element is calculated.

One figure of merit used is the detector specific responsivity in volts/watt/volt, a useful quantity in comparing detector elements without regard to the optimum bias voltage usually determined by maximum signal-to-noise ratio in incoherent detection. The specific responsivity is thus the more meaningful parameter for mixer elements.

A. CONVERSION GAIN

The equivalent circuit of the mixer with finite dark conductance is given in Figure 8:

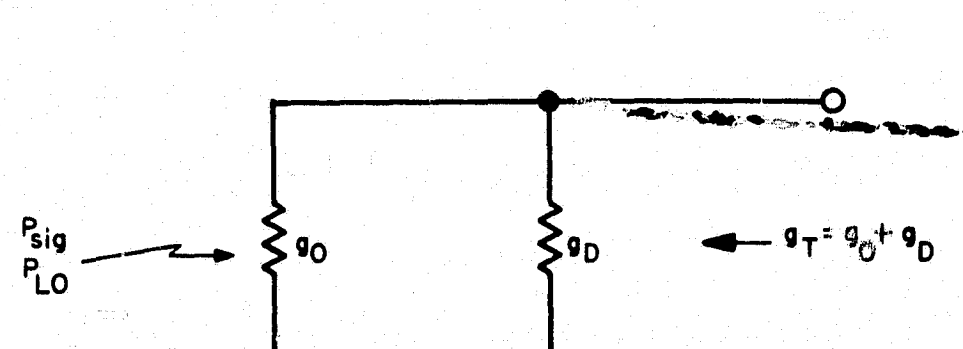

FIGURE 8. EQUIVALENT CIRCUIT FOR MIXER WITH FINITE DARK CONDUCTANCE

Here

g_D = mixer dark conductance

g_o = LO-induced conductance

g_T = total mixer conductance = $g_o + g_D$

The available conversion gain, or the ratio of the available IF output power to the available infrared signal power, is then

$$G = \frac{P_{IF}}{P_s} \frac{|I(\omega)|^2}{8P_s g_T} = \frac{|I(\omega)|^2}{8P_s\, g_o \left(1 + \frac{g_D}{g_o}\right)} \tag{11}$$

Using the same development used in Section II,

$$G = \frac{\eta q\, \mu \tau}{2h\nu_s\, (1 + \omega^2 \tau^2)} \left(\frac{V}{L}\right)^2 \frac{1}{\left(1 + \frac{g_D}{g_o}\right)} \tag{12}$$

where all quantities are defined as in Section II. The DC power dissipated is

$$P_{DC} = V^2\, (g_o + g_D) \tag{13}$$

and from reference 1,

$$g_o = \frac{q\, \mu \tau\, \eta\, P_{LO}}{L^2\, h\nu_{LO}} \tag{14}$$

It can be shown that

$$G = \frac{P_{DC}}{2\, P_{LO}} \frac{1}{1 + \omega^2 \tau^2} \frac{1}{\left(1 + \frac{g_D}{g_o}\right)^2} \tag{15}$$

This expression is the same as equation 7 in Section II except that $\frac{g_D}{g_o} \neq 0$.

B. OPTIMUM RATIO OF BIAS TO LO POWER

The dark and LO induced conductance for a square mixer element with thickness D are

$$g_D \approx \mu_e q\, D\, n_o$$

$$g_o \approx \mu_e q\, D\, n_e \tag{16}$$

A general derivation of the optimum bias/LO power ratio is given below starting from equations 14, 15, and 16. The conductance ratio in the presence of LO power

$$\frac{g_D}{g_o} = \frac{\text{Vol}\, n_o\, h\nu_{LO}}{\eta\, P_{LO}\, \tau} \tag{17}$$

where

Vol = mixer volume

n_o = dark electron concentration

τ = lifetime (assumed independent of P_{LO} in this section)

Therefore, using equations 14 and 17 $g_T = g_o + g_D = \mu_e qD\,(n_o + n_e)$ where n_e is the LO induced electron concentration and μ_e is assumed to be independent of P_{LO}. Therefore, $g_o/g_D = n_e/n_o$.

From equation 17

$$\frac{g_D}{g_o} = \frac{\text{Vol}\, n_o\, h\nu_{LO}}{\tau\, P_T}\left(1 + \frac{P_{DC}}{\eta\, P_{LO}}\right) = \frac{n_o}{n_e} \tag{18}$$

where $P_T = P_{DC} + \eta\, P_{LO}$, is the total power dissipated in the mixer element and τ is assumed to be independent of P_{LO}.

The small-signal specific responsivity $\mathcal{R}/V$ where the detector conductance change induced by the absorbed signal power is very small, is given (Appendix I) by

$$\frac{\mathcal{R}}{V} = \frac{\eta \tau}{\text{Vol } n_o h\nu} \tag{19}$$

Therefore, from equations 18 and 19

$$\frac{g_D}{g_o} = \frac{\eta}{(\mathcal{R}/V)P_T} \left(1 + \frac{P_{DC}}{\eta P_{LO}}\right) \tag{20}$$

Letting

$$y = \frac{P_{DC}}{\eta P_{LO}} \tag{21}$$

$$x = \frac{\eta}{\left(\frac{\mathcal{R}}{V}\right) P_T} \tag{22}$$

Then

$$\frac{g_D}{g_o} = x\,(1 + y) \tag{23}$$

and from equations 15, 21, 22, and 23

$$G = \frac{\eta\, y\, (1 + \omega^2 \tau^2)^{-1}}{2\left[1 + x(1 + y)\right]^2} \tag{24}$$

and therefore

$$G = \frac{\eta\,(1 + \omega^2\tau^2)^{-1}}{2\left[x^2 y + 2x\,(1 + x) + \dfrac{(1 + x)^2}{y}\right]} \tag{25}$$

and the optimum power ratio can be calculated:

$$x^2 y_{opt} = \frac{(1 + x)^2}{y_{opt}} \tag{26}$$

$$y_{opt} = \frac{1 + x}{x} = 1 + \frac{1}{x} \tag{27}$$

The optimum power ratio is given by

$$\left(\frac{P_{DC}}{P_{LO}}\right)_{opt} = 1 + \left(\frac{\mathcal{R}}{V}\right) P_T \tag{28}$$

The maximum conversion gain using the optimum power ratio for $x \ll 1$ is

$$G_{max} = \frac{\eta\,(1 + \omega^2\tau^2)^{-1}}{8x\,(1 + x)} \approx \frac{\eta\,(1 + \omega^2\tau^2)^{-1}}{8x} \tag{29}$$

$$G_{max} = \frac{(\mathcal{R}/V)\,P_T}{8\,(1 + \omega^2\tau^2)}, \quad x \ll 1 \tag{30}$$

From equations 23 and 27

$$\left(\frac{g_D}{g_o}\right)_{opt} = 2x + 1 \approx 1^{*}, \text{ for } x << 1 \qquad (31)$$

The calculated maximum conversion gain, optimum power ratio, and optimum conductance ratio as a function of y are given in Figure 9. It should be noted that:

- The abscissa includes the total dissipated power budget P_T, mixer volume, dark electron concentration and mixer carrier lifetime.
- This analysis breaks down for the large modulation condition ($g_D/g_o << 1$) since there would be a large change of τ with P_{LO} and the $(1 + g_D/g_o)^{-1}$ term in equation 11 would approach unity,
- As expected from equation 30, the maximum gain occurs when the total power dissipation and mixer signal responsivity per volt are maximized.

The mixer is likely to be optimum at only one temperature. Thus, it is suggested that the LO and DC bias powers be fixed so that the available conversion gain be maximized at those temperatures indicating poorest receiver performance.

Figure 9 specifies the required mixer parameters for a given level of receiver performance. For example, assuming a nanosecond mixer with a quantum efficiency of 0.5 using equation 4, page 6, Section I, justified later in report ($P_{MIN} = 2h\nu B/\eta = 7.5 \times 10^{-20}$), a mixer temperature of 100 K and an IF amplifier noise factor of 1.5 db (yielding $T_{IF} \cong 120$ K and $P_{TH} \cong 3.03 \times 10^{-21}$ w/Hz), we calculate that a mixer conversion gain of approximately -9 db or greater is required to obtain a receiver NEP less than 10^{-19} w/Hz (Figure 3 and page 6).

---

* This result is inconsistent with the assumption of constant τ, so $g_D/g_o > 1$ may be more desirable for this case.

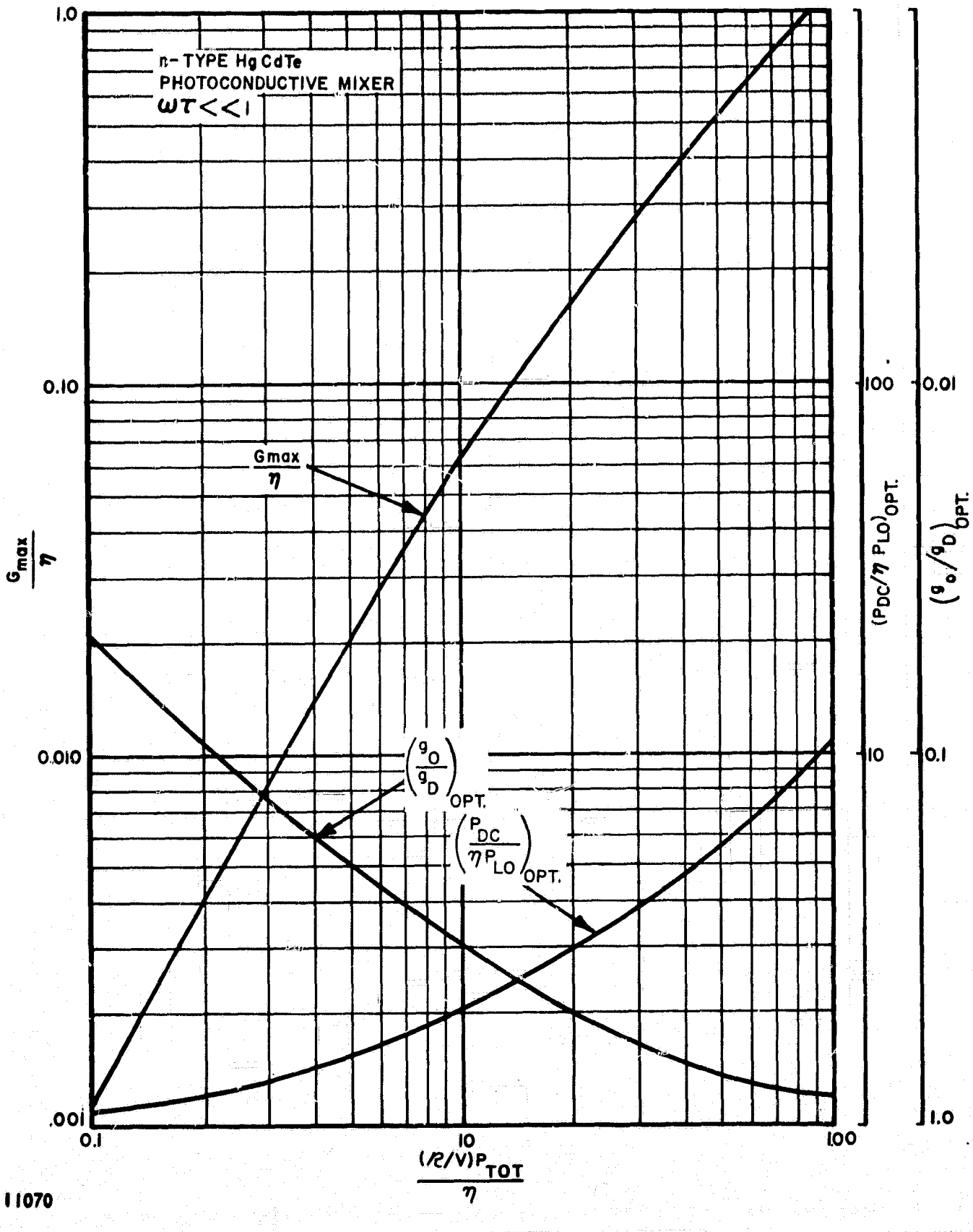

FIGURE 9. OPTIMUM CONDUCTANCE AND BIAS/LO POWER RATIO FOR PHOTOCONDUCTIVE HgCdTe

From Figure 9, a mixer gain of -9 db and $\eta = 0.5$ corresponds to a required small-signal specific responsivity of 680 volts/watt/volt for a total power dissipation of 2 mw. Also, from Figure 9, we obtain $(P_{DC}/\eta P_{LO})_{opt} = 3.6$, so that $P_{DC} = 1.57$ mw and $\eta P_{LO} = 0.43$ mw for $P_T = 2$ mw. The optimum value of ηP_{LO} sets the optimum conductance ratio, also available from Figure 9.

IV. HETERODYNE AND LOCAL-OSCILLATOR LIFETIMES IN PHOTOCONDUCTIVE HgCdTe MIXERS

This section analyzes the effect of LO power on the lifetimes of PC-HgCdTe elements operated as mixers. The analysis indicates three distinct lifetimes:

- Heterodyne lifetime τ_{het}, which is a small-signal lifetime inversely proportional to the change in recombination rate with excess carrier concentration
- Local oscillator-induced lifetime τ_{LO}, which is inversely proportional to the recombination rate, and
- Dark lifetime τ_D, which occurs when $P_{LO} = 0$.

For the large modulation case ($g_o/g_D >> 1$), we obtain in the limit of large LO power:

- For radiative recombination: $\tau_{het} \approx \frac{\tau_{LO}}{2}$
- For Auger recombination: $\tau_{het} \approx \frac{\tau_{LO}}{3}$.

A. DERIVATION OF HETERODYNE LIFETIME

The continuity equation for the spatially homogeneous case with band-to-band generation and recombination can be written from equation 420.5 on page 191 of reference 5

$$\frac{\partial n}{\partial t} + (r - g) = g_E \qquad (32)$$

where

g_E = excess rate of generation of carriers per unit volume due to external radiation,

$r - g$ = net rate of recombination over thermal generation per unit volume,

n = electron concentration.

Now for the condition of fixed n_o and p_o

$$r - g = R\,(n_e) \tag{33}$$

where

n_o = dark electron concentration

p_o = dark hole concentration

n_e = LO-induced electron concentration

$n = n_o + n_e$, $p = p_o + n_e$

Then

$$\frac{\partial n}{\partial t} + R\,(n_e) = g_E \tag{34}$$

Let the steady-state value of $n_e = n_{eo}$ such that $R\,(n_{eo}) = g_E$. Suppose g_E is increased by Δg_E. Let $n_e = n_{eo} + \Delta n_e$. Therefore

$$\frac{\partial\,(\Delta n_e)}{\partial t} + R\,(n_{eo} + \Delta n_e) = g_E + \Delta g_E \tag{35}$$

Since

$$\begin{aligned} R(n_{eo} + \Delta n_e) &\equiv R(n_{eo}) + \Delta n_e \left(\frac{dR}{dn_e}\right)_{n_e = n_{eo}} \\ &= g_E + \Delta n_e \left(\frac{dR}{dn_e}\right)_{n_e = n_{eo}} \end{aligned} \tag{36}$$

we obtain

$$\frac{\partial(\Delta n_e)}{\partial t} + \Delta n_e \left(\frac{dR}{dn_e}\right)_{n_e = n_{eo}} = \Delta g_E \tag{37}$$

The terms Δg_E and $(dR/dn_e)_o$ are constants in equations 36 and 37. Solving, we obtain

$$\Delta n_e = \frac{\Delta g_E}{(dR/dn_e)_{n_e = n_{eo}}} \left[1 - e^{-\left(\frac{dR}{dn_e}\right)_o t}\right] \tag{38}$$

Hence, we may define a <u>heterodyne lifetime</u>

$$\tau_{het} \equiv \frac{1}{\left(dR/dn_e\right)_{n_e = n_{eo}}} \tag{39}$$

In contrast, the steady-state bulk definition which Blakemore (page 193 of reference 5) uses for the lifetime is

$$\tau_{LO} = \frac{n_e}{R(n_e)} = \frac{1}{R(n_e)/n_e} \tag{40}$$

Since $R(n_e) = 0$ for $n_e = 0$, these two lifetimes expressions agree if, and only if, $R(n_e)$ is linear in n_e. This is not so for either radiative or Auger recombination. The difference may be a factor of two in the former or a factor of three in the latter.

1. RADIATIVE RECOMBINATION

For radiative recombination, the recombination rate from equation 511.13 of reference 5, where $np = (n_o + n_e)(p_o + n_e)$, is

$$R(n_e) = G_r \frac{n_e (p_o + n_o + n_e)}{n_i^2} \tag{41}$$

where G_r is the radiative recombination constant for the mixer element (equation 511.13 of reference 5).

Using equations 39, 40, and 41, we obtain for the heterodyne and LO lifetimes

$$\tau_{LO} = \frac{n_i^2}{G_r (n_o + p_o + n_e)} \tag{42}$$

and

$$\tau_{het} = \frac{n_i^2}{G_r (n_o + p_o + 2n_e)} \tag{43}$$

2. BAND-TO-BAND AUGER RECOMBINATION

For this case, the recombination rate from equation 612.5 of reference 5 is

$$R(n_e) = \frac{n_e (n_e + p_o + n_o) [G_{ee} p_o (n_o + n_e) + G_{hh} n_o (p_o + n_e)]}{n_i^4} \tag{44}$$

$$R(n_e) = \frac{n_e (n_e + p_o + n_o) \left[(G_{ee} p_o + G_{hh} n_o) n_e + (G_{ee} + G_{hh}) n_i^2\right]}{n_i^4} \tag{45}$$

where G_{ee} and G_{hh} are the Auger recombination constants for the mixer material. They vary with mixer temperature, band gap, mass ratio, and dielectric constant (see reference 5, equations 611.7 and 611.8).

We obtain for the heterodyne and LO lifetimes

$$\tau_{LO} = \frac{n_i^4}{(G_{ee}\, p_o + G_{hh}\, n_o)\, n_e^2 + \left[(G_{ee}\, p_o + G_{hh}\, n_o)\,(p_o + n_o) + (G_{ee} + G_{hh})\, n_i^2\right] n_e + (G_{ee} + G_{hh})\,(p_o + n_o)\, n_i^2} \tag{46}$$

and

$$\tau_{het} = \frac{n_i^4}{3(G_{ee}\, p_o + G_{hh}\, n_o)\, n_e^2 + 2\left[(G_{ee}\, p_o + G_{hh}\, n_o)\,(p_o + n_o) + (G_{ee} + G_{hh})\, n_i^2\right] n_e + (G_{ee} + G_{hh})\,(p_o + n_o)\, n_i^2} \tag{47}$$

In the previous photoconductive mixing analysis it was assumed that the heterodyne (small signal) and LO-induced lifetimes were equal.

B. VARIATION OF HETERODYNE AND LO LIFETIMES, CONDUCTANCE RATIO, AND LO POWER

For the 10.6 micron heterodyne operation near 100 K in n-type HgCdTe, Auger band-to-band recombination is believed to dominate (reference 6). Equation 44 can be written:

$$R(n_e) = K_{ee}\, \frac{n_e (n_o + n_e)\,(n_o + p_o + n_e)}{n_i^2} \tag{48}$$

$$\approx K_{ee}\, \frac{n_e (n_o + n_e)^2}{n_i^2} \text{ for } n_o \gg p_o \text{ and} \tag{49}$$

$$K_{ee} \equiv \frac{G_{ee}}{n_o} \gg K_{hh} \equiv \frac{G_{hh}}{p_o} \tag{50}$$

The heterodyne or small-signal lifetime τ_{het} is

$$\tau_{het}^{-1} = K_{ee}\left\{3\left(\frac{n_e}{n_i}\right)^2 + 2\left[2\left(\frac{n_o}{n_i}\right) + \frac{n_i}{n_o}\right]\frac{n_e}{n_i} + \frac{n_o}{n_i}\left(\frac{n_o}{n_i} + \frac{n_i}{n_o}\right)\right\} \tag{51}$$

$$\approx K_{ee}\left\{3\left(\frac{n_e}{n_i}\right)^2 + 4\left(\frac{n_o}{n_i}\right)\left(\frac{n_e}{n_i}\right) + \left(\frac{n_o}{n_i}\right)^2\right\}, \; n_o >> p_o \tag{52}$$

The dark lifetime τ_D is obtained by setting $n_e = 0$ in the above equation.

$$\tau_D^{-1} = K_{ee}\left(\frac{n_o}{n_i}\right)\left(\frac{n_o}{n_i} + \frac{n_i}{n_o}\right) \approx K_{ee}\left(\frac{n_o}{n_i}\right)^2, \; n_o >> p_o \tag{53}$$

Combining equations 52 and 53

$$\frac{\tau_{het}}{\tau_D} \approx \frac{1}{3\left(\frac{n_e}{n_o}\right)^2 + 4\left(\frac{n_e}{n_o}\right) + 1}, \text{ for } n_o >> p_o \tag{54}$$

For the large modulation case $n_e/n_o = g_o/g_D >> 1$, then

$$\frac{\tau_{het}}{\tau_D} \approx \frac{1}{3}\left(\frac{n_o}{n_e}\right)^2 = \frac{1}{3}\left(\frac{g_D}{g_o}\right)^2 \tag{55}$$

For $n_e/n_o = g_o/g_D = 1$, we obtain $\tau_{het}/\tau_D = 0.125$. The LO lifetime ratio is (equations 49 and 53)

$$\frac{\tau_{LO}}{\tau_D} = \frac{n_e/R(n_e)}{K_{ee}^{-1}\left(\frac{n_o}{n_i}\right)^{-2}} = \frac{1}{\left(\frac{n_e}{n_o}\right)^2 + 2\left(\frac{n_e}{n_o}\right) + 1} \tag{56}$$

The heterodyne and LO lifetimes normalized to the mixer dark lifetime are plotted as a function of conductance ratio (g_o/g_D) in Figure 10.

The variation of (g_o/g_D) with LO power is derived as follows. The LO-induced electron concentration is related to the LO power by

$$n_e = \frac{\eta P_{LO} \tau_{LO}}{Vol\ h\nu_{LO}} \tag{57a}$$

Thus the conductance ratio is

$$\frac{g_o}{g_D} = \frac{n_e}{n_o} = \left(\frac{\eta \tau_D}{Vol\ n_o\ h\nu_{LO}}\right)\left(\frac{\tau_{LO}}{\tau_D}\right) P_{LO} \tag{57b}$$

The first term in brackets on the right side is the specific responsivity of equation 19 of Section III-B. Substitution of equation 19 of Section III-B and equation 54 into equation 56 then gives

$$P_{LO} = \frac{(g_o/g_D)\,(1 + g_o/g_D)^2}{\mathcal{R}/V} \tag{57c}$$

where $\mathcal{R}/V$ is the mixer responsivity normalized to the applied bias voltage. This expression is plotted in Figure 11.

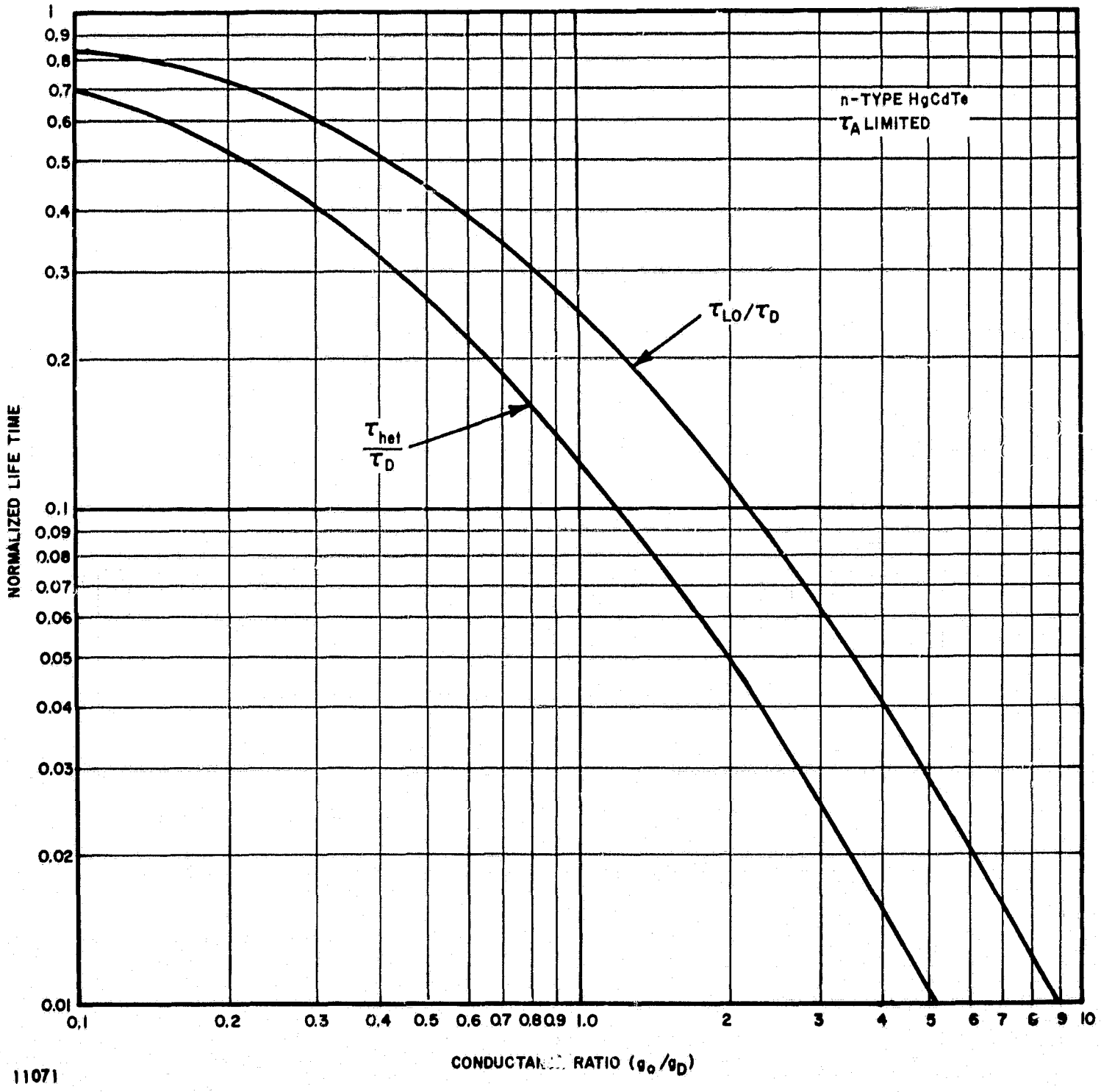

FIGURE 10. NORMALIZED HETERODYNE AND LO LIFETIME VS CONDUCTANCE RATIO FOR n-TYPE, AUGER LIFETIME LIMITED, HgCdTe

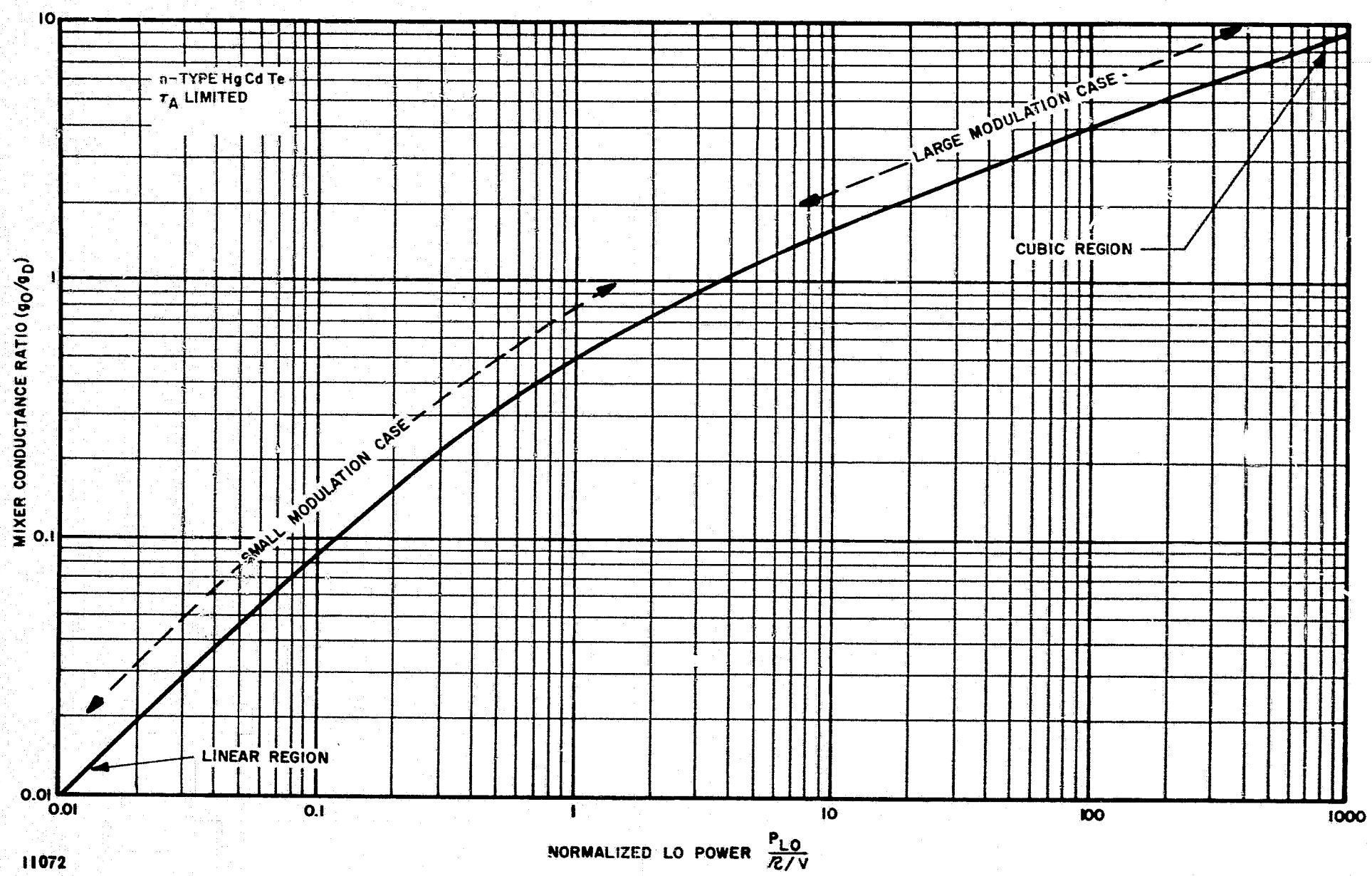

FIGURE 11. MIXER CONDUCTANCE RATIO VS NORMALIZED LO POWER FOR n-TYPE HgCdTe

The normalized heterodyne and LO lifetimes versus normalized LO power are given in Figure 12.

We conclude the following from this analysis and Figures 10, 11, and 12:

- The heterodyne lifetime is always smaller than the LO lifetime and the limit for large P_{LO} can be as low as one third the LO lifetime.
- τ_{het}/τ_D and τ_{LO}/τ_D approach unity for small P_{LO}.
- τ_{het} and τ_{LO} decrease with increasing LO power.
- Although g_o is initially linear in P_{LO}, g_o varies as $P_{LO}^{1/3}$ above $g_o/g_D > 5$.
- The applied LO power required to obtain a specified τ_{het}/τ_D ratio and g_o/g_D ratio is determined by the mixer responsivitity and bias voltage.

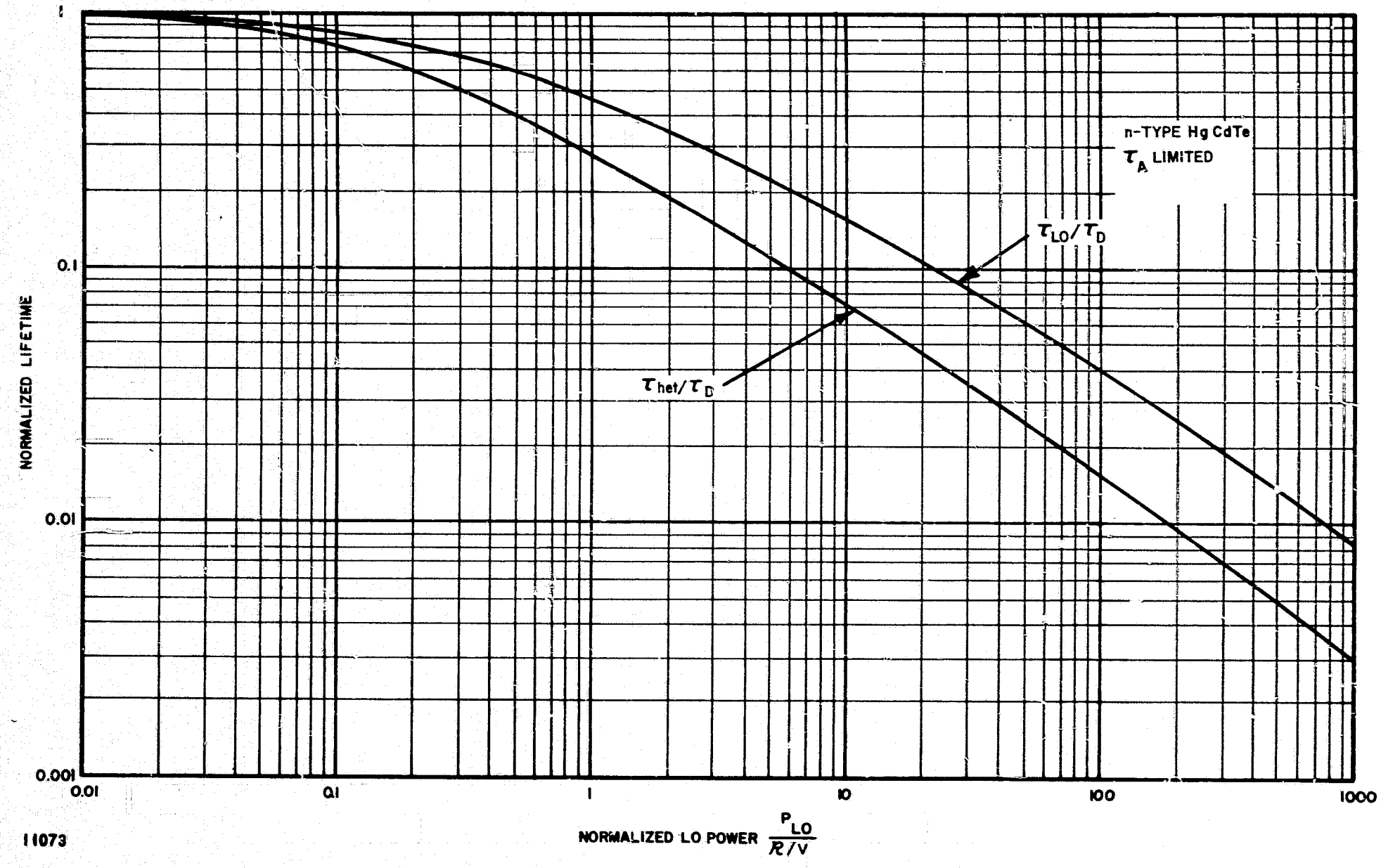

FIGURE 12. NORMALIZED MIXER LIFETIMES VS NORMALIZED APPLIED LO POWER FOR n-TYPE HgCdTe

V. ANALYSIS OF MIXING IN PC-HgCdTe FOR VARYING LIFETIME AND FINITE DARK CONDUCTANCE

A. INTRODUCTION

Based on the concepts of a heterodyne (small-signal) lifetime and LO lifetime introduced in Section IV, the analyses in Sections II, III, and reference 1 are further expanded to where the carrier lifetime is a function of LO power. The effect of appreciable dark conductance is also included. Many of the previous equations required modification; others are unchanged, but are included here for completeness.

B. ANALYSIS

The IF photocurrent generator is given by

$$I(\omega) = \eta\, q\, F_1\, A \left(\frac{\tau_{het}}{T_r}\right) \frac{1}{1 + j\,\omega\,\tau_{het}} \tag{58}$$

where

η = quantum efficiency = $\dfrac{(1 - R)\,(1 - e^{-\alpha D})}{1 - R\,e^{-\alpha D}}$ (reference 7)

R = reflection coefficient = $\left(\dfrac{n - 1}{n + 1}\right)^2$

n = index of refraction of photoconductor

α = photoconductor absorption coefficient

D = depth of photoconductor in direction of illumination

q = electronic charge

$F_1 A$ = peak photon flux at IF

A = illuminated area of photoconductor = L × W

L = interelectrode spacing

W = other dimensions of photoconductor in plane of illumination

τ_{het} = small-signal lifetime of principal carriers under steady illumination

T_r = transit time of principal carrier = $L^2/\mu V$

μ = mobility of principal carriers

ω = IF angular frequency

V = bias voltage

The available conversion gain, or the ratio of the available IF output power to the available infrared signal power, is

$$G = \frac{P_{IF,\ available}}{P_s} = \frac{|I(\omega)|^2}{8\ (g_o + g_D)\ P_s} \tag{59}$$

where

g_o = LO-induced mixer conductance

g_D = dark conductance of mixer

Using the definition of T_r, the LO-induced mixer conductance is

$$g_o = \frac{I_o}{V} = \frac{\eta\, q\, F_o\, A\, \tau_{LO}}{V\, T_r} = \frac{\eta\, q\, \mu\, F_o\, A\, \tau_{LO}}{L^2} \tag{60}$$

where

I_o = DC photocurrent = $\dfrac{\eta\, q\, \mu\, F_o\, A\, \tau_{LO}}{L^2}$

F_oA = average photon flux

τ_{LO} = large-signal lifetime of principal carriers

Substitution of equations 58 and 60 into 59 then gives

$$G = \frac{\eta\, q\, V\, \tau_{het}}{2h\nu_s\, T_r\, (1 + \omega^2\, \tau_{het}^2)} \left(\frac{\tau_{het}/\tau_{LO}}{1 + g_D/g_o}\right) \tag{61}$$

$$= \frac{\eta\, q\, \mu\, \tau_{het}}{2h\nu_s\, (1 + \omega^2\, \tau_{het}^2)}\, \frac{V^2}{L^2} \left(\frac{\tau_{het}/\tau_{LO}}{1 + g_D/g_o}\right)$$

In obtaining 61, use has been made of the relation for modulation index, namely

$$\frac{F_1 A}{F_o A} \approx 2\sqrt{\frac{F_s A}{F_{LO} A}}, \qquad F_{LO} >> F_s \tag{62}$$

where the photon flux at signal frequency is

$$F_s A = \frac{P_s}{h\nu_s}, \tag{63}$$

and the photon flux at LO frequency is

$$F_{LO} A \approx F_o A = \frac{P_{LO}}{h\nu_{LO}} \tag{64}$$

In equations 63 and 64

h = Planck's constant

ν_s = infrared signal frequency

P_{LO} = infrared LO power

ν_{LO} = LO frequency

The conversion gain depends on the LO power directly through its effect on g_o and indirectly through possible effects on the lifetimes τ_{het} and τ_{LO} and the transit time T_r (through an effect on mobility μ).

An alternative expression for the conversion gain in terms of the total absorbed bias power (P_{dc}) and the LO power (P_{LO}) is useful for gain calculations and for optimization of the ratio of bias to LO power. The total absorbed bias power is

$$P_{DC} = V^2 (g_o + g_D) \tag{65}$$

Since $\nu_s \approx \nu_{LO}$, substitution of equations 60, 64, and 65 into 61 gives

$$G = \frac{P_{DC}}{2P_{LO}} \left(\frac{\tau_{het}}{\tau_{LO}} \right)^2 \left(\frac{1}{1 + g_D/g_o} \right)^2 \frac{1}{1 + \omega^2 \tau_{het}^2} \tag{66}$$

If the carrier mobility is assumed to be independent of LO power, equation 66 shows that for $\omega\tau_{het} < 1$ the available mixer gain is independent of carrier mobility and depends only on the power, conductance, and lifetime ratios.

The overall mean-square noise current generator consists of three component noise generators

$$\overline{i_N^2} = \overline{i_{GR}^2} + \overline{i_G^2} + \overline{i_{IF}^2} \tag{67}$$

$\overline{i_{GR}^2}$ is the G-R noise, given by (Appendix II)

$$\overline{i_{GR}^2} = 4q \left(\frac{\tau_{het}}{T_r} \right) \left(\frac{\tau_{het}}{\tau_{LO}} \right) \left(1 + \frac{p_o}{n_e} \right) \frac{I_o B}{1 + \omega^2 \tau_{het}^2} \tag{68}$$

where B is the IF bandwidth, p_o is the dark hole concentration, and n_e is the excess electron-hole pair concentration due to the local oscillator. In equation 68 the local-oscillator induced, and dark contributions to G-R noise correspond to the terms 1 and p_o/n_e, respectively, in the factor $(1 + p_o/n_e)$. Qualitatively, the former is much greater than the latter ($1 >> p_o/n_e$) because the G-R noise is proportional to the minority carrier concentration, which increases much faster than the dc current (equivalently, majority carrier concentration) as hole-electron pairs are generated by the local oscillator. This statement is believed to have general applicability to HgCdTe intrinsic photodetectors although equation 68 was specifically derived for n-type HgCdTe with Auger band-to-band recombination dominant (see Appendix II).

An alternative form of the factor $(1 + p_o/n_e)$ is obtained by substituting $g_D/g_o = n_o/n_e$ and $n_o p_o = n_i^2$, where n_i is the intrinsic carrier concentration:

$$1 + \frac{p_o}{n_e} = 1 + \frac{g_D}{g_o}\left(\frac{n_i}{n_o}\right)^2 \tag{69}$$

$\overline{i_G^2}$ is the thermal noise of the total mixer conductance and is

$$\overline{i_G^2} = 4\,k\,T_M\,(g_o + g_D)\,B \tag{70}$$

where

k = Boltzmann's constant

T_M = physical temperature of mixer

$\overline{i_{IF}^2}$ is the IF amplifier noise referred to the output terminals of the mixer, and is

$$\overline{i_{IF}^2} = 4\,k\,T'_{IF}\,(g_o + g_D)\,B \tag{71}$$

where

T'_{IF} = effective input noise temperature of IF amplifier referred to the output terminals of the mixer = $(F'_{IF} - 1)T_o$

F'_{IF} = noise factor of IF amplifier referred to the output terminals of the mixer

T_o = reference temperature = 290 k

The IF output signal-to-noise power ratio is

$$\left(\frac{S}{N}\right)_{POWER} = \frac{|I(\omega)|^2}{2\,\overline{i_N^2}} \tag{72}$$

Substitution of equations 59 to 61 and 67 to 71 into 72 then gives

$$\left(\frac{S}{N}\right)_P = \left(\frac{\eta P_s}{2h\nu_s B}\right) \frac{1}{1 + \frac{g_D}{g_o}\left(\frac{n_i}{n_o}\right)^2 + \frac{k(T_M + T'_{IF})}{q\,V}\left(\frac{T_r}{\tau_{het}}\right)\left(\frac{\tau_{LO}}{\tau_{het}}\right)\left(1 + \frac{g_D}{g_o}\right)\left(1 + \omega^2\tau_{het}^2\right)} \tag{73}$$

Thus, the NEP, or the value of signal power to give an IF S/N ratio equal to unity, is

$$NEP = \frac{2h\nu_s B}{\eta}\left\{1 + \frac{g_D}{g_o}\left(\frac{n_i}{n_o}\right)^2 + \frac{k(T_M + T'_{IF})}{qV}\left(\frac{T_r}{\tau_{het}}\right)\left(\frac{\tau_{LO}}{\tau_{het}}\right)\left(1 + \frac{g_D}{g_o}\right)\left(1 + \omega^2\tau_{het}^2\right)\right\}$$

$$= \frac{2h\nu_s B}{\eta}\left\{1 + \frac{g_D}{g_o}\left(\frac{n_i}{n_o}\right)^2 + \frac{1}{40V}\left(\frac{T_M + T'_{IF}}{T_o}\right)\left(\frac{T_r}{\tau_{het}}\right)\left(\frac{\tau_{LO}}{\tau_{het}}\right)\left(1 + \frac{g_D}{g_o}\right)\left(1 + \omega^2\tau_{het}^2\right)\right\} \tag{74}$$

with V in volts. In terms of the conversion gain (equation 61), equation 74 can be written

$$NEP = \frac{2h\nu_s B}{\eta}\left[1 + \frac{g_D}{g_o}\left(\frac{n_i}{n_o}\right)^2\right] + \frac{k(T_M + T'_{IF})\,B}{G}$$

$$\approx P_{min} + \frac{k(T_M + T'_{IF})\,B}{G} \tag{75}$$

where $P_{min} = 2h\nu_s B/\eta$.

Note that all these expressions reduce to the simpler ones of Section II for $\tau_{het} = \tau_{LO} = \tau_D$ and $g_D/g_o \approx 0$.

VI. PARAMETRIC ANALYSIS AND MIXER DESIGN IN AUGER-LIFETIME-LIMITED n-TYPE PHOTOCONDUCTIVE HgCdTe

A. PARAMETRIC ANALYSIS

A closed analysis has been conducted on Auger-lifetime-limited photoconductive n-type HgCdTe that examines both the physical and engineering parameters. This analysis yields information on the variation of receiver properties such as NEP, conversion gain, IF frequency response, and mixer conductance ratio with LO power, DC bias power, mixer temperature, mixer volume and such material properties as quantum efficiency, carrier mobility, dark carrier lifetime, dark electron concentration, and mixer dark conductance.

This parametric study includes the variation of material lifetime with incident power density and gives expressions for gain and NEP in terms of measurable engineering quantities.

1. MIXER LIFETIME

The dark lifetime for Auger-lifetime-limited PC n-type HgCdTe is given by equation 53.

$$\tau_D = \frac{n_i^2}{n_o G_{ee}} \equiv \frac{n_i^2}{n_o^2 K_{ee}} \tag{76}$$

where

n_i = intrinsic carrier concentration,

n_o = dark electron concentration,

G_{ee} = thermal equilibrium generation rate due to electron-electron processes,

$K_{ee} \equiv \frac{G_{ee}}{n_o}$.

In the presence of LO power, the LO-induced lifetime is

$$\tau_{LO} = \frac{n_i^2}{K_{ee}\left(n_o + n_e\right)^2} = \frac{\tau_D}{\left(1 + g_o/g_D\right)^2} \tag{77}$$

where n_e = LO-induced electron concentration.

From equation 54, the heterodyne lifetime is

$$\tau_{het} = \frac{n_i^2}{K_{ee}\left(n_o + n_e\right)\left(n_o + 3n_e\right)} = \frac{\tau_D}{\left(1 + g_o/g_D\right)\left(1 + 3g_o/g_D\right)} \tag{78}$$

Under the condition of large LO power ($n_e >> n_o$), $\tau_{het} \approx \frac{\tau_{LO}}{3}$.

From equation 78, the thermal equilibrium dark electron concentration is

$$n_o^2 = \frac{n_i^2}{\left(\tau_{het} K_{ee}\right)\left(\frac{n_e}{n_o} + 1\right)\left(3\frac{n_e}{n_o} + 1\right)} \tag{79}$$

and from equation 59 we define

$$z \equiv \frac{n_e}{n_o} = \frac{g_o}{g_D} = \frac{\eta P_{LO} \tau_{het}}{h\nu_{LO} Vol} \frac{\tau_{LO}}{\tau_{het}} \frac{1}{n_o} \tag{80}$$

where

g_D = dark mixer conductance,
g_o = photo-induced mixer conductance,
Vol = mixer volume,
η = mixer quantum efficiency,

P_{LO} = applied LO power,

h = Planck's constant,

ν_{LO} = LO frequency.

Substituting equations 77, 78, and 79 into 80,

$$z = \frac{\eta\, P_{LO}\, \tau_{het}}{h\nu_{LO}\, Vol} \frac{(3z+1)}{(z+1)} \frac{\tau_{het}^{1/2}\, K_{ee}^{1/2}\, (z+1)^{1/2}\, (3z+1)^{1/2}}{n_i} \qquad (81)$$

We define a temperature dependent variable which changes with the power budget and mixer volume

$$\chi \equiv \frac{P_T\, \tau_{het}^{3/2}\, K_{ee}^{1/2}}{h\nu_{LO}\, Vol\, n_i} \qquad (82)$$

where P_T = total power dissipation = $P_{DC} + \eta\, P_{LO}$.

We also define a variable y such that

$$y \equiv \frac{P_{DC}}{\eta\, P_{LO}} \qquad (83)$$

Combining equations 81, 82, and 83

$$z = \frac{\chi(3z+1)^{3/2}}{(1+y)(z+1)^{1/2}} \qquad (84)$$

and from equations 83 and 84,

$$1 + y = \frac{\chi (3z + 1)^{3/2}}{z (z + 1)^{1/2}} = \frac{P_T}{\eta P_{LO}} \tag{85}$$

2. MIXER CONVERSION GAIN

The available conversion gain for a photoconductive mixer is (equations 66, 77, and 78)

$$G = \frac{P_{DC}}{2 P_{LO}} \cdot \frac{1}{\left(1 + \omega^2 \tau_{het}^2\right)} \cdot \frac{\left(\tau_{het}/\tau_{LO}\right)^2}{\left(1 + g_D/g_o\right)^2} \tag{86}$$

$$= \frac{P_{DC}}{2 P_{LO}} \frac{1}{\left(1 + \omega^2 \tau_{het}^2\right)} \cdot \frac{1}{\left(3 + g_D/g_o\right)^2}$$

where ω = angular IF frequency.

For $\omega\tau_{het} << 1$, then from equations 80, 83, and 86, the appropriate gain is

$$G_{\omega=o} = \frac{\eta}{2} \frac{y}{\left(3 + \frac{1}{z}\right)^2} \tag{87}$$

Using equations 85 and 87

$$G_{\omega=o} = \frac{\eta z}{2\left(3z + 1\right)^2} \frac{\chi (3z + 1)^{3/2} - z (z + 1)^{1/2}}{\left(z + 1\right)^{1/2}} \tag{88}$$

which expresses the available conversion gain in terms of the conductance ratio g_o/g_D, and the mixer parameter χ. There is no simple optimum gain that can be calculated from equation 88. The value of χ is fixed by the selection of mixer temperature, IF lifetime, and total power density. Using equation 88, the mixer conversion gain has been calculated as a function of conductance ratio g_o/g_D for five values of the mixer parameter χ and is plotted in Figure 13. As Figure 13 shows, for values $0 < \chi < 0.237$, there is an optimum conductance ratio for each value of χ, which yields maximum conversion gain. For larger χ, the gain monotonically increases with the conductance ratio.

3. OPTIMUM CONDUCTANCE AND POWER RATIOS

Differentiating equation 88 with respect to z and solving for z_{OPT} in terms of χ, we obtain

$$\chi = \frac{2z_{OPT}\left(z_{OPT}+1\right)^{3/2}}{\left(3z_{OPT}+1\right)^{3/2}\left(2z_{OPT}+1\right)} \tag{89}$$

This expression for optimum conductance ratio has been plotted in Figure 14. For $\chi > 0.237$, the optimum conductance ratio approaches infinity.

The low-frequency conversion gain for optimum conductance ratio is obtained by substituting equation 89 into equation 88

$$G_{\omega=o} = \frac{\eta}{2}\,\frac{z_{OPT}^2}{\left(2z_{OPT}+1\right)\left(3z_{OPT}+1\right)^2} \tag{90}$$

Figure 15 shows the maximum conversion gain as a function of mixer parameter χ. As can be seen from Figure 15 (and Figure 13) the maximum achievable conversion gain increases directly with χ, and changes relatively slowly with g_o/g_D and χ. A conversion gain near -10 db is calculated for $g_o/g_D = 0.5$ and $\chi = 1$.

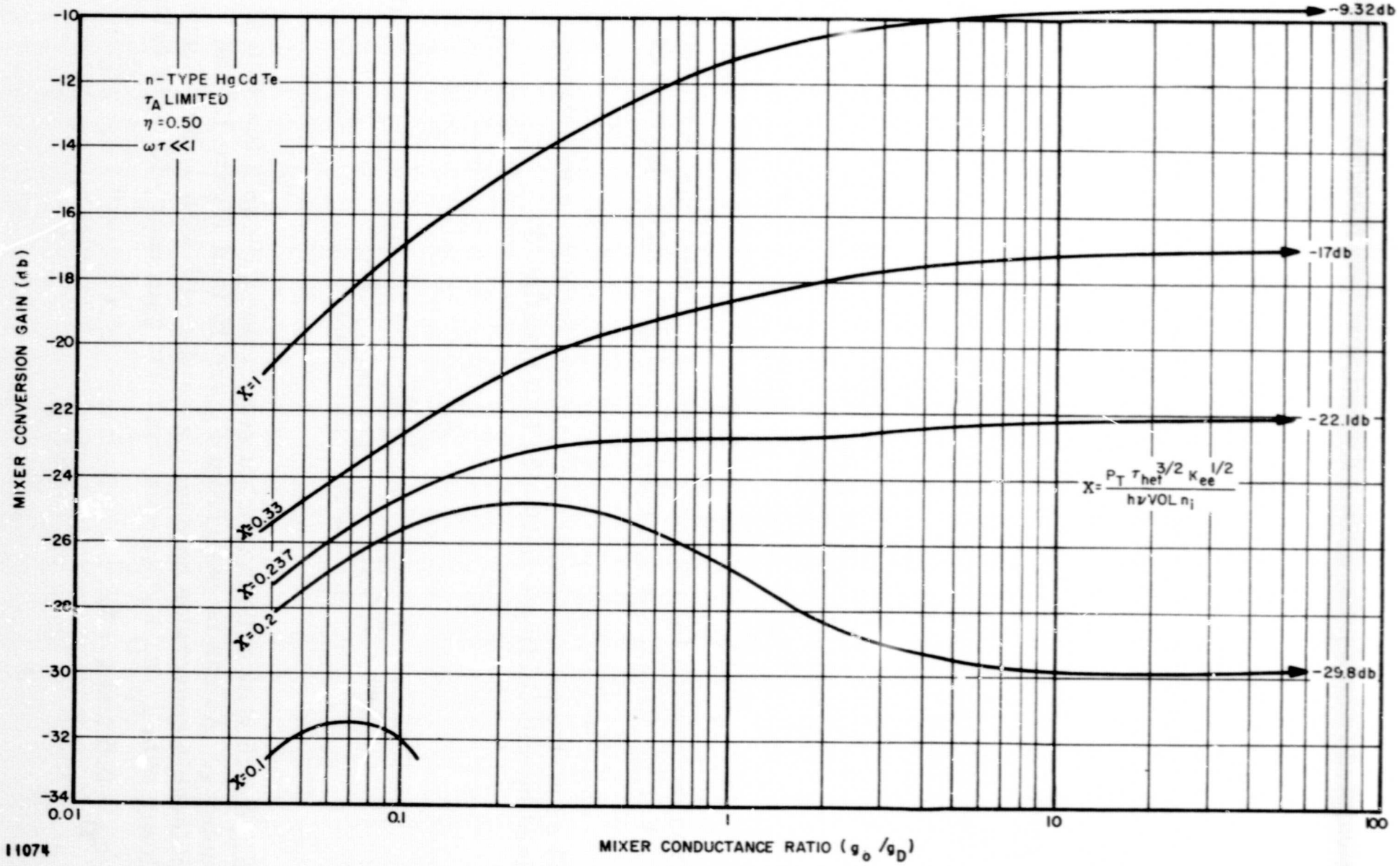

FIGURE 13. CALCULATED MIXER CONVERSION GAIN VS MIXER CONDUCTANCE RATIO FOR n-TYPE HgCdTe

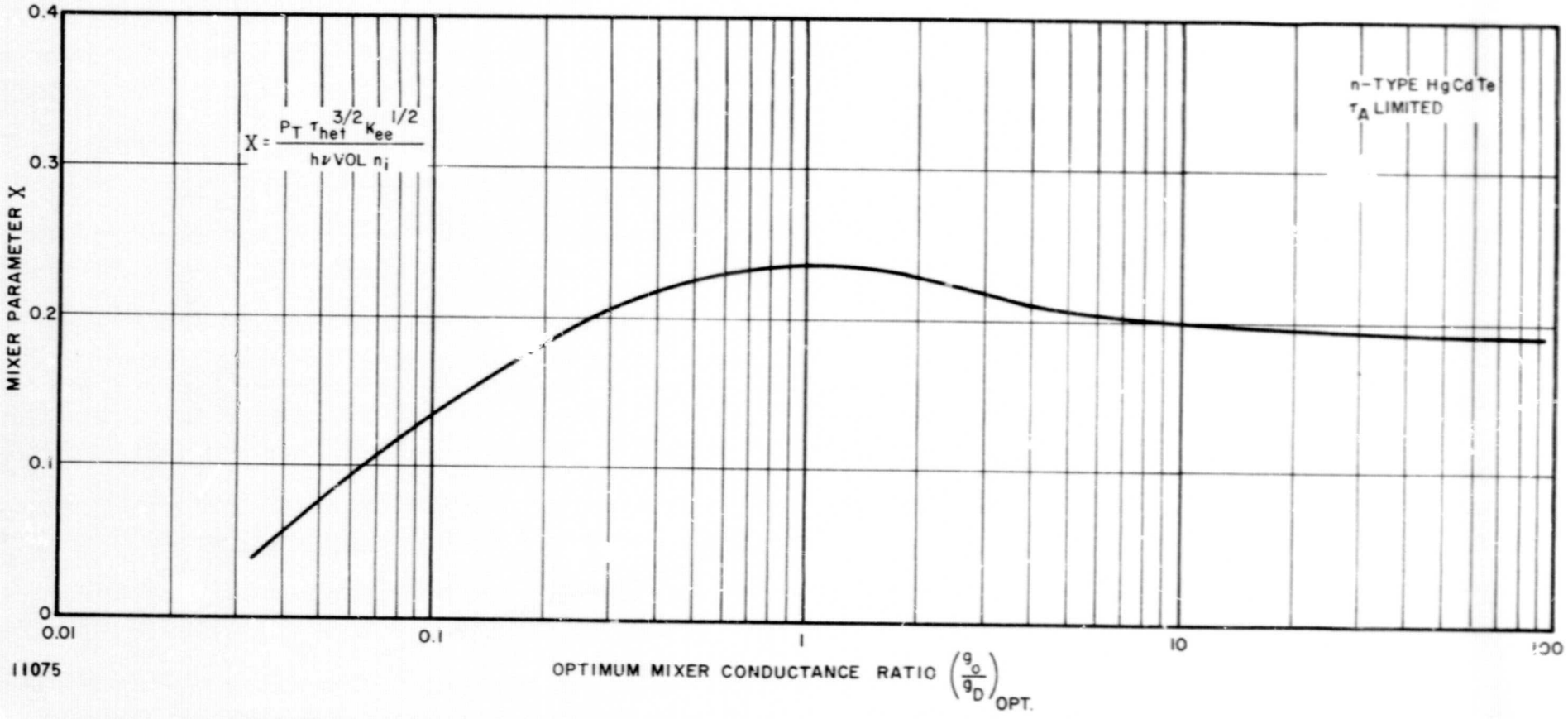

FIGURE 14. CALCULATED OPTIMUM CONDUCTANCE RATIO AS A FUNCTION OF MIXER PARAMETER χ, IN n-TYPE HgCdTe

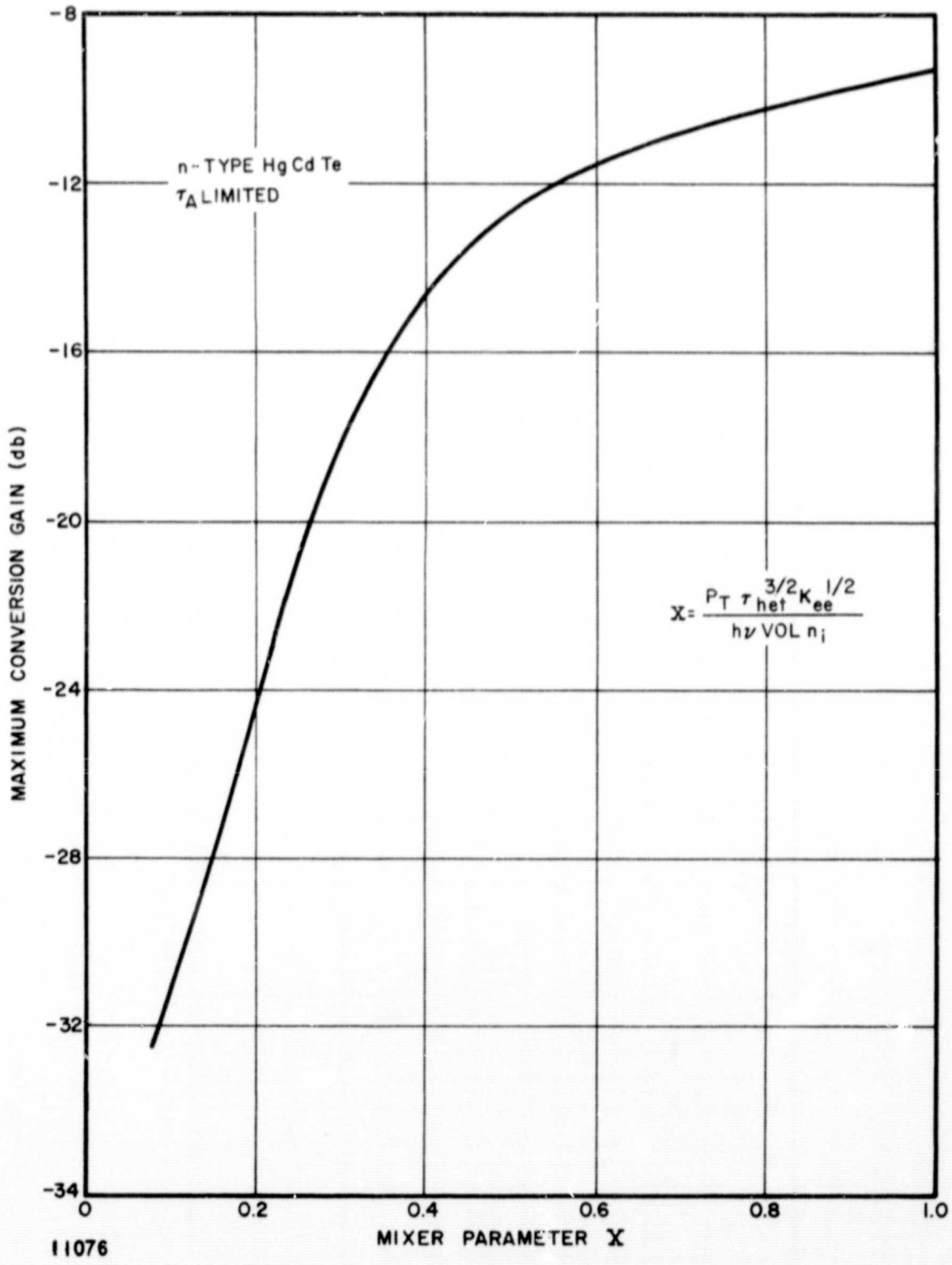

FIGURE 15. MAXIMUM CONVERSION GAIN VS MIXER PARAMETER χ FOR n-TYPE HgCdTe

Using equations 85 and 89, the power ratio at the optimum conductance ratio is

$$y_{OPT} + 1 = \frac{2(z_{OPT} + 1)}{(2z_{OPT} + 1)} \tag{91}$$

and

$$y_{OPT} = \frac{1}{2z_{OPT} + 1} \tag{92}$$

The optimum power ratio has been plotted in Figure 16 as a function of mixer parameter χ, using equations 92 and 89.

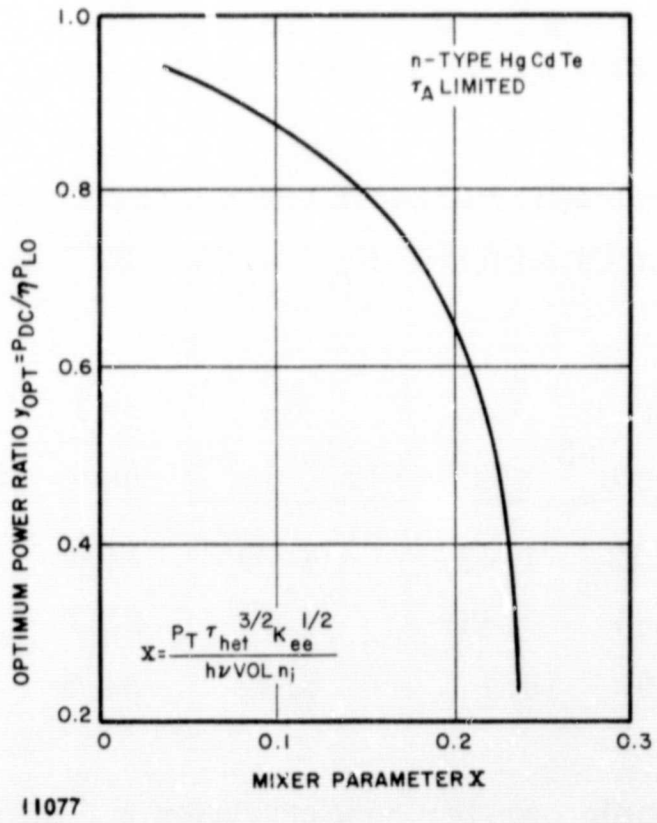

FIGURE 16. CALCULATED OPTIMUM POWER RATIO AS A FUNCTION OF MIXER PARAMETER χ

Since the power ratio $P_{DC}/\eta\ P_{LO}$ must remain a positive number, equation 85 is plotted in Figure 17 to establish the allowable operating region for this analysis. For example, when $\chi = 0.1$, power considerations require that $g_o/g_D < 0.180$.

B. MIXER DESIGN

This section applies the parametric analysis of Section VI, part A to a specific mixer design. The variation of receiver performance as a function of such variables as operating temperature, LO power, bias power, and mixer volume is calculated using representative values for the parameters in the mixer parameter χ.

Since χ (defined in equation 82) must exceed 0.237 to meet the objectives of the proposed LCE, there is no finite value of conductance ratio g_o/g_D which maximizes mixer conversion gain (Figure 13). Therefore a g_o/g_D and τ_{het} were selected for a T_m of 100 K and equations 76, 78, and 79 were used to determine the required n_o, and therefore the required N_D.

The values used in the calculations are given in Table 1 for three mixer temperatures and, x = 0.18 (Appendix III) using data from reference 6:

TABLE 1. MATERIAL PARAMETERS USED FOR PC-Hg_{1-x} Cd_xTe MIXER CALCULATIONS ($N_D = 4.68 \times 10^{15}$ cm^{-3}; x = 0.18)

Temperature (K)	n_i $\times 10^{14}$ cm^{-3}	K_{ee} $\times 10^5$	n_o $\times 10^{15}$ cm^{-3}	τ_D nsec	g_D 10^{-2} mhos	μ 10^4 $cm^2/Vsec$
80	2.32	1.68	4.69	14.6	11.8	13.15
100	6.39	7.45	4.77	23.2	8.15	8.9
120	12.9	19.1	5.02	34.3	6.23	6.47

The intrinsic carrier concentration n_i, dark lifetime τ_D electron mobility μ, and normalized thermal equilibrium generation rate K_{ee}, as well as the mixer thermal noise power (kT_MB) all vary with mixer temperature. The calculated variation of dark conductance and dark lifetime with mixer

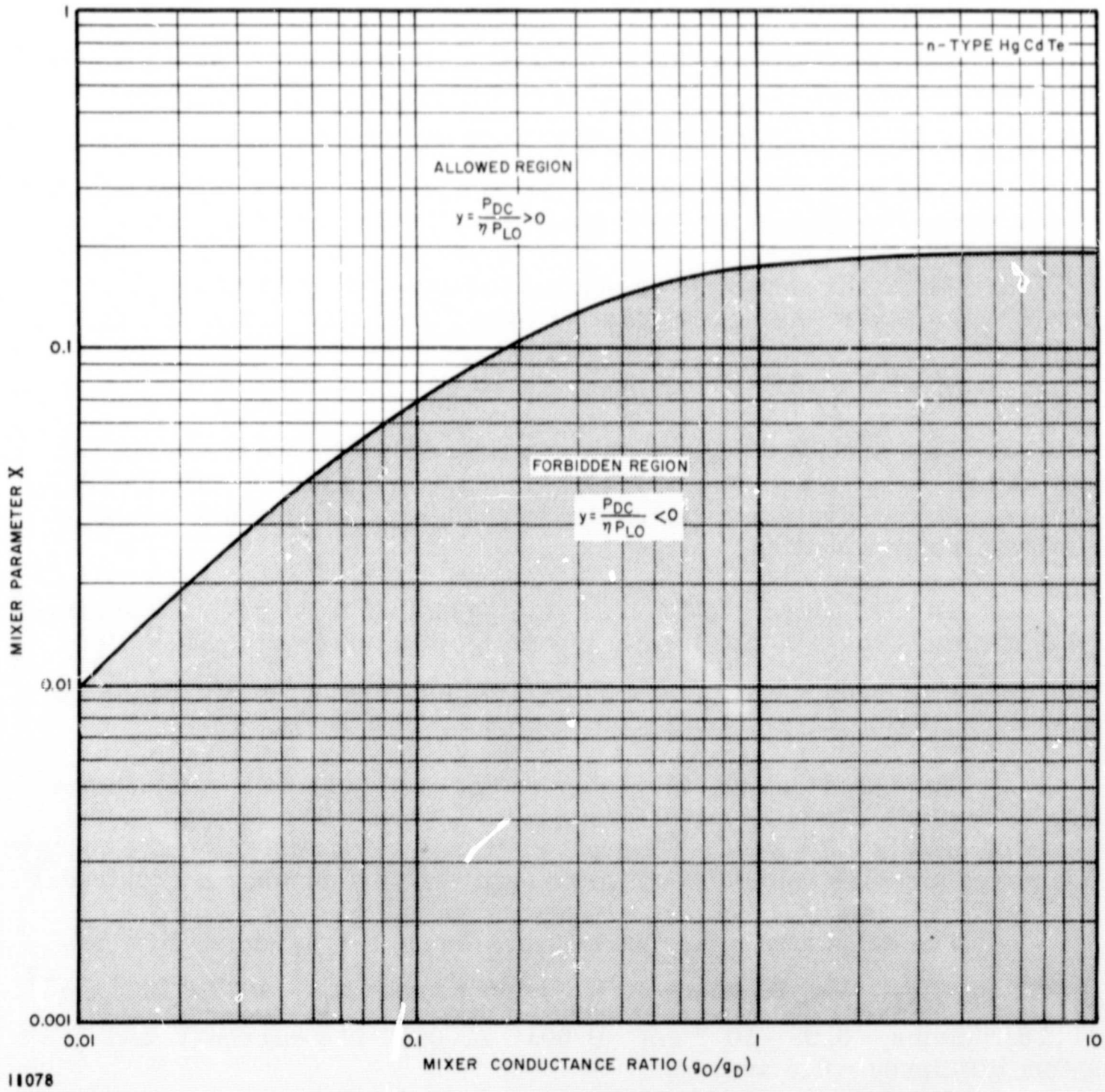

FIGURE 17. ALLOWED VALUES OF MIXER PARAMETER χ VS MIXER CONDUCTANCE RATIO

temperature are plotted in Figures 18 and 19 for $N_D = 4.68 \times 10^{15}$ cm^{-3}. The mixer dark conductance decreases and the dark lifetime increases with increasing mixer temperature.

1. BEHAVIOR OF CONVERSION GAIN AT CONSTANT TEMPERATURE

The calculated variation of mixer conversion gain ($\omega\tau << 1$) with total power dissipation ($P_{DC} + \eta P_{LO}$) is shown in Figure 20 for a mixer volume of 6.98×10^{-18} cm^3(0.003" × 0.003" × 12 microns), $g_o/g_D = 1$, and a mixer temperature of 100 K. As expected, the mixer gain increases with increasing power dissipation for fixed applied LO power (set by T_m and g_o/g_D).

Figure 21 shows the calculated variation of conversion gain ($\omega\tau << 1$) with mixer volume for constant total power dissipation, at 100 K.

2. MIXER PERFORMANCE OVER 80 TO 120 K RANGE

This section discusses mixer performance where the laser LO power and DC bias voltage are both kept constant in the spacecraft, and the radiation cooler temperature varies due to changing thermal load, seasonal variations, solar radiation, etc.

The LO power and DC bias voltage are selected so that a heterodyne lifetime of 3 nsec is obtained in the designated mixer sample ($N_D = 4.68 \times 10^{15}$ cm^{-3} and $x = 0.18$) at a mixer temperature of 100 K. The mixer is then permitted to vary in temperature over a $\pm$20 K range.

The behavior over this temperature range of mixer conductance ratio, heterodyne lifetime, mixer resistance, total power dissipation, and conversion gain is calculated. (In practice it may be possible to make changes in LO power and bias voltage to optimize receiver performance if required.)

The calculated mixer parameters for an n-type Auger-lifetime-(τ_A) limited, $Hg_{1-x}Cd_xTe$ mixer at $T_m = 100$ K, with $N_D = 4.68 \times 10^{15}$ cm^{-3}, $x = 0.18$, volume = 6.98×10^{-8} cm^3 (0.003" × 0.003" × 12 microns), and quantum efficiency = 0.5 are:

Mixer parameter	χ	1.5
Conductance ratio	g_o/g_D	1.0
Heterodyne lifetime	τ_{het}	2.93 nsec

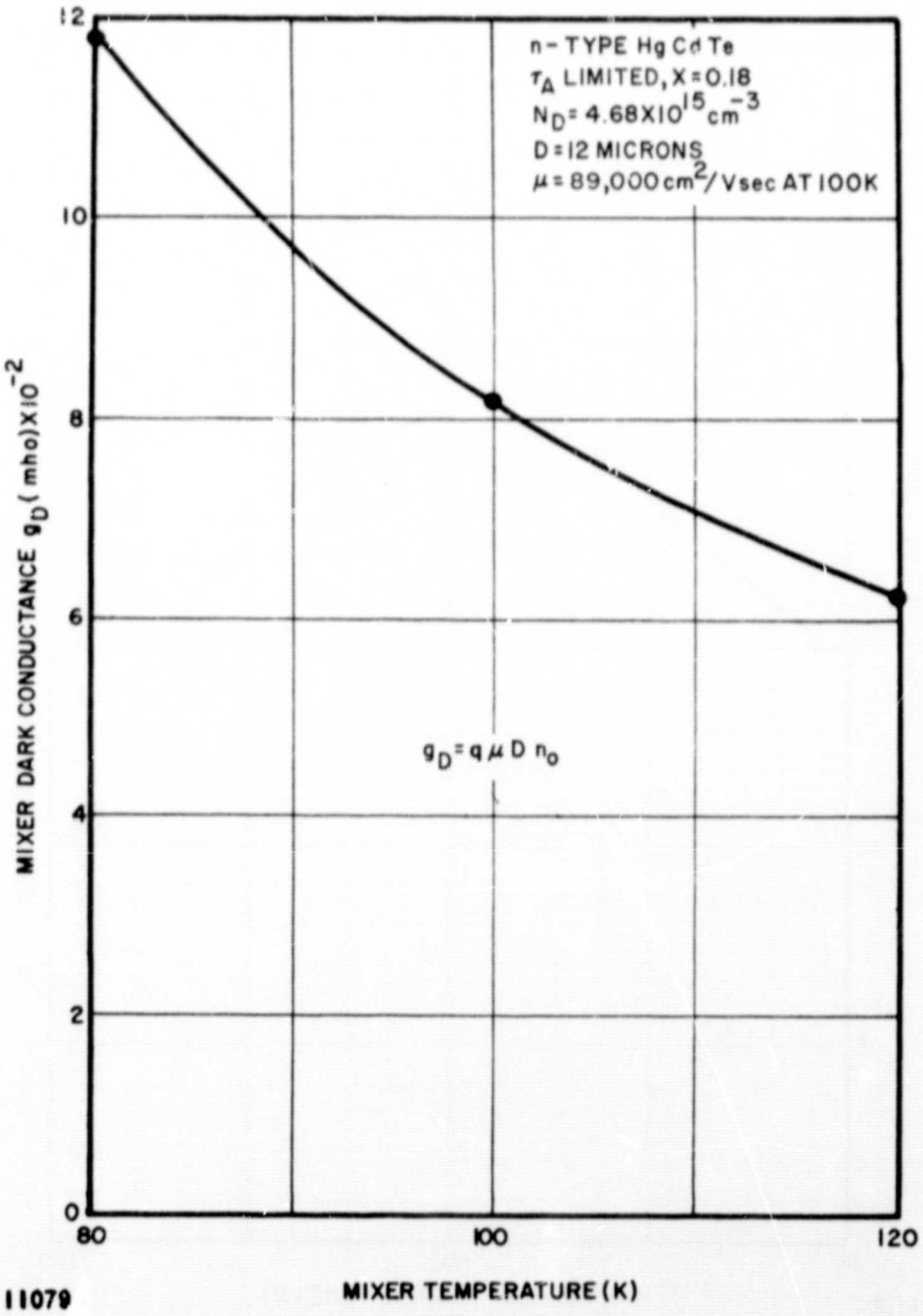

FIGURE 18. CALCULATED VARIATION OF MIXER DARK CONDUCTANCE WITH TEMPERATURE IN n-TYPE HgCdTe

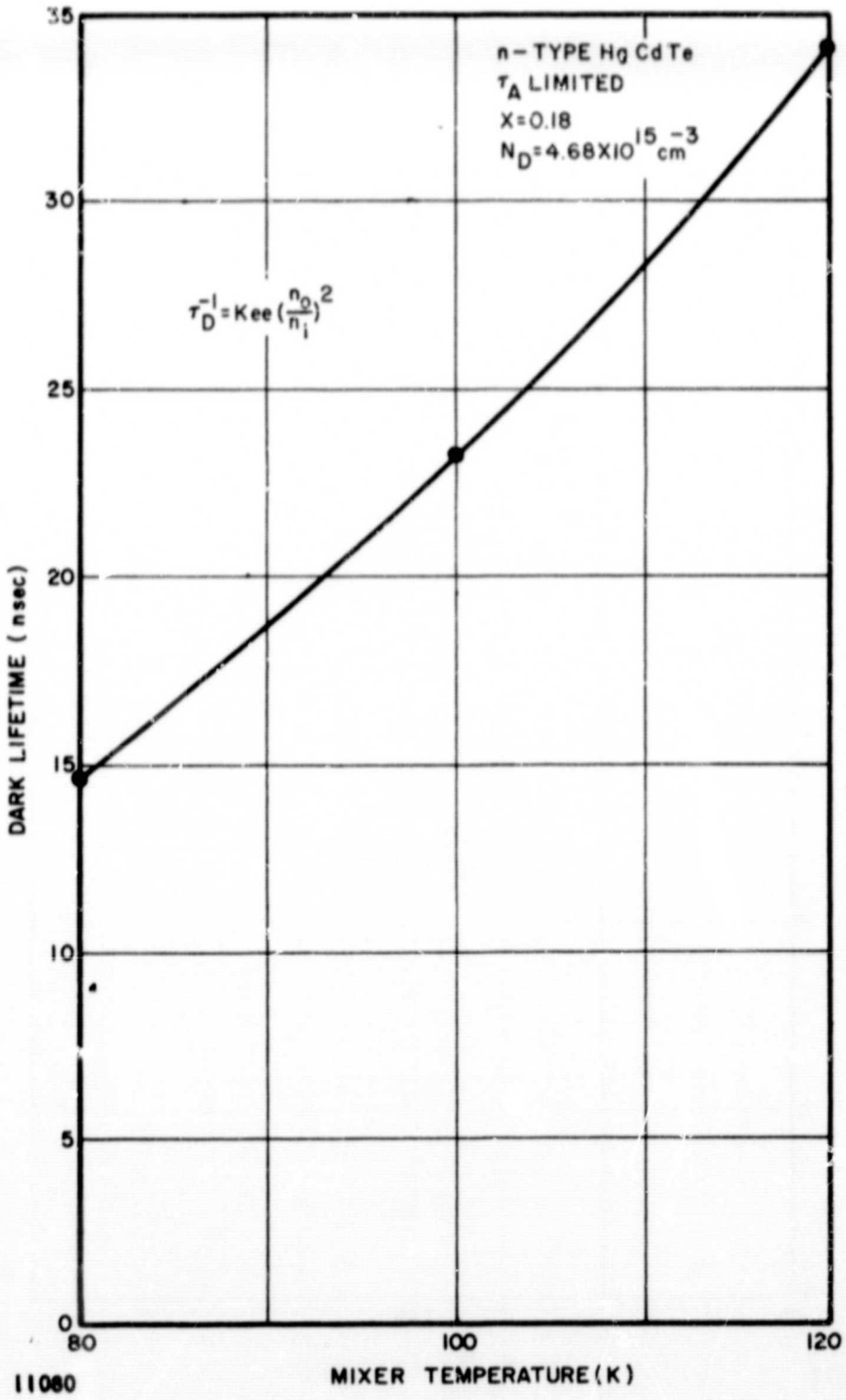

FIGURE 19. CALCULATED VARIATION OF DARK LIFETIME WITH MIXER TEMPERATURE IN n-TYPE HgCdTe

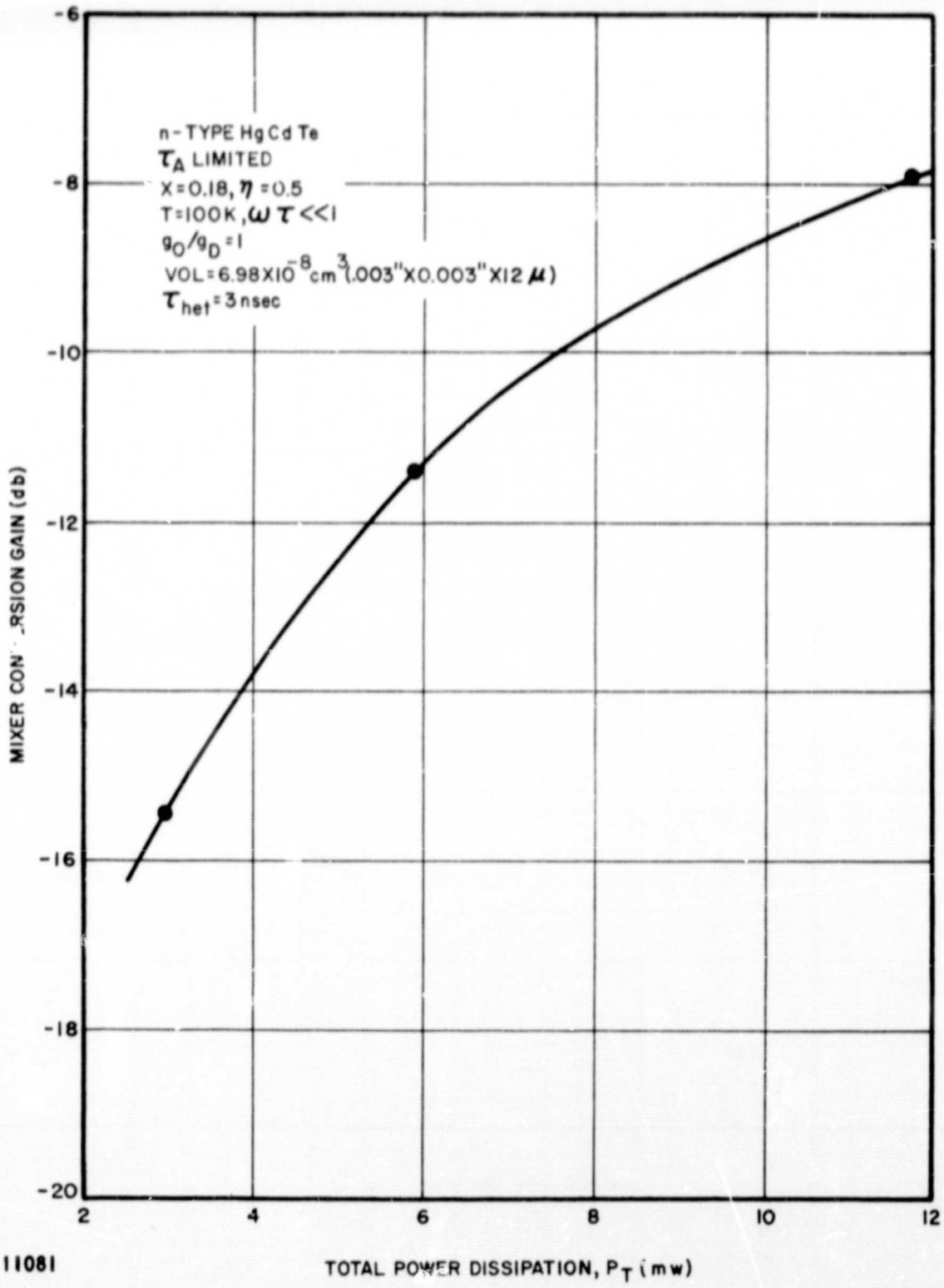

FIGURE 20. CALCULATED MIXER CONVERSION GAIN VS TOTAL POWER DISSIPATION IN n-TYPE HgCdTe MIXER

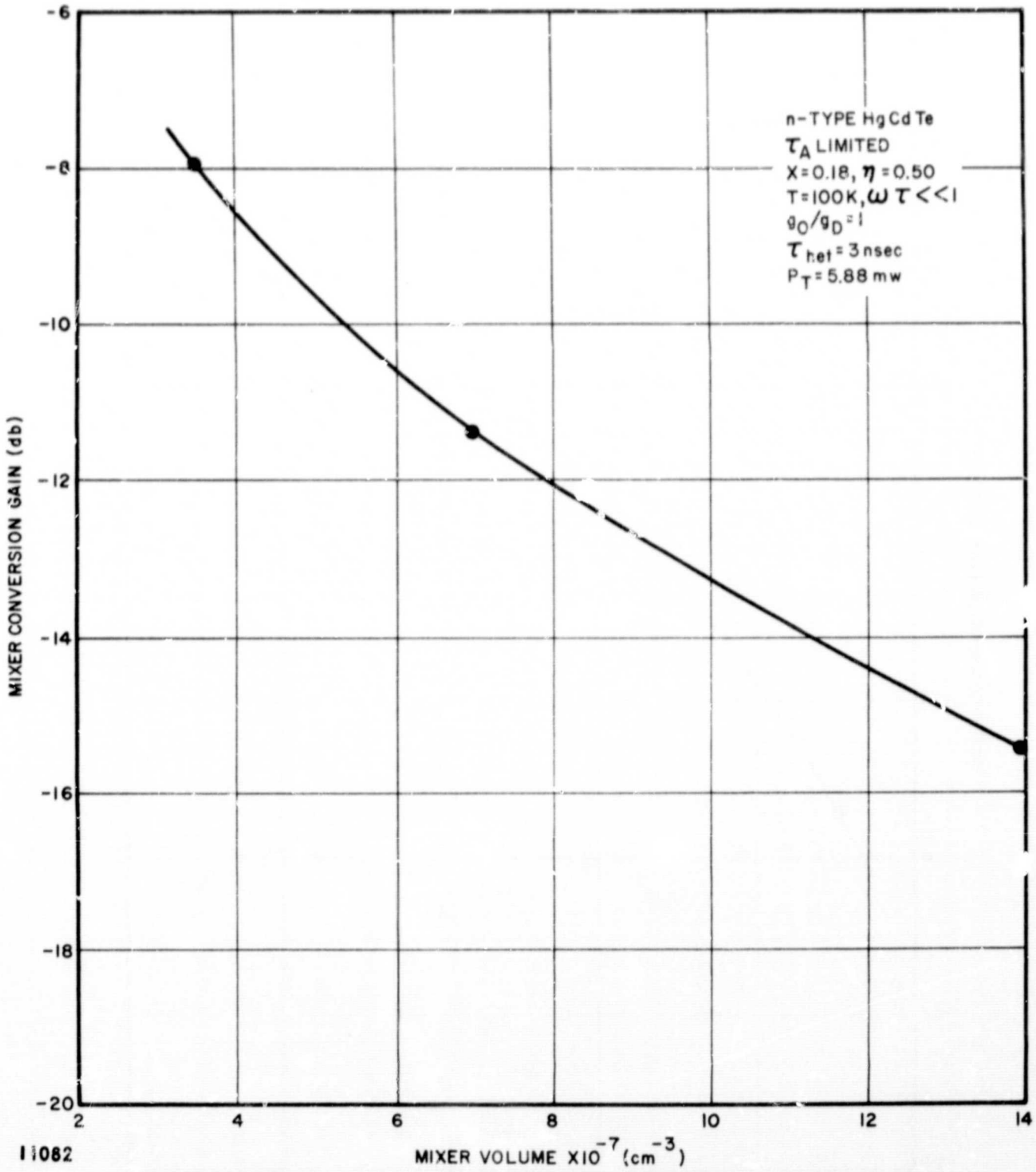

FIGURE 21. CALCULATED MIXER CONVERSION GAIN VS MIXER VOLUME IN n-TYPE HgCdTe MIXER

LO lifetime	τ_{LO}	5.9 nsec
LO-induced conductance	g_o	8.15×10^{-2} mhos
LO power applied	P_{LO}	2.14 mw
LO power absorbed	ηP_{LO}	1.07 mw
DC bias power	P_{DC}	7.54 mw
Total power absorbed	P_T	8.61 mw
Power ratio	$\frac{P_{DC}}{\eta P_{LO}}$	7.06
Mixer conductance	$g_T = g_o + g_D$	16.3×10^{-2} mhos
Mixer resistance	$R_T = g_T^{-1}$	6.14 ohms
DC bias voltage	V	0.215 volts
DC electric field	E	28.3 volts/cm
Conversion gain (low frequency)	G_o	-9.57 db
Conversion gain (20 MHz)	G	-10.1 db

Figures 22, 23, and 24 show the calculated variation of g_o/g_D, τ_{het} and mixer resistance, $R_T = \frac{1}{g_o + g_D}$ (equal to IF source resistance) as a function of mixer temperature for a constant applied LO power of 2.14 mw, and constant DC bias voltage of 0.215 volt.

As can be see in Figure 23, the heterodyne lifetime varies from 2.39 to 3.47 nsec, or by a factor of only 1.45 to 1 over the 80 to 120 K temperature range. This is an encouraging result.

The source impedance of the IF amplifier varies by a factor of about 1.6 to 1 over the 80 to 120 K range (Figure 24). This is sufficiently small so that no significant receiver sensitivity degradation caused by IF noise contribution should be encountered (Section II-E).

The power dissipation and conversion gain as a function of mixer temperature are shown in Figures 25 and 26 for P_{LO} fixed at 2.14 mw and DC bias voltage constant at 0.215 volt. As Figure 25 shows, the total power dissipated in the mixer element varied from 10.8 mw, at 80 K down to 7.4 mw at 120 K. From Figure 26, the low frequency conversion gain varies from -9.0 db at 80 K to -10.0 db at 120 K. This calculated conversion gain change of only 1 db is remarkably small.

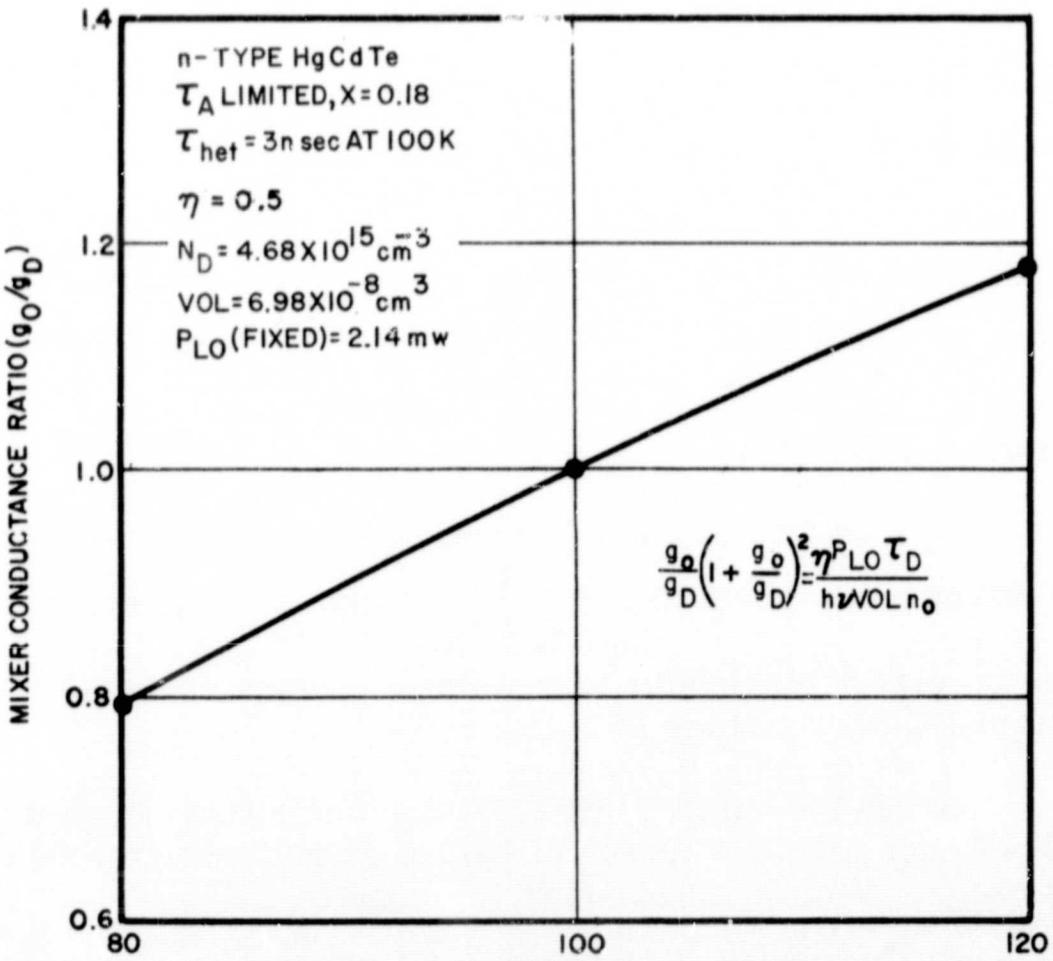

FIGURE 22. CALCULATED VARIATION OF MIXER CONDUCTANCE RATIO WITH MIXER TEMPERATURE FOR CONSTANT APPLIED LO POWER IN n-TYPE HgCdTe

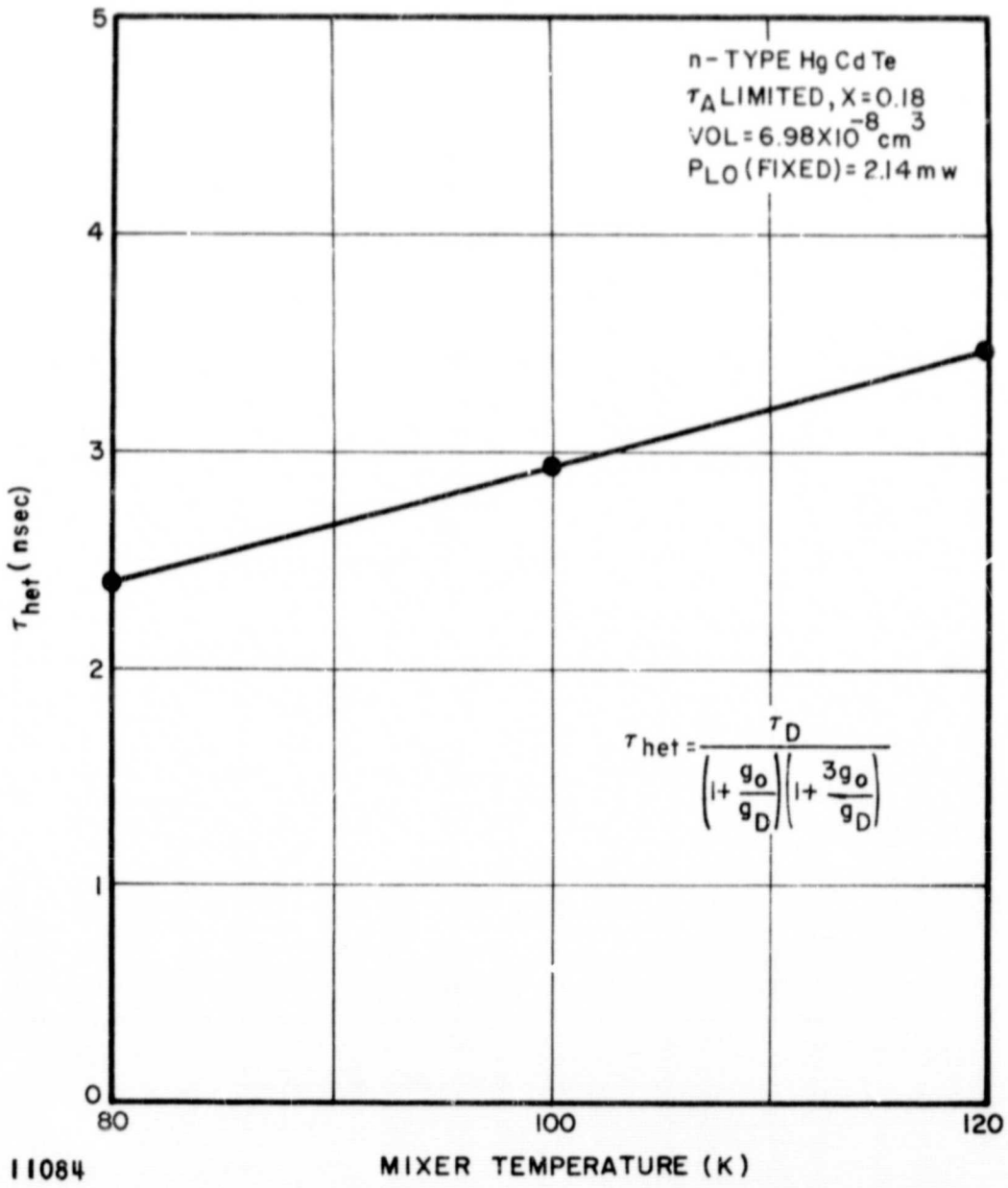

FIGURE 23. CALCULATED HETERODYNE LIFETIME VS MIXER TEMPERATURE IN n-TYPE HgCdTe FOR FIXED APPLIED LO POWER

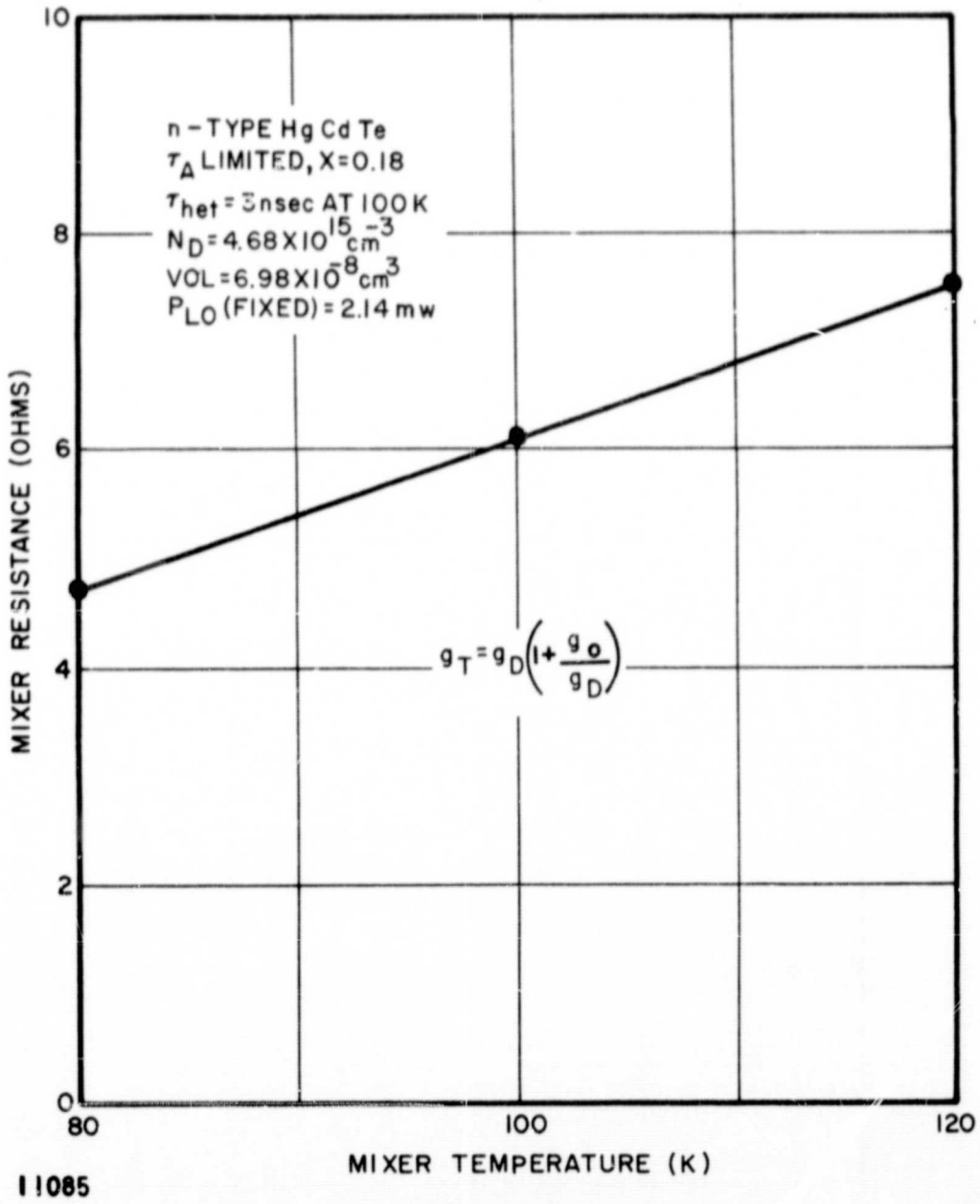

FIGURE 24. CALCULATED MIXER RESISTANCE VS MIXER TEMPERATURE IN n-TYPE HgCdTe FOR FIXED APPLIED LO POWER

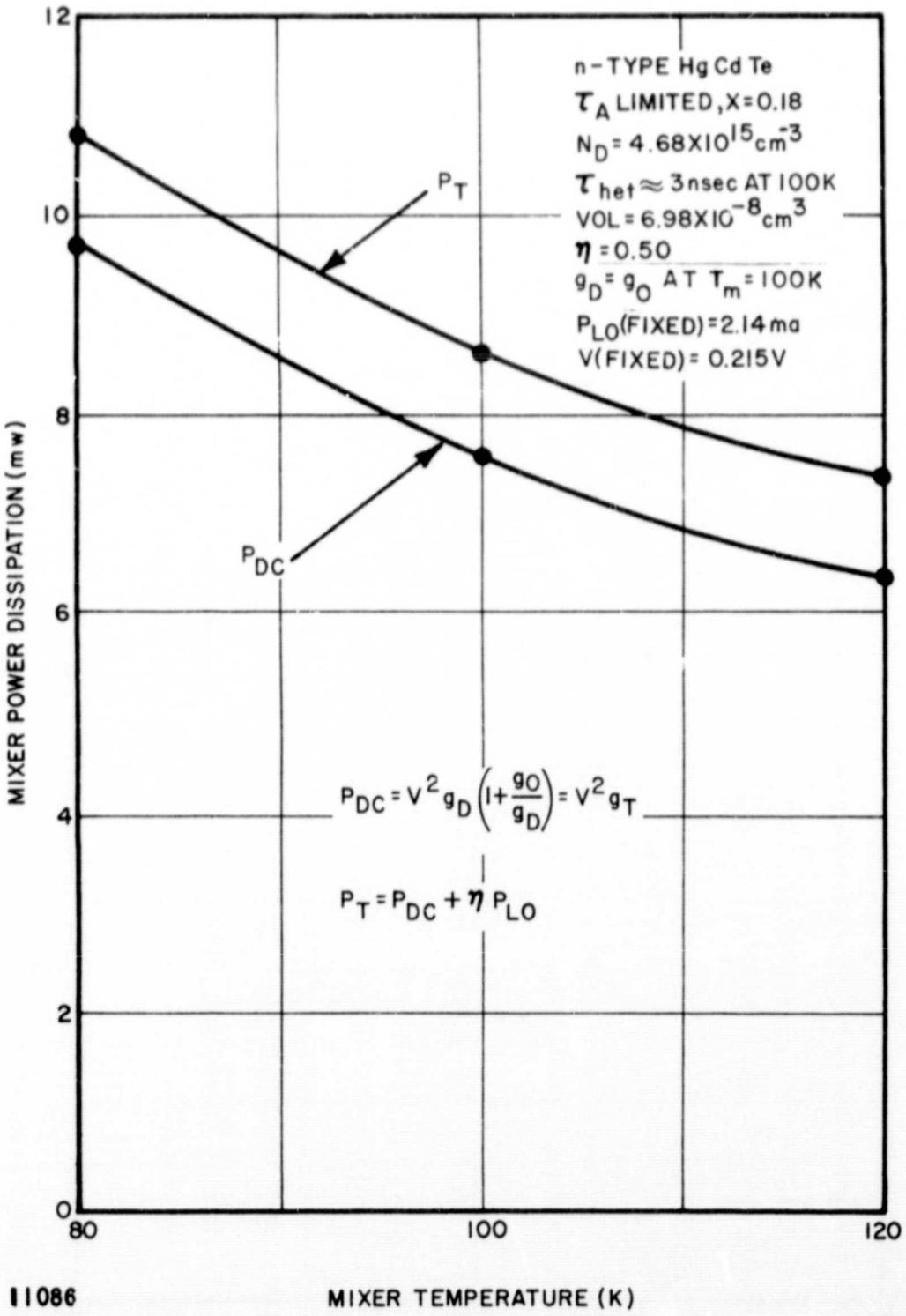

FIGURE 25. CALCULATED MIXER POWER DISSIPATION VS MIXER TEMPERATURE FOR CONSTANT APPLIED LO POWER AND DC BIAS VOLTAGE IN n-TYPE HgCdTe

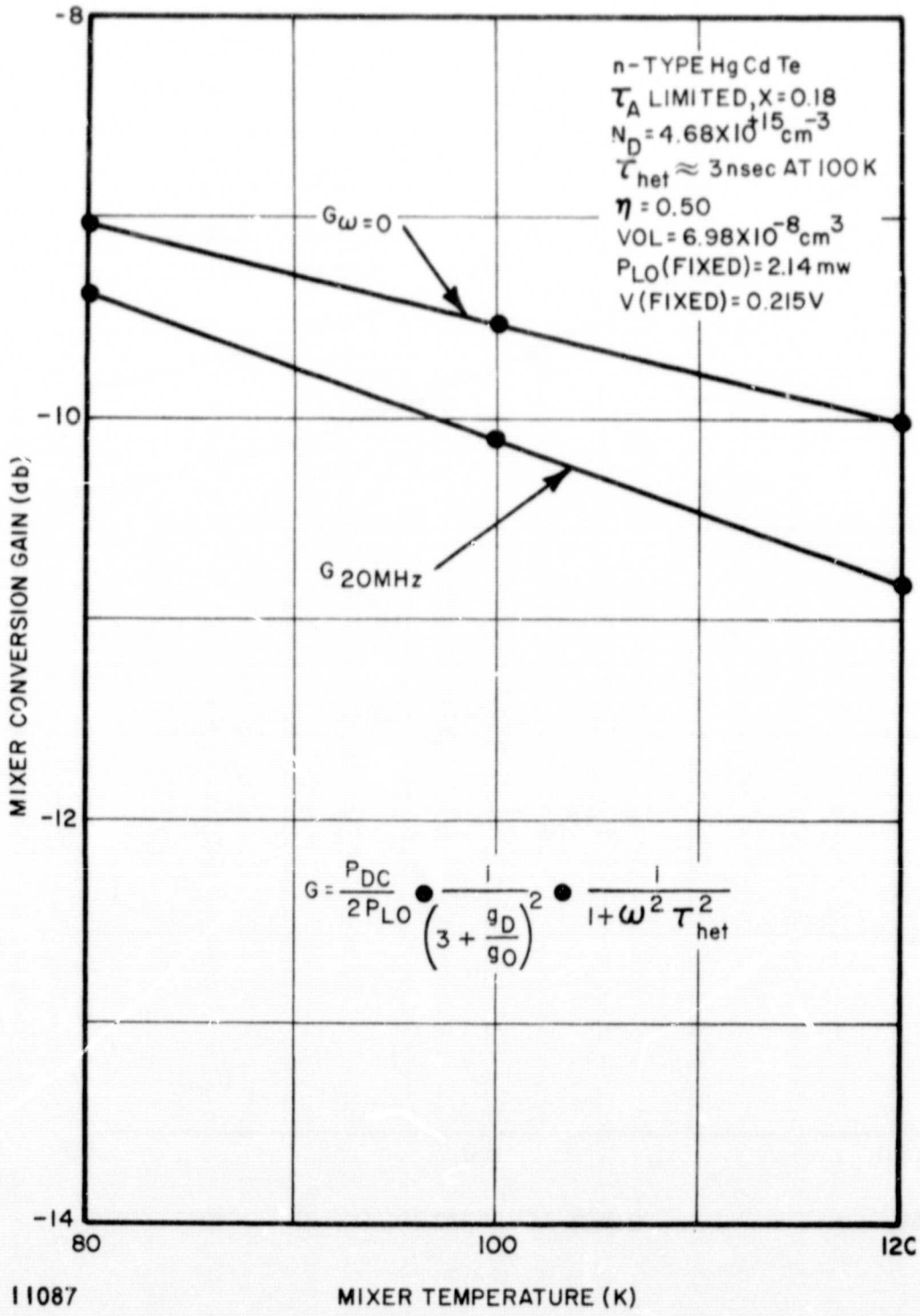

FIGURE 26. CALCULATED MIXER CONVERSION GAIN VS MIXER TEMPERATURE FOR CONSTANT APPLIED LO POWER AND DC BIAS VOLTAGE IN n-TYPE HgCdTe

The theory thus indicates that a large variation in receiver sensitivity would not be expected as the temperature varies over the 80 to 120 K temperature range. The calculated variation of mixer power dissipation has a negative rather than the desired positive slope with temperature. A positive slope is desirable to increase conversion gain at the higher temperatures, since the radiation cooler can handle larger thermal loads at the higher temperature. Since the mixer operates slightly into the roll-off region of the mixer response, the gain at an IF of 20 MHz is also shown in Figure 26. The conversion gain at an IF of 20 MHz varies from -9.4 db at 80 K to -10.8 db at 120 K, a 1.5 db variation.

A mixer conversion gain of -9.3 db is required to achieve a receiver NEP of 10^{-19} w/Hz at 100 K for $F_{IF} \approx 1.5$ db. Hence, additional bias power (or a smaller mixer element) must be used to obtain an NEP of 10^{19} w/Hz at all temperatures in the 80 to 120 K range. Since detector fabrication and quantum efficiency considerations (reference 6) make it difficult to reduce the mixer volume and the total dissipated power calculated at 80 K was 10.8 mw, possibly taxing the capacity of present-day radiation coolers, it may be difficult to simultaneously meet the sensitivity, frequency response, and power dissipative objectives of the proposal LCE using n-type photoconductive HgCdTe.

VII. RESULTS ON p-TYPE PHOTOCONDUCTIVE HgCdTe

This section presents:

- Preliminary analysis on p-type HgCdTe,
- Measurements on conductance variation with LO power,
- Measurements of frequency response of p-type PC-HgCdTe sample.

A. PHOTOCONDUCTANCE-TO-DARK CONDUCTANCE RATIO IN p-TYPE INTRINSIC PC-HgCdTe WITH AUGER RECOMBINATION

The conductance ratio of n-type intrinsic photoconductors with Auger recombination has been derived in Section IV-B. The corresponding derivation for p-type material is more complicated, since additional terms may be significant. The starting point is the dark conductivity

$$\sigma_D = n_o \mu_e q + p_o \mu_h q \tag{93}$$

where

σ_D = dark conductivity,
n_o = dark electron concentration,
μ_e = electron mobility,
q = electronic charge,
p_o = dark hole concentration ($>> n_o$),
μ_h = hole mobility ($<< \mu_e$).

Under photoexcitation, the conductivity becomes

$$\sigma = (n_o + n_e) \mu_e q + (p_o + n_e) \mu_h q \tag{94}$$

where n_e = excess hole-electron pair concentration due to photoexcitation.

The photoconductance-to-dark-conductance ratio is

$$\frac{g_o}{g_D} = \frac{\sigma - \sigma_D}{\sigma_D} = \frac{n_e(\mu_e + \mu_h)}{n_o\mu_e + p_o\mu_h} \tag{95}$$

$$\approx \frac{\frac{n_e}{p_o}}{\frac{1}{b} + \frac{n_o}{p_o}}$$

where $b \equiv \frac{\mu_e}{\mu_h} >> 1$

Next evaluate the ratio n_e/p_o in terms of material constants and LO power. As previously, the excess hole-electron pair concentration is related to the LO power by

$$n_e = \frac{\eta P_{LO} \tau_{LO}}{Vol\ h \nu_{LO}} \tag{96}$$

where

η = quantum efficiency,

P_{LO} = local oscillator incident power,

τ_{LO} = large signal lifetime of electron-hole pairs,

Vol = volume,

h = Planck's constant,

ν_{LO} = local oscillator frequency.

The lifetime τ_{LO} is in turn a function of the excess concentration n_e by the following reasoning. From Section IV-A, for Auger recombination, the net recombination rate for p-type material is

$$R(n_e) \approx \frac{n_e(n_e + p_o)\,(K_{ee}\, n_e + K_{ee}\, n_o + K_{hh}\, p_o)}{n_i^2} \tag{97}$$

where

K_{ee} = normalized electron-electron generation rate
K_{hh} = normalized hole-hole generation rate ($\ll K_{ee}$),
n_i = intrinsic carrier concentration.

The large signal, or local oscillator, lifetime is thus

$$\tau_{LO} = \frac{n_e}{R(n_e)} = \frac{n_i^2}{(n_e + p_o)\,(K_{ee}\, n_e + K_{ee}\, n_o + K_{hh}\, p_o)} \tag{98}$$

$$\approx \frac{n_i^2}{K_{ee}\, n_e\,(n_e + p_o) + p_o(K_{ee}\, n_o + K_{hh}\, p_o)}$$

The small signal, or heterodyne lifetime for p-type, Auger-lifetime-limited photoconductors is

$$\tau_{het} = \frac{1}{\frac{dR}{dn_e}} = \frac{n_i^2}{p_o\left(K_{ee}\, n_o + K_{hh}\, p_o\right) + 2\, K_{ee}\, p_o\, n_e + 3\, K_{ee}\, n_e^{\,2}} \tag{99}$$

$$\approx \frac{n_i^2}{K_{ee}\, n_e\,(3n_e + 2p_o) + p_o(K_{ee}\, n_o + K_{hh}\, p_o)}$$

The dark lifetime τ_D is given by the value of τ_{LO} or τ_{het} for $n_e = 0$ (equivalently, $P_{LO} = 0$), or

$$\tau_D = \frac{n_i^2}{p_o(K_{ee}\, n_o + K_{hh}\, p_o)} \tag{100}$$

From equations 98 and 100, the ratio of large signal and dark lifetimes is

$$\frac{\tau_{LO}}{\tau_D} = \frac{p_o(K_{ee}\, n_o + K_{hh}\, p_o)}{K_{ee}\, n_e(n_e + p_o) + p_o(K_{ee}\, n_o + K_{hh}\, p_o)} \tag{101}$$

$$= \frac{1}{1 + \dfrac{\dfrac{n_e}{p_o}\left(1 + \dfrac{n_e}{p_o}\right)}{\dfrac{K_{hh}}{K_{ee}} + \dfrac{n_o}{p_o}}}$$

In terms of the conductance ratio in equation 95, equation 100 becomes

$$\frac{\tau_{LO}}{\tau_D} = \frac{1}{1 + \dfrac{\dfrac{g_o}{g_D}\left[1 + \dfrac{g_o}{g_D}\left(\dfrac{1}{b} + \dfrac{n_o}{p_o}\right)\right]}{\left[\dfrac{\dfrac{K_{hh}}{K_{ee}} + \dfrac{n_o}{p_o}}{\dfrac{1}{b} + \dfrac{n_o}{p_o}}\right]}} \tag{102}$$

The ratio of heterodyne lifetime to dark lifeti:e s

$$\frac{\tau_{het}}{\tau_D} = \frac{1}{1 + \dfrac{2\,K_{ee}\,p_o\,n_e + 3\,K_{ee}\,n_e^2}{p_o(K_{ee}\,n_o + K_{hh}\,p_o)}} \tag{103}$$

$$= \frac{1}{1 + \dfrac{\dfrac{n_e}{p_o}\left(2 + 3\,\dfrac{n_e}{p_o}\right)}{\dfrac{n_o}{p_o} + \dfrac{K_{hh}}{K_{ee}}}}$$

Using equation 95, we obtain

$$\frac{\tau_{het}}{\tau_D} = \frac{1}{1 + \dfrac{g_o/g_D\left[2 + 3\left(1/b + n_o/p_o\right)\,g_o/g_D\right]}{\dfrac{K_{hh}/K_{ee} + n_o/p_o}{1/b + n_o/p_o}}} \tag{104}$$

The open-circuit responsivity $\mathcal{R}$, a useful measurable parameter, is related to the dark lifetime. $\mathcal{R}$ is defined as the open circuit voltage developed per unit of incident power at low power levels. In terms of the bias voltage V, it can be shown that the specific responsivity; that is, the responsivity per volt, is (Appendix I)

$$\frac{\mathcal{R}}{V} = \lim_{P_{LO} \to 0} \left\{ \frac{\left(\dfrac{g_o}{g_D}\right)}{P_{LO}} \right\} \tag{105}$$

Substitution of equations 95 and 96 into equation 105 (recognizing that $\tau_{LO} \longrightarrow \tau_D$ as $P_{LO} \longrightarrow 0$) then yields

$$\frac{\mathcal{R}}{V} = \frac{\eta \tau_D}{\text{Vol}\, h\, \nu_{LO}\, p_o \left(\frac{1}{b} + \frac{n_o}{p_o}\right)} \tag{106}$$

Finally, substitution of equations 95, 102 and 106 into equation 96 yields the desired relationship:

$$P_{LO}\left(\frac{\mathcal{R}}{V}\right) = \frac{g_o}{g_D} \left\{ 1 + \frac{\frac{g_o}{g_D}\left[1 + \frac{g_o}{g_D}\left(\frac{1}{b} + \frac{n_o}{p_o}\right)\right]}{\left[\frac{\frac{K_{hh}}{K_{ee}} + \frac{n_o}{p_o}}{\frac{1}{b} + \frac{n_o}{p_o}}\right]} \right\} \tag{107}$$

Examination of equation 107 shows that it is

$$a_1 \times P_{LO} = \frac{g_o}{g_D} + a_2 \left(\frac{g_o}{g_D}\right)^2 + a_3 \left(\frac{g_o}{g_D}\right)^3 \tag{108}$$

where $a_2 >> a_3$. Figure 27 shows a calculated curve, describing the general behavior based on equation 107, the photoconductance-to-dark conductance ratio as a function of local oscillator power on a log-log plot.

As Figure 27 shows, the conductance varies directly as P_{LO} for low LO power, changing first to a $P_{LO}^{1/2}$ dependence and then to a $P_{LO}^{1/3}$ dependence with increasing LO power. Initial measurements on the conductance variation on a p-type sample are reported in the next section.

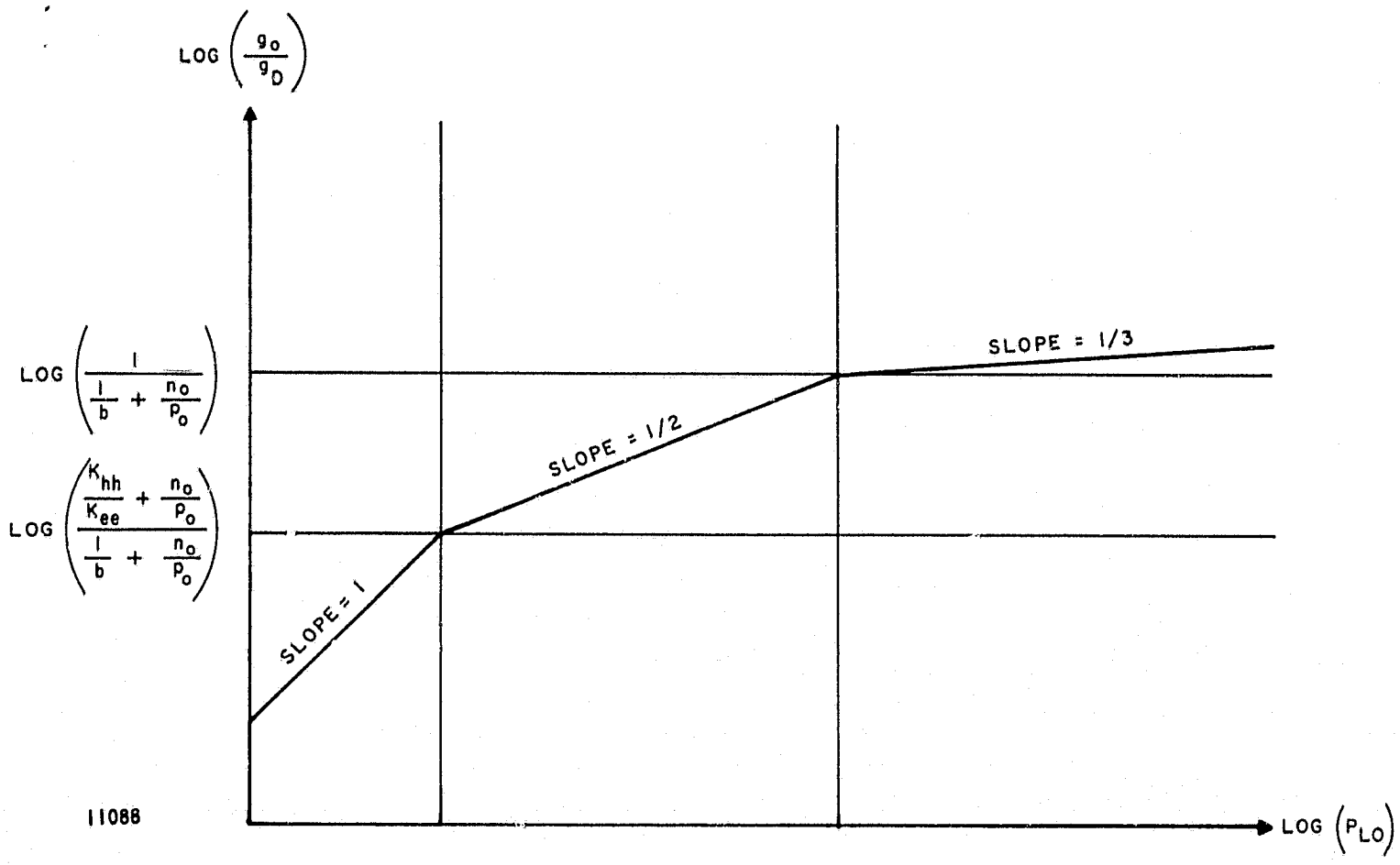

FIGURE 27. THEORETICAL CONDUCTANCE RATIO VS LO POWER FOR p-TYPE HgCdTe (AUGER RECOMBINATION)

B. MEASUREMENTS OF CONDUCTANCE VARIATION

Figure 28 shows the change in the current-voltage characteristic of a p-type PC-HgCdTe sample having a nanosecond time constant at 77 K, as the applied LO power is varied from 0 to 90 mw. The detector area was 0.016 × 0.016 inch and the dark resistance was 25 ohms. As Figure 28 shows, the mixer resistance has decreased to approximately 10.5 ohms for 90 mw of applied LO power.

The results of a more detailed measurement of conductance ratio g_o/g_D as a function of LO power are shown in Figure 29. A calculated curve for the conductance variation of Auger-lifetime-limited p-type PC-HgCdTe based on the analysis of Section VII-A, has been fitted to the experimental results in Figure 29. The measured and theoretical curves are seen to be in agreement.

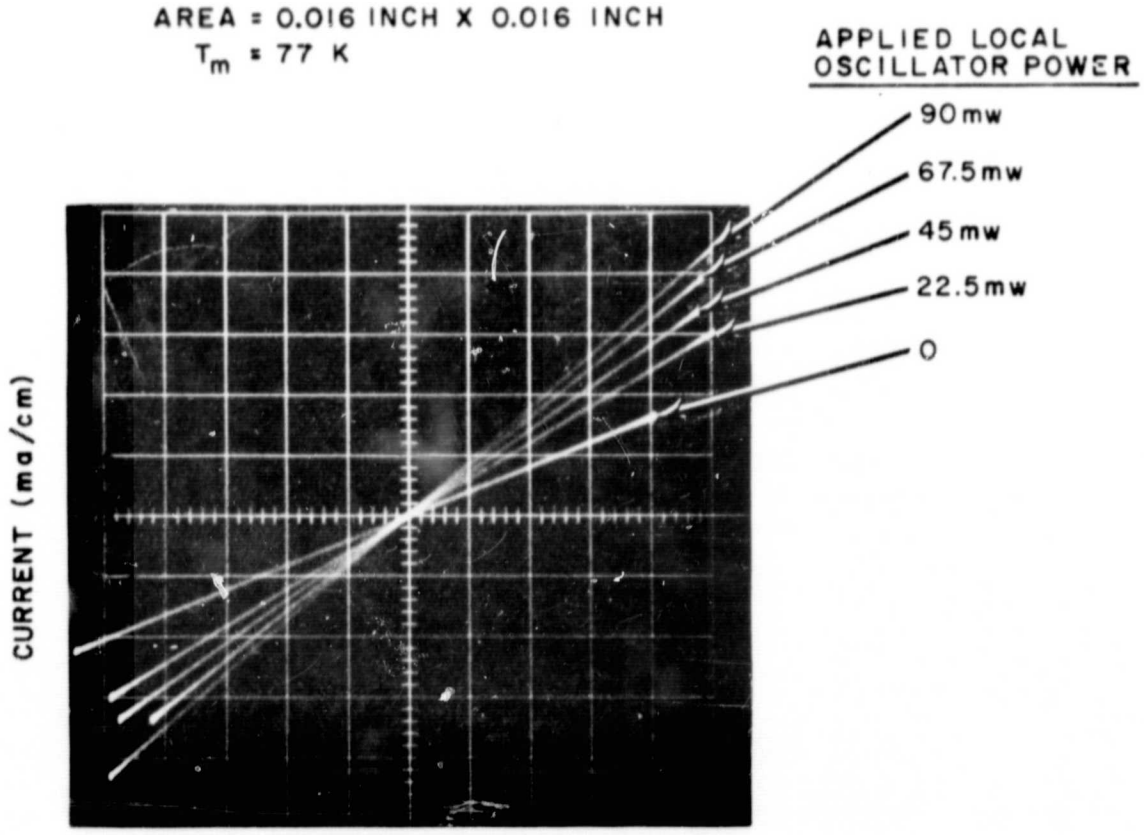

FIGURE 28. I-V CHARACTERISTICS OF p-TYPE HgCdTe MIXER ELEMENT FOR SEVERAL VALUES OF LO POWER

The ability to depress the detector resistance as required for mixer operation in this relatively fast element was extremely encouraging. The higher operating resistance of p-type samples compared to fast n-type samples assists in matching into the low-noise IF amplifier.

C. FREQUENCY RESPONSE MEASUREMENTS

1. RESULTS

Preliminary measurements were carried out on the frequency response of a p-type PC-HgCdTe element using an indirect sensitivity measurement method which compares the thermal noise to the receiver (GR plus thermal) noise.

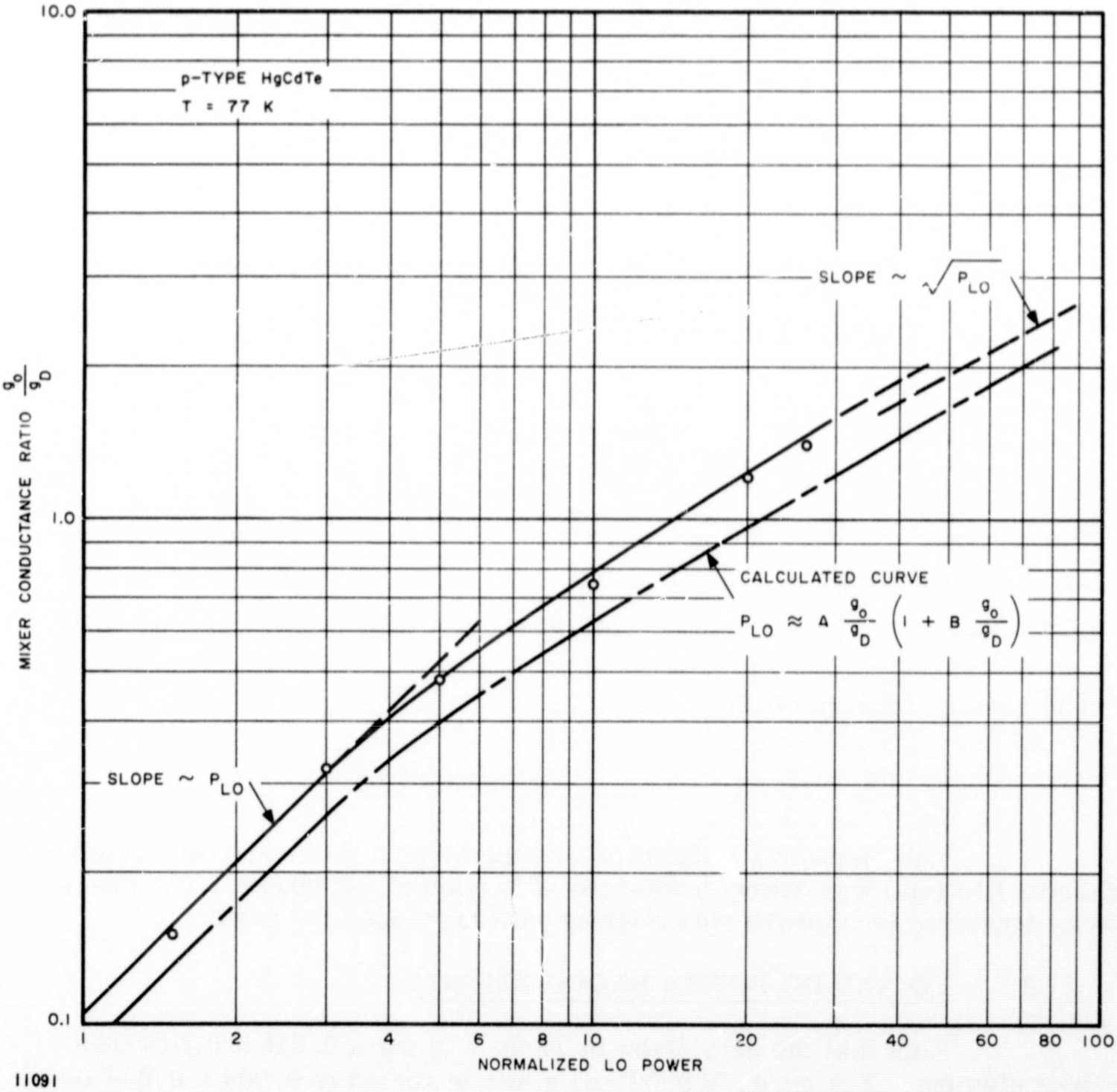

FIGURE 29. MEASURED AND CALCULATED VARIATION OF CONDUCTANCE RATIO WITH LO POWER IN p-TYPE HgCdTe

Figure 30 shows the measured data on relative mixer sensitivity, referred to P_{min}, as a function of IF frequency at 77 K.

The measurements were made using two values of conductance ratio $g_o/g_D = 1.1$ and $g_o/g_D = 0.38$, in an attempt to determine the variation of mixer lifetime and sensitivity with LO power.

The results of the sensitivity measurements are tabulated in Table 2.

TABLE 2. VARIATION OF p-TYPE HgCdTe MIXER PARAMETERS WITH APPLIED LO POWER (MIXER AREA ≈0.016" × 0.016") AT T_m = 77 K

g_o/g_D	Applied P_{LO} (mw)	P_{DC} (mw)	Total Power $P_T = P_{DC} + \eta P_{LO}$* (mw)	$f_{3\,db}$ (MHz)	τ_{LO} (nsec) (calc)	NEP/P_{min} ($\omega\tau < 1$)
1.1	76.5	21	60	40	4	2.05
0.38	20.2	17.35	27.5	41	3.9	2.65

* It is assumed that $\eta = 0.50$.

The measured 3-db cutoff frequency (and therefore the calculated carrier lifetime) was nearly unchanged with applied LO power. The sensitivity appeared to improve only slightly with increased LO power.

2. LO AND DC POWER REQUIREMENTS

Note that the data given in Table 2 is for a 0.016 × 0.016 inch mixer element. For $g_o/g_D = 0.38$ and a mixer scaled to 0.004 × 0.004 inch, the power requirements are only $P_{DC} \approx 1.1$ mw and $P_{LO} \approx 1.3$ mw.

In addition, the mixer gain can be increased by increasing the DC bias power.

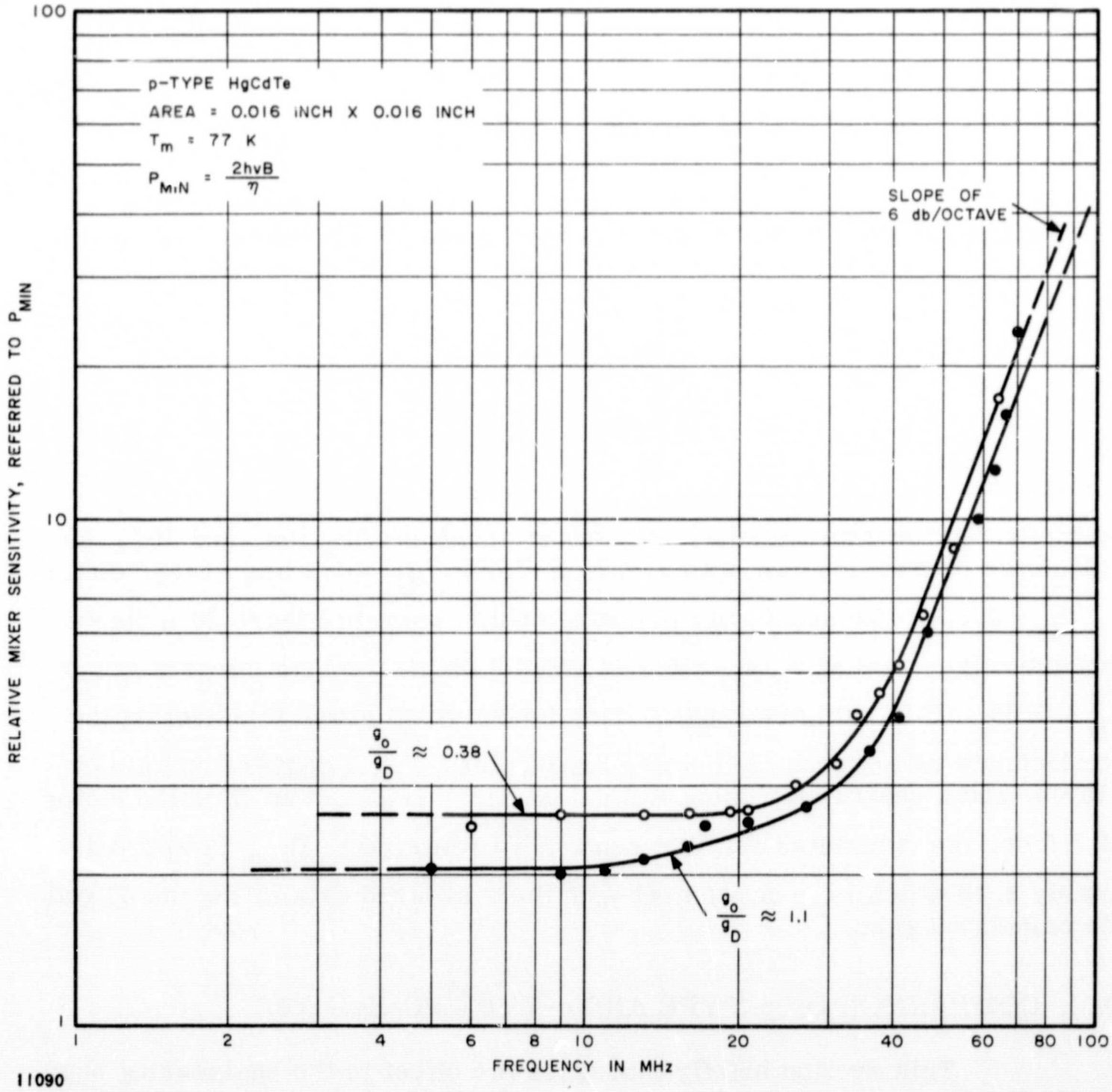

FIGURE 30. RELATIVE MIXER SENSITIVITY VS IF FREQUENCY FOR TWO VALUES OF LO POWER IN p-TYPE HgCdTe

3. COMPARISON TO ANALYSIS

The available conversion gain is

$$G = \frac{P_{DC}}{P_{LO}} \frac{1}{\left(1 + g_D/g_o\right)^2} \left(\frac{\tau_{het}}{\tau_{LO}}\right)^2 \frac{1}{1 + \omega^2 \tau_{het}^2} \qquad (109)$$

as developed in Section V. From Figures 27 and 28 a breakpoint of

$$\frac{\frac{K_{hh}}{K_{ee}} + \frac{n_o}{p_o}}{1/b + n_o/p_o} \approx 0.73$$

was selected for gain calculations. Using equations 93, 104, and 109, the calculated conversion gain was -15.72 db for $g_o/g_D = 1.1$ and -14.28 db for $g_o/g_D = 0.38$. The sensitivity measurements shown in Figure 30 indicate that the mixer gain at $g_o/g_D = 1.1$ is about 2 db higher than the gain at $g_o/g_D = 0.38$. This gain discrepancy may be due to an error in selecting the conductance ratio versus LO power breakpoint. For a conversion gain of -15 db, and a quantum efficiency of 0.5 at $T_m = 77$ K and an IF noise factor of 1.5 db, the calculated relative sensitivity referred to P_{min} is approximately 2.19 which is in agreement with the measured data in Figure 30 and the calculated gain.

D. COMPARISON OF p-TYPE AND n-TYPE PC-HgCdTe

This section briefly discusses the effect in the engineering equations when a p-type material is considered instead of an n-type PC-HgCdTe mixer element. We assume a small-modulation case and $\tau_{het} \approx \tau_{LO}$. This p-type detector has a carrier mobility approximately 100 times lower than that for the n-type material. Both materials are assumed to have the same lifetime and geometry.

Based on the engineering equations in Section III and other considerations, we obtain:

- The p-type sample's resistance is about 100 times higher than the n-type samples. Therefore, it will be easier to match into the IF amplifier for the highly-doped nanosecond elements being considered.
- The reduced mobility of the p-type sample requires that a 10 times higher bias voltage be used to obtain the same conversion gain.
- The dissipated DC bias and LO powers are then about the same as for the n-type element.

E. SUMMARY

Preliminary measurements on p-type HgCdTe mixers indicate that it may be possible to achieve in combination:

- Lifetime in the nanoseconds (frequency response to beyond 20 MHz),
- Reasonably good receiver sensitivity,
- Moderate total power dissipation.

Presently, the absolute mixer sensitivity at 10 kHz, the quantum efficiency, and the variation of mixer element parameters with temperature have not been measured. Photovoltaic effects have been observed at the contacts of a poorer p-type HgCdTe sample. These results must be considered preliminary until more extensive data has been measured and the detector uniformity and other parameters have been investigated.

VIII. ANALYSIS OF PHOTOVOLTAIC MIXING IN HgCdTe

An analysis on heterodyne operation of PV-HgCdTe is presented with expressions for noise equivalent power, conversion gain, cutoff frequency, etc. An initial analysis on photovoltaic (PV) mixing was conducted on a previous program at AIL sponsored by the Office of Naval Research. A mixer analysis in this report examines the feasibility of using photovoltaic HgCdTe mixer elements in the LCE.

A. AVAILABLE IF SIGNAL POWER

The equivalent circuit at IF frequencies for a reverse biased PV infrared mixer is shown in Figure 31A. The mixer analysis assumes a non-zero leakage conductance and neglects any lead inductance which may be present. This is representative of present-day HgCdTe photovoltaic elements. The square of the peak IF signal current is [reference 8 (equations 15 and 17) and equations 62 to 64 of this report].

$$I_S^2 = 4\left(\frac{\eta q}{h\nu}\right)^2 P_{sig}\, P_{LO} \tag{110}$$

where

I_S = peak IF signal current,

ν = signal frequency,

η = quantum efficiency,

P_{sig} = signal power,

P_{LO} = LO power $>>$ P_{sig}.

From Figure 31A, the ratio of the short-circuit current to the signal current is

$$\frac{I_{SC}}{I_S} = \frac{1}{(1 + G_D R_S) + j\,\omega\, C_D R_S} \tag{111}$$

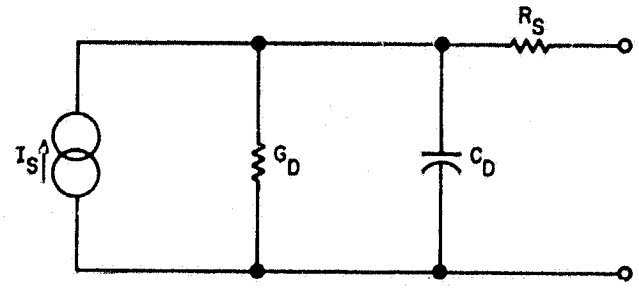

A. BASIC CIRCUIT

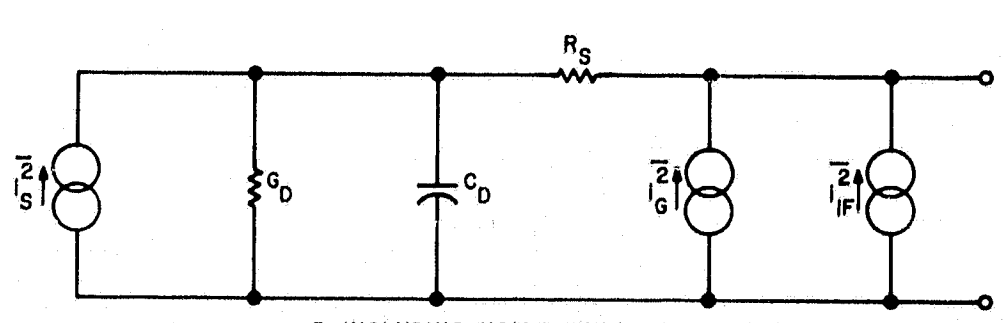

B. INCLUDING NOISE GENERATORS

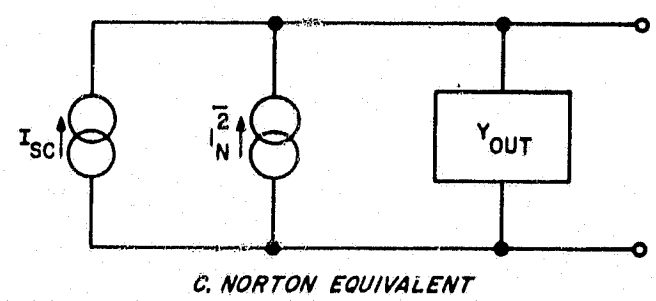

C. NORTON EQUIVALENT

A1103

FIGURE 31. EQUIVALENT CIRCUIT FOR INFRARED PHOTOVOLTAIC MIXER

where

I_{SC} = short-circuit current,

G_D = small-signal shunt conductance (slope of I-V curve in reverse direction),

R_S = series resistance,

C_D = junction capacitance.

The mixer output admittance can be expressed as

$$Y_{out} = \frac{G_D + R_S\left(G_D^2 + \omega^2 C_D^2\right) + j\,\omega\, C_D}{\left(1 + G_D R_S\right)^2 + \omega^2 \quad C_D^2 R_S^2} \tag{112}$$

The real component of the output admittance is

$$G'_{out} = \frac{G_D + R_S\left(G_D^2 + \omega^2 C_D^2\right)}{\left(1 + G_D R_S\right)^2 + \left(\omega C_D R_S\right)^2} \tag{113}$$

The short-circuit current is

$$\left|I_{SC}\right|^2 = \frac{\left|I_S\right|^2}{\left(1 + G_D R_S\right)^2 + \left(\omega C_D R_S\right)^2} \tag{114}$$

and the available output power from the photovoltaic mixer is

$$\left(P_{IF}\right)_{available} = \frac{\left|I_{SC}\right|^2}{8\, G'_{out}} = \frac{\left|I_S\right|^2}{8\left[G_D\left(1 + G_D R_S\right) + \omega^2 R_S C_D^2\right]} \tag{115}$$

The output power is 3 db down at an IF frequency given by

$$f_c = \frac{\left(1 + R_S G_D\right)^{1/2}}{2\pi C_D \left(R_S/G_D\right)^{1/2}} \approx \frac{1}{2\pi C_D \left(R_S/G_D\right)^{1/2}}, \; R_S G_D \ll 1 \qquad (116)$$

B. NOISE

The equivalent noise circuit for the photovoltaic mixing case including noise generators is shown in Figures 31B and C. The overall mean-square noise current generator is

$$\overline{i_N^2} = \overline{i_G^2} + \overline{i_{IF}^2} + \frac{\overline{i_S^2}}{\left(1 + G_D R_S\right)^2 + \left(f/f_c\right)^2} \qquad (117)$$

where

$\overline{i_G^2}$ = thermal noise = $4kT_m B\, G'_{out}$,

$\overline{i_{IF}^2}$ = IF amplifier noise = $4kT'_{IF} B\, G'_{out}$,

$\overline{i_S^2}$ = shot noise $\approx 2q\, I_o B$ for condition $f_{IF} < \frac{1}{8T_r}$,

k = Boltzmann's constant,

T_m = physical temperature of mixer,

B = IF bandwidth,

T'_{IF} = effective input noise temperature of IF amplifier which is a function of its source impedance,

I_o = DC photocurrent induced by LO,

T_r = carrier transit time.

C. MIXER GAIN

The available photovoltaic mixer gain, that is, the ratio of the available IF output power to the available infrared signal power, is

$$G = \frac{P_{IF(available)}}{P_{sig}} = \frac{\left|I_S\right|^2}{8\, P_{sig}\left[G_D\left(1 + G_D\, R_S\right) + \omega^2\, R_S\, C_D^2\right]} \qquad (118)$$

which from equation 110 and 118 can be written

$$G = \frac{\left(\frac{\eta q}{h\nu}\right)^2 P_{LO}}{2\left[G_D\left(1 + G_D\, R_S\right) + \omega^2\, R_S\, C_D^2\right]} \qquad (119)$$

for a photovoltaic mixer, $\tau/T_r = 1$. Therefore (reference 1), under the condition that, $P_{LO} >> P_{sig}$, the DC photocurrent due to absorbed LO power is

$$I_o = \frac{\eta q}{h\nu}\left(\frac{\tau}{T_r}\right) P_{LO} = \frac{\eta q}{h\nu}\, P_{LO} \qquad (120)$$

Combining these equations,

$$G = \eta \frac{qI_o}{2h\nu} \frac{1}{G_D\left(1 + R_S\, G_D\right) + \omega^2\, R_S\, C_D^2} \qquad (121)$$

and for $R_S\, G_D << 1$

$$G = \frac{\eta\, q\, I_o}{2\, h\, \nu\, G_D\left[1 + \left(f/f_c\right)^2\right]} \qquad (122)$$

It can be seen, from this expression that the available conversion gain is 3 db down at the IF frequency (f_c) previously defined (equation 116).

Note that the conversion gain varies with LO power through its effect on the photocurrent I_o and is relatively independent of the applied bias voltage except for changes in shunt conductance or junction capacitance with bias voltage.

D. SIGNAL-TO-NOISE RATIO

The signal-to-noise ratio for the photovoltaic mixer is

$$\frac{S}{N} = \frac{\left|I_{SC}\right|^2}{2\,\overline{i_N^2}} \tag{123}$$

Substituting expressions for the noise current and the short-circuit current gives

$$\frac{S}{N} = \frac{\left|I_S\right|^2}{8k\left(T_m + T'_{IF}\right) B\left[G_D + R_S\left(G_D^2 + \omega^2 C_D^2\right)\right] + 4qI_oB} \tag{124}$$

$$= \frac{\left(\frac{\eta q}{h\nu}\right) P_{sig}\, I_o}{I_o qB + 2k\left(T_m + T'_{IF}\right) B\left[G_D\left(1 + R_S G_D\right) + \omega^2 R_S C_D^2\right]} \tag{125}$$

Thus, the NEP, that is, the value of signal power to give an IF signal-to-noise ratio equal to unity, is

$$NEP = \frac{h\nu B}{\eta}\left\{1 + \frac{2k\left(T_m + T'_{IF}\right)}{qI_o}\left[G_D\left(1 + R_S G_D\right) + \omega^2 R_S C_D^2\right]\right\} \tag{126}$$

This is reducible to

$$NEP = \frac{h\nu B}{\eta} + \frac{k\left(T_m + T'_{IF}\right) B}{G} \tag{127}$$

which is the same expression as that derived for the photoconductive mixing case, with the exception of the factor of two in the quantum noise term due to the generation-recombination noise in photoconductors.

E. LOCAL OSCILLATOR POWER REQUIRED TO ACHIEVE QUANTUM-NOISE-LIMITED OPERATION

When the photovoltaic mixer is operated in the flat portion of its frequency response, that is $f_{IF} < f_c$, the NEP is

$$NEP = \frac{h\nu B}{\eta}\left\{1 + \frac{2k\left(T_m + T'_{IF}\right) G_D}{qI_o}\right\} \tag{128}$$

Quantum-noise-limited operation is obtained for sufficient absorbed LO power so that

$$I_o >> \frac{2k\left(T_m + T'_{IF}\right) G_D}{q} \tag{129}$$

Using the above expression, a photoexcited current of 150 micro-amperes is calculated to obtain an NEP of $2h\nu B/\eta$ for the following values:

$$k = 1.38 \times 10^{-23} \text{ joules/K}$$

$$T_m = 80 \text{ K}$$

$$F_{IF} = 1.7 \text{ db } (T_{IF} = 139 \text{ K})$$

$$G_D^{-1} = 250 \text{ ohms}$$

$$q = 1.6 \times 10^{-19} \text{ coulombs}$$

For an assumed photovoltaic mixer quantum efficiency of 0.30, the best achievable receiver sensitivity under the condition of equation 129 is

$$P_{MIN} = \frac{h\nu B}{\eta} = 6.2 \times 10^{-20} \text{ Watt/Hz} \qquad (130)$$

Consider the case where a 25-percent degradation due to thermal noise contributions (equation 127) can be tolerated. Then the overall receiver sensitivity will be 7.8×10^{-20} watt/Hz. The required photoexcited current is 0.6 milliampere. This current corresponds to a calculated absorbed LO power (ηP_{LO}) of 0.108 milliwatt and applied LO power (P_{LO}) of only 0.36 milliwatt. These are very favorable values.

IX. EXPERIMENTAL RESULTS ON MIXING IN PHOTOVOLTAIC-HgCdTe

A. CURRENT-VOLTAGE CHARACTERISTIC

This section presents detailed measurements on mixing in photovoltaic HgCdTe with results on NEP, frequency response, power dissipation, conversion gain, and quantum efficiency. The photovoltaic HgCdTe mixer element tested had a spectral peak near 12.5 microns at 77 K (Figure 32). The measured I-V characteristic, with and without LO power applied to the junction, is shown in Figure 33. The forward I-V characteristic shows no change in impedance with absorbed LO power. The reverse I-V characteristic shows the expected increase in current with LO power. The induced photocurrent in the reverse direction increased linearly with increasing LO power over the 0 to 3.0 mw range measured.

The parameters of the photovoltaic mixer at 77 K were as follows:

Area	$A = 0.09\ mm^2$
Peak Wavelength	$\lambda p = 12.7$ microns
Series Resistance	$R_S = 8.2$ ohms
Slope Shunt Resistance	$G_D^{-1} \approx 190$ ohms at V = 0.3 volts
Responsivity	$\mathcal{R} = 39$ volts/watt at zero bias
Quantum Efficiency	$\eta = 0.09$ at 10.6 microns

B. NOISE MEASUREMENTS

For quantum-noise-limited operation in photovoltaic mixers, the mean-square shot-noise current induced by the absorption of LO power must dominate the sum of all other mean-square noise currents in the mixer (equation 117). (The induced shot noise power varies linearly with LO power as shown in Figure 34 and therefore the required LO power is determined by the system noise in the absence of laser LO.)

1. INDUCED SHOT NOISE

The induced shot noise was found to vary essentially linearly with LO power, as shown in Figure 34. Although this is theoretically to be expected from equation 120, the linearity will only occur for the case where G_D

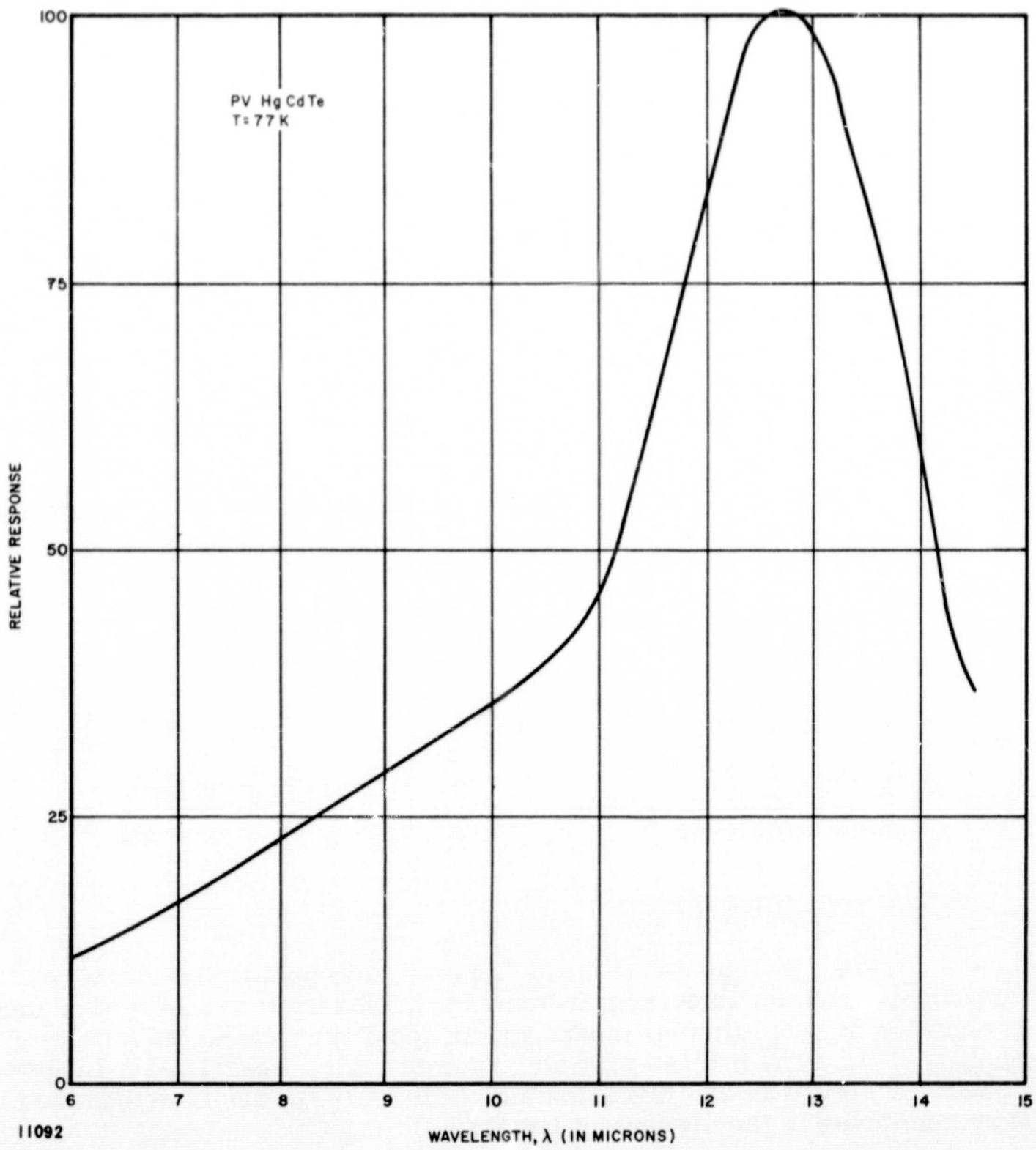

FIGURE 32. SPECTRAL RESPONSE OF PV HgCdTe MIXER

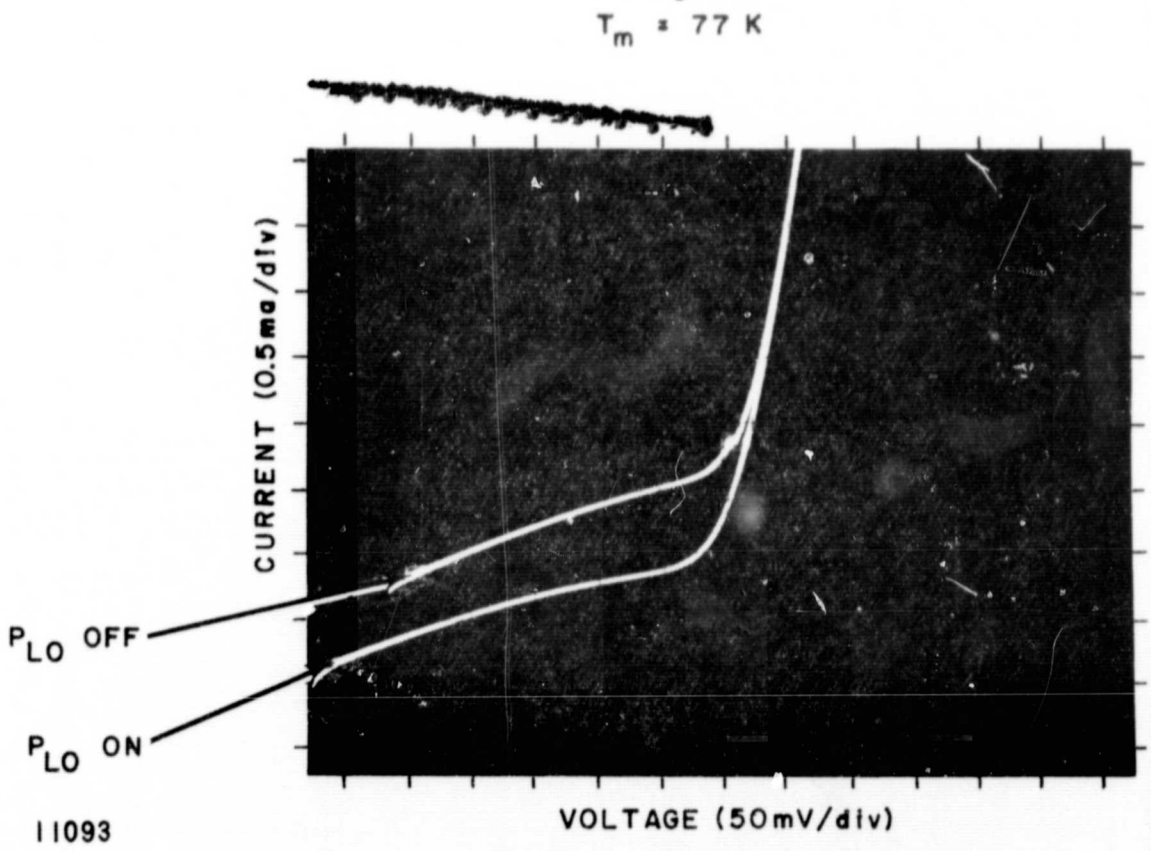

FIGURE 33. CURRENT-VOLTAGE CHARACTERISTIC OF PHOTOVOLTAIC HgCdTe MIXER WITH LO POWER AS A PARAMETER

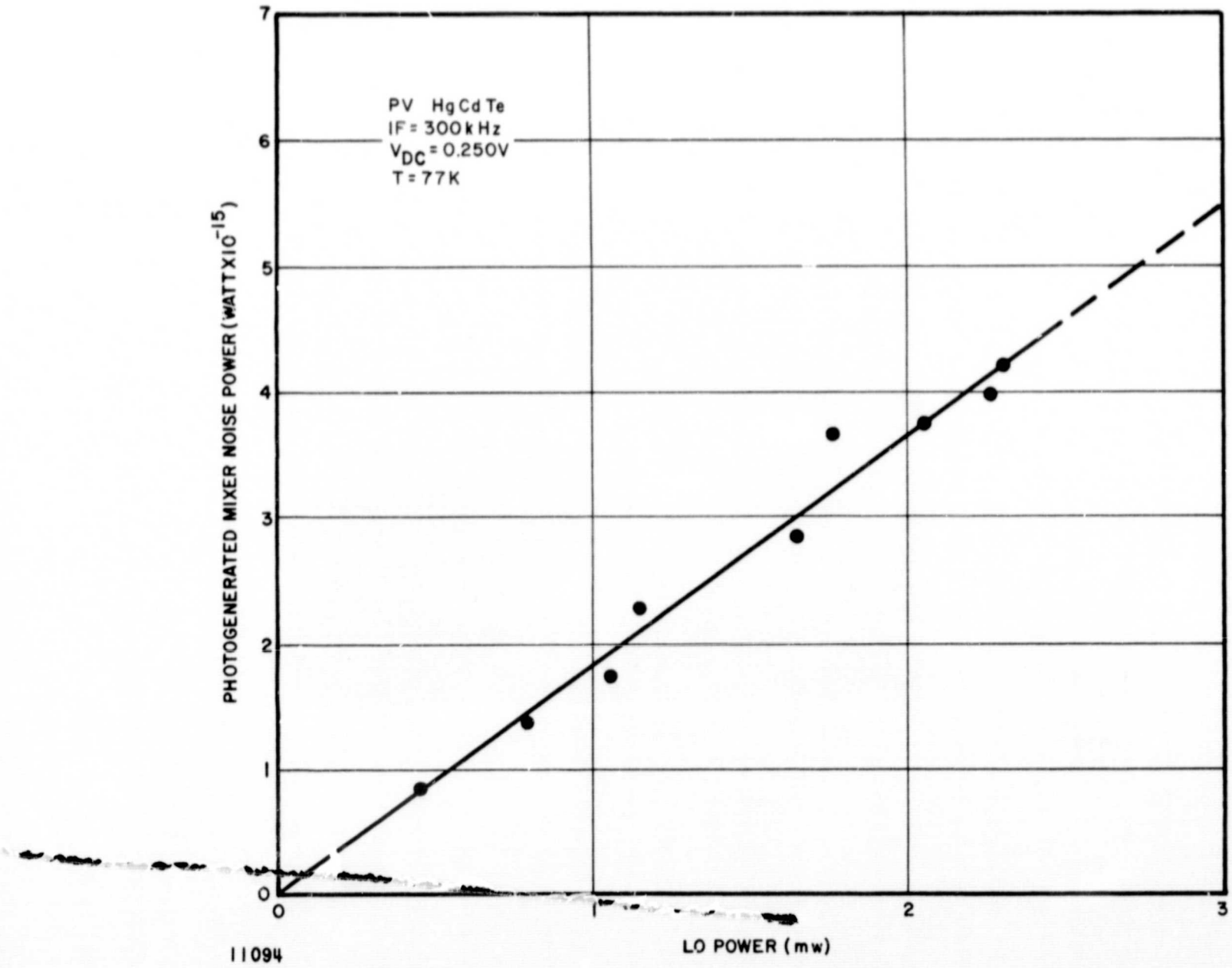

FIGURE 34. PHOTOGENERATED MIXER NOISE VS LO POWER IN PV HgCdTe

remains independent of P_{LO}. This was true to a good approximation for the DC bias value utilized (Figure 33).

2. 1/f NOISE

Contact or (1/f) noise was observed at IF frequencies between 10 KHz and 1 MHz which tends to increase the nonphoto excited noise power. The mean square (1/f) noise is

$$\overline{i^2_{1/f}} \approx \frac{K_1 I^2 B}{f} \tag{131}$$

where I = bias current, and K_1 = proportionality factor which includes the mixer volume and bandwidth of the measurement setup.

As can be seen from equation 131, the 1/f noise decreases with increasing IF frequency and decreasing bias current.

Figure 35 shows the measured noise voltage output versus frequency under three sets of bias conditions. The noise voltage rolls off at the expected 3 db per octave rate and approaches the IF amplifier noise level in the region between 1 and 5 MHz.

The 1/f noise can thus be expected to be essentially negligible at frequencies from 20 to 30 MHz. Therefore, the mixer IF amplifier noise measured at an IF of 300 kHz was used for mixer NEP calculations in order that the low frequency 1/f noise does not obscure the results.

C. HOMODYNE MEASUREMENTS

Homodyne measurements were made on the photovoltaic HgCdTe mixer at a mixer temperature of 77 K to determine the effects of such variables as LO power, DC bias voltage and system bandwidth on the receiver sensitivity. The CO_2 laser output was split into a signal and LO beam and then recombined using germanium beam splitters. The signal beam was 100 percent intensity modulated at a 10-kHz rate using a mechanical chopper.

The measured mixed signal voltage output versus input power with LO power as a parameter is shown in Figure 36. The nonlinear effects for power levels above P_S = 3 μw may be due to mixer saturation. The measured

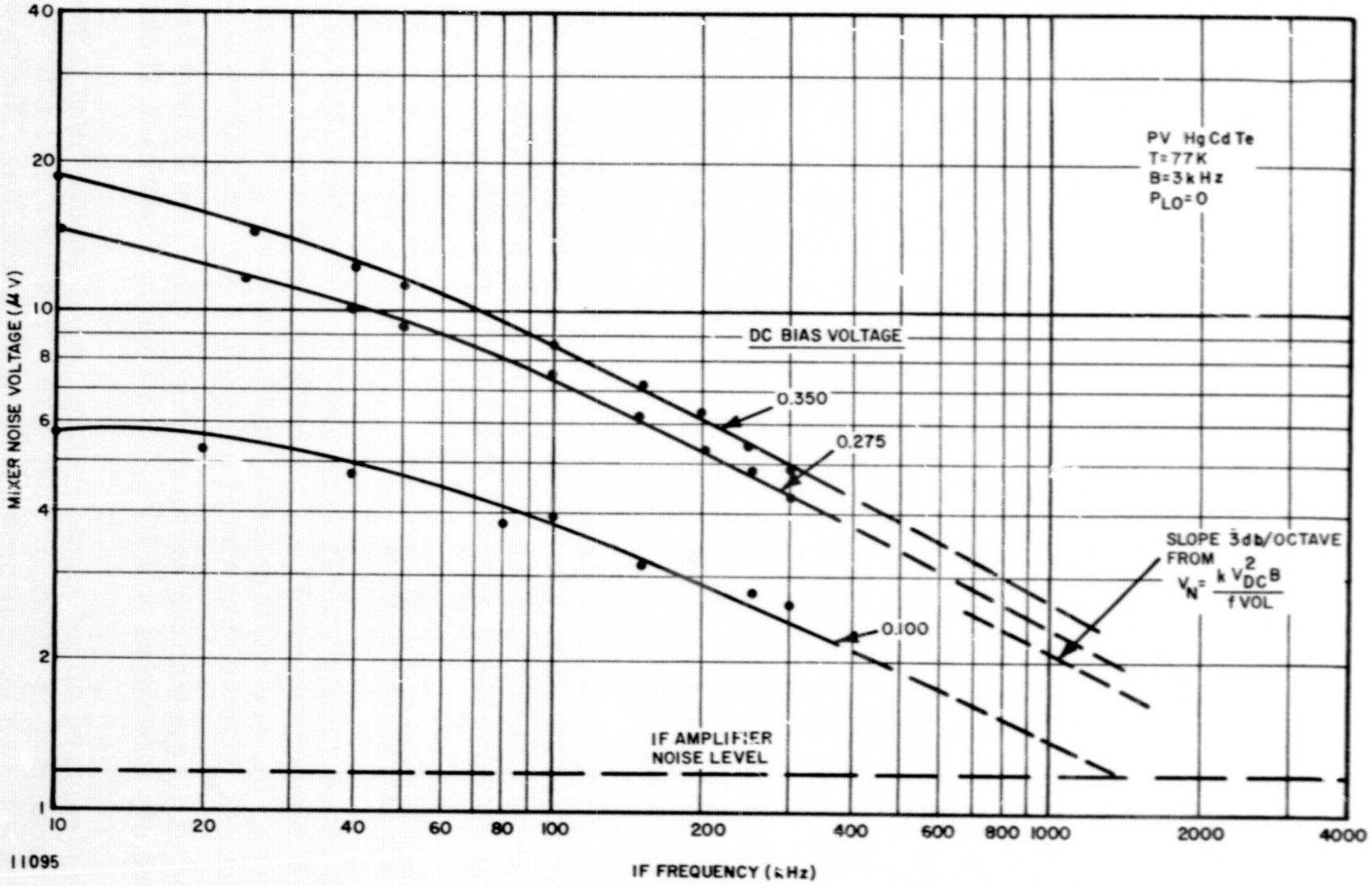

FIGURE 35. 1/f NOISE VS IF FREQUENCY (kHz) IN PV HgCdTe

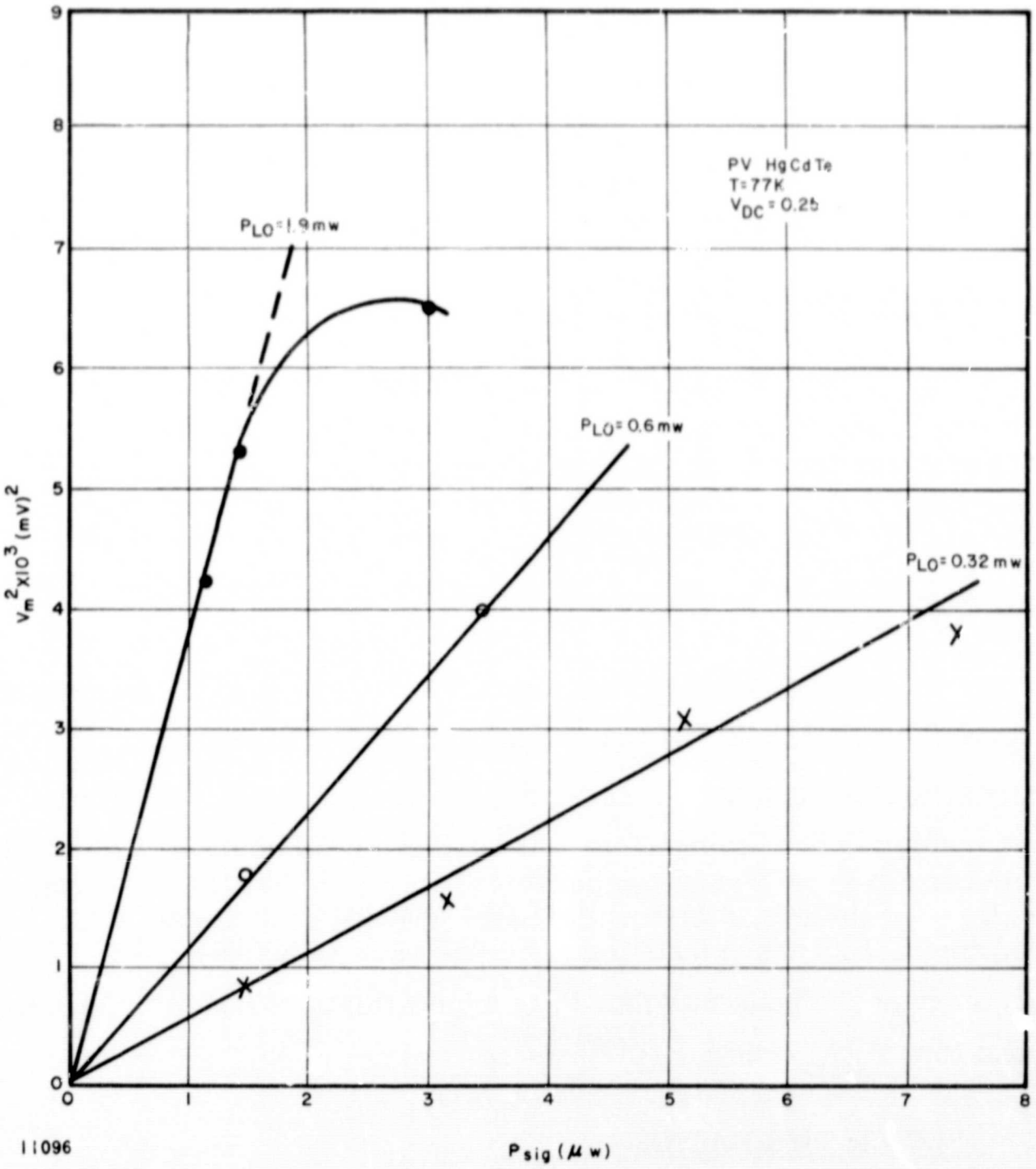

FIGURE 36. SQUARE OF MIXED SIGNAL VOLTAGE VS SIGNAL POWER FOR VARIOUS VALUES OF LO POWER IN PV HgCdTe

mixed signal current output was found to vary as the square-root of the signal power (for $P_S < 1$ μw) as predicted from equation 110.

Figure 37 is a plot of the square of the mixed signal voltage output normalized to the input power, versus LO power which demonstrates the expected linear relationship. Since the square of the mixed signal voltage is proportional to the power delivered to the IF amplifier, the ordinate of Figure 37 can be reduced to P_{IF}/P_S which is the available mixer gain.

D. NOISE EQUIVALENT POWER

For a measured quantum efficiency of 0.09 at 77 K, $P_{MIN} = h\nu B/\eta$ is calculated to be 2.08×10^{-19} w/Hz. Measured NEP as a function of LO power for the PV-HgCdTe mixer at a bias voltage of 0.25 volt and mixer temperature of 77 K is shown in Figure 38. As expected from equations 122 and 127, the NEP approaches P_{MIN} as the LO-induced shot noise begins to override the system noise. The noise voltage was measured at 300 kHz as previously noted.

The measured NEP was 7.2×10^{-19} w/Hz for an applied LO of 0.50 mw. For an applied LO of 2.0 mw, the NEP was 2.2×10^{-19} w/Hz, thus approaching the quantum-noise-limited value of $P_{MIN} = 2.08 \times 10^{-19}$ w/Hz. The quantum-noise-limited NEP at 10.6 microns could be reduced by operating the mixer at higher temperatures in order that the wavelength of peak response of the mixer element (Figure 32) will shift toward 10.6 microns, resulting in increased quantum efficiency and reduced P_{MIN}. The quantum efficiency at the peak wavelength is approximately 0.20 which would correspond to a P_{MIN} of 9.4×10^{-20} w/Hz.

E. POWER DISSIPATION

The applied LO power of 2.0 mw used to obtain quantum-noise-limited operation corresponds to an absorbed power (ηP_{LO}) of only 180 μw. The DC power dissipation was 1 mw. The total power dissipation in the mixer was thus approximately 1.2 mw.

Based on these results, it is concluded that operation at megahertz frequencies could be obtained with an absorbed LO power of 120 μw and a DC power dissipation of 0.8 mw, since the second stage thermal noise at 20 or 30 MHz would be less than the thermal noise measured at 10 kHz.

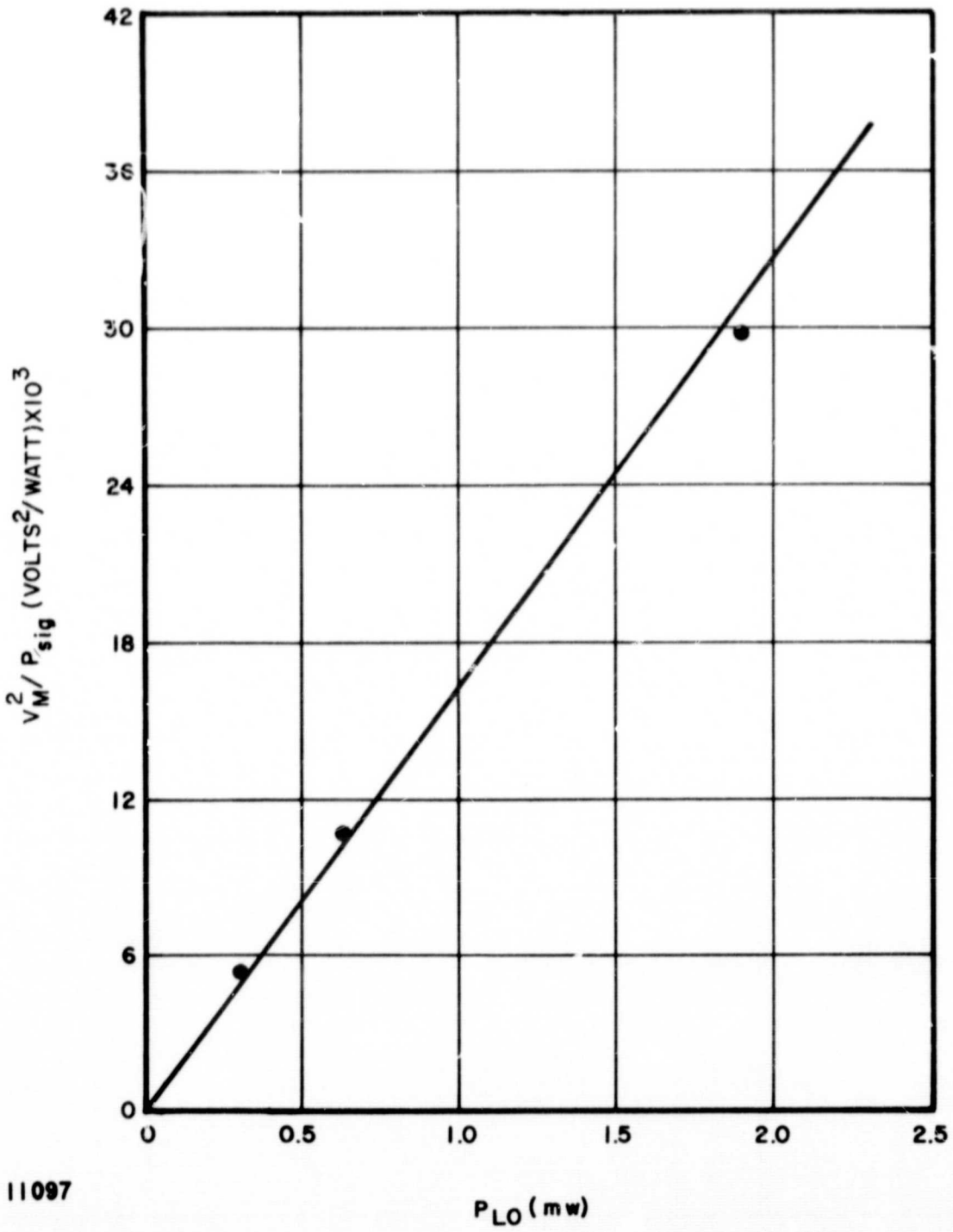

FIGURE 37. SQUARE OF MIXED SIGNAL VOLTAGE TO SIGNAL POWER RATIO VS LO POWER IN PV HgCdTe

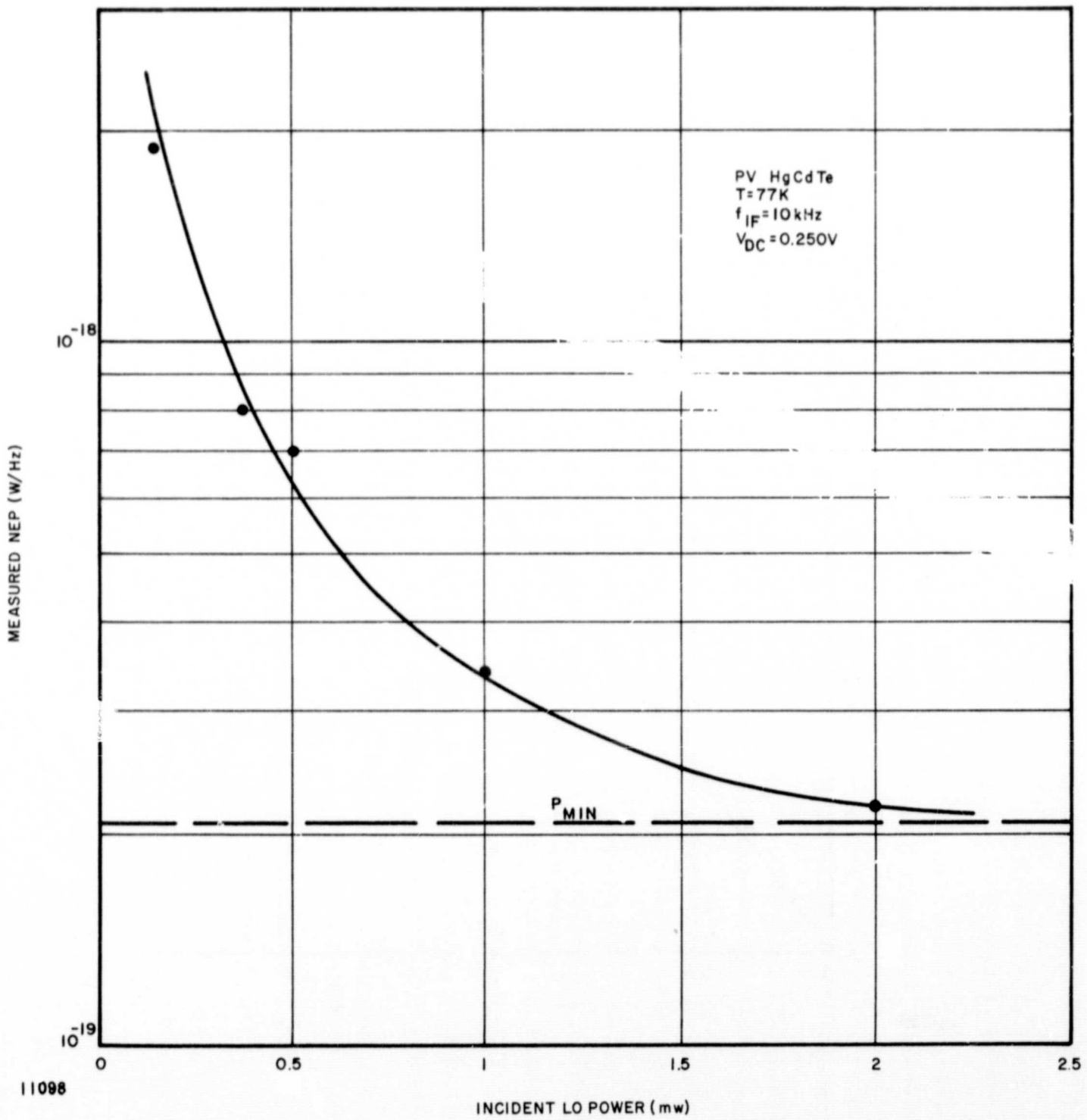

FIGURE 38. MEASURED NEP VS LO POWER (NOISE MEASURED AT 300 kHz) IN PV HgCdTe

F. AVAILABLE CONVERSION GAIN

Using equation 122, the calculated available conversion gain of the PV HgCdTe mixer for an applied LO power of 1.9 mw, $\eta = 0.09$ and $G_D^{-1} = 190$ ohms is -8.6 db. Using the measured data in Figure 37 for P_{LO} of 1.9 mw, the calculated gain is -7.7 db and using the measured data in Figure 38 for $F_{IF} \approx 1.5$ db, $P_{MIN} = 2.08 \times 10^{-19}$ w/Hz and $T_M = 77$ K, the calculated gain is -6.5 db. This small gain spread of only 2 db is encouraging.

G. INDIRECT SENSITIVITY MEASUREMENTS

The linewidth of CO_2 lasers limits the practical IF frequency offset in a two-laser heterodyne setup. Hence, an alternative technique, developed to indirectly measure mixer sensitivity, was used to measure the frequency response of the photovoltaic mixer element. The technique is similar to one which was used to evaluate receiver sensitivity of a photoconductive Ge:Cu mixer in a 10.6-micron receiver at IF frequencies up to 1.2 GHz. The accuracy of this indirect measurement technique has been previously verified by making direct receiver sensitivity measurements using a GaAs electro-optic modulator with 30-MHz modulation sidebands. For the photovoltaic HgCdTe mixer, the ratio of the thermal noise to the receiver (thermal and shot) noise was measured and referred to the quantum-noise-limited sensitivity.

The indirectly measured sensitivity of the photovoltaic HgCdTe mixer as a function of IF frequency at 77 K is shown in Figure 39. The measurements were made with 450 millivolts of reverse bias, a 5- to 90-MHz IF amplifier with a 1.7-db noise factor and 0.8 mw of LO power ($\eta P_{LO} = 0.072$ mw). A 3-db (50 ohm) pad was inserted between the infrared mixer and IF amplifier which minimized any loading of the IF amplifier as the mixer source impedance changed with frequency. It also had the disadvantage of attenuating the LO-excited shot noise current delivered to the IF amplifier, and reducing the mixer's transducer gain by about 3 db.

As can be seen from Figure 39, the measured frequency response of the photovoltaic mixer was flat to 40 MHz. No attempt was made to increase the cutoff frequency by resonating the PV diode or matching the input impedance of the IF amplifier to the diode. For a measured forward resistance of 7.7 ohms and shunt conductance of $(190 \text{ ohms})^{-1}$, the calculated junction capacitance is approximately 67 pf (equation 116).

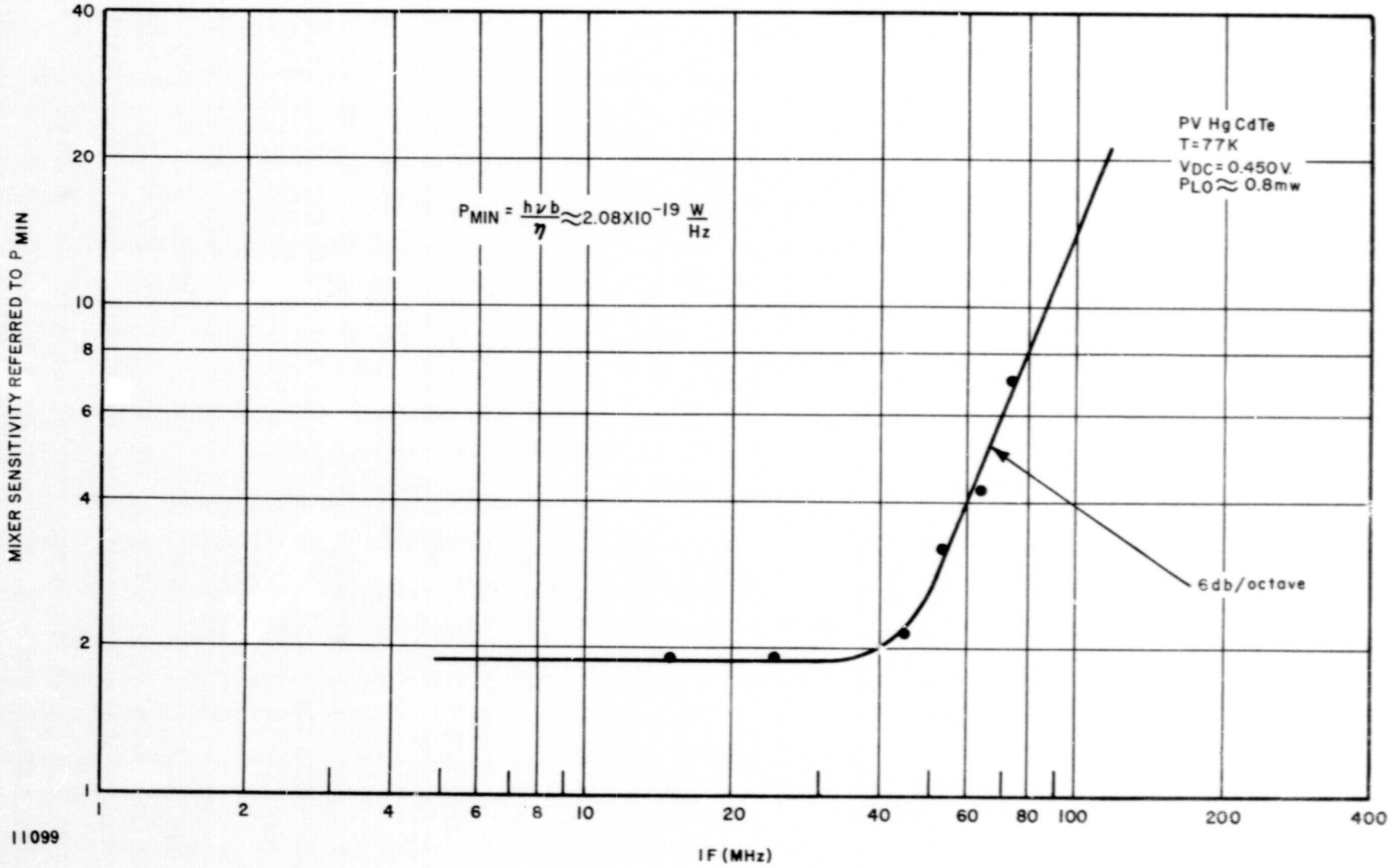

FIGURE 39. MIXER SENSITIVITY VS IF FREQUENCY IN PV HgCdTe

The indirectly measured receiver sensitivity was 1.9 $h\nu B/\eta$ at IF frequencies below 40 MHz. It would be reduced to approximately 1.45 $h\nu\beta/\eta$ if the mixer IF amplifier combination were operated without the 3-db pad. The sensitivity measurement results differ slightly from those obtained in the homodyne setup because a different IF amplifier was employed.

Indirect mixer sensitivity measurements as a function of photo-induced current were made at an IF of 35 MHz and the available photovoltaic mixer gain was calculated using equation 127. The results shown in Figure 40 indicate that the PV mixer gain increased linerarly with induced mixer current (which is proportional to absorbed LO power) as predicted by the gain equation 122.

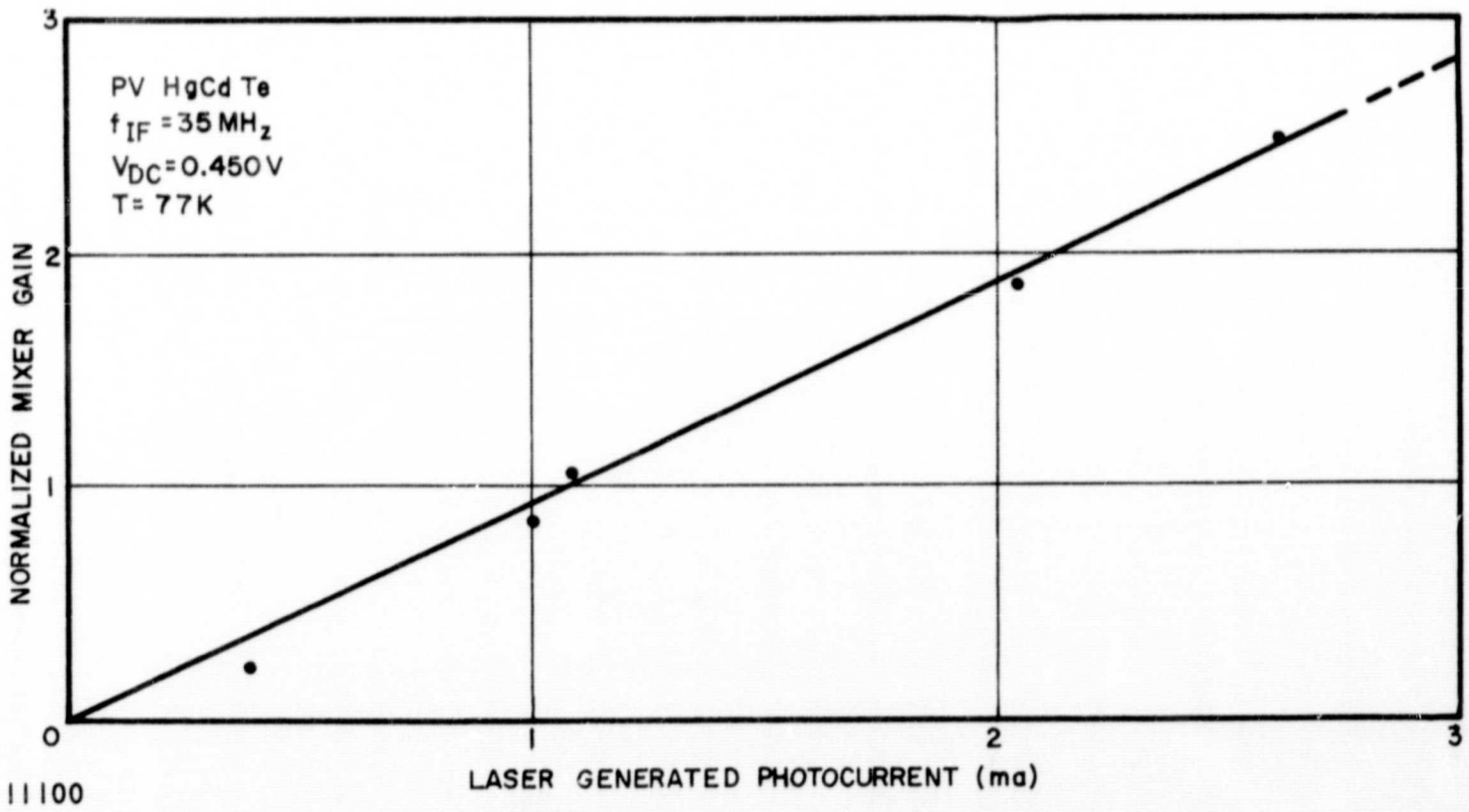

FIGURE 40. MIXER GAIN VS PHOTOCURRENT AT AN IF OF 35 MHz

X. MIXER CONFIGURATIONS FOR ERROR-SENSING AND SIGNAL DETECTION

A laser communication link in space requires means for accurately aligning transmitter and receiver antenna beams with their remote counterparts to effect the efficient transfer of information-bearing energy. A key element in the link is the pointing-error sensor in the receiver. Sensing displacement of the received beam from the receiver pointing axis may be accomplished by either:

- Sequentially misaligning a single beam in a predetermined pattern, or
- Simultaneously comparing the outputs of an array of receiving antenna beams.

The most popular embodiment of the sequential technique is the conical-scan receiver in which the single lobe of the receiver antenna is nutated about the pointing axis of the receiver at fixed offset angle and rate. A point source on the pointing axis of the receiver produces a constant signal output. However, an angular offset between the source and the receiver pointing axis results in an amplitude-modulated signal in which:

- Phase with respect to the nutating beam gives the angular direction of the error, and
- Amplitude is proportional to the magnitude of the pointing error.

Comparing the detector output with reference signals synchronized with the nutator drive gives the azimuth and elevation error voltages for driving the position servos. A block diagram of such a receiver is given in Figure 41.

The simplest form of the multiple beam array is the amplitude sensing monopulse. At microwaves, four antenna feeds are generally used. At infrared wavelengths, the four feeds are replaced by four detector elements.

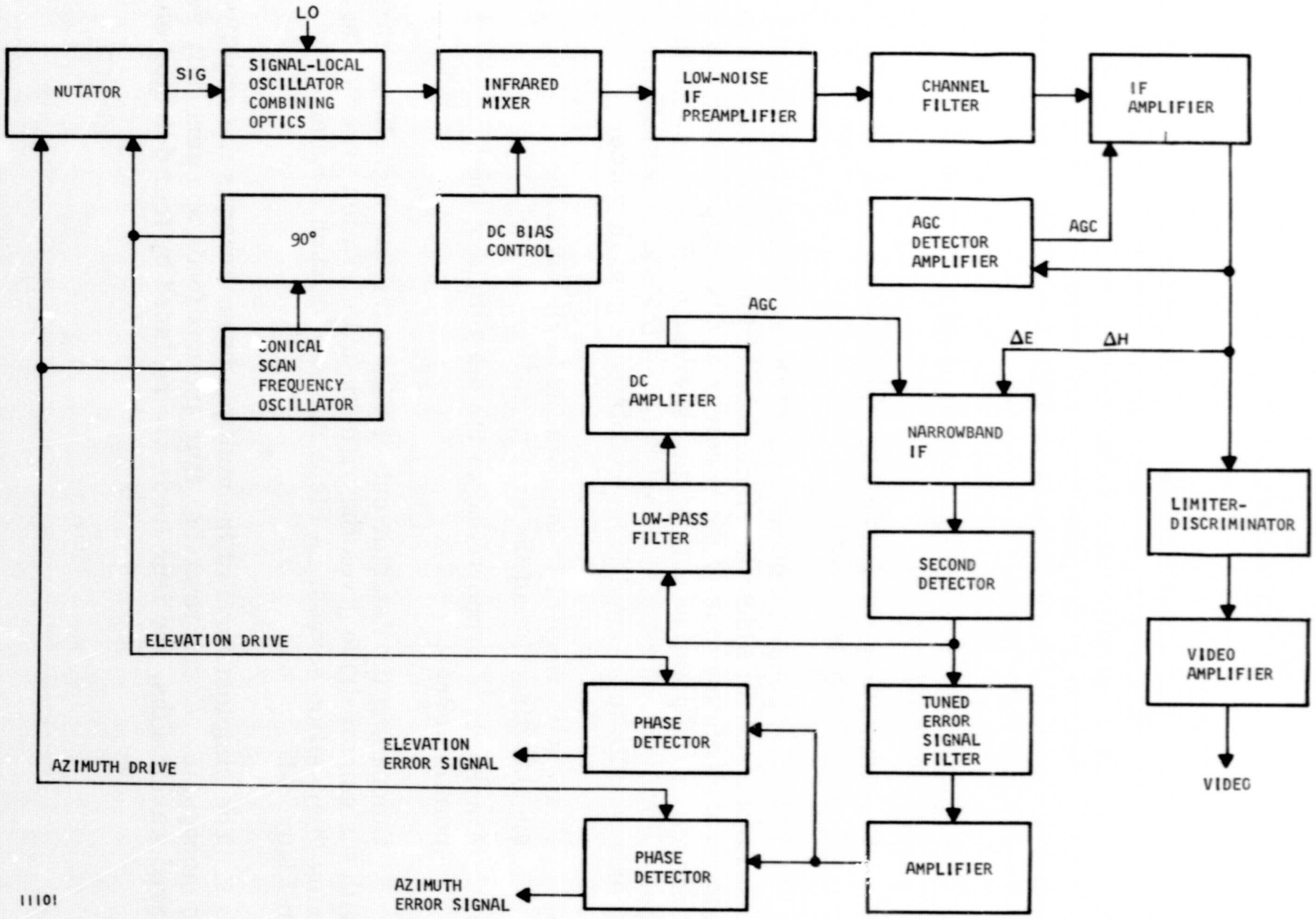

FIGURE 41. SINGLE MIXER HETERODYNE RECEIVER WITH NUTATOR

These elements may be used as:

- Direct detectors with reduced sensitivity, or
- Heterodyne mixers with sensitivity approaching the quantum-noise-limit.

For the LCE application it appears that the ultimate sensitivity is required. Therefore, the heterodyne mixer array with phase sensitive processing at IF is selected for further discussion. This is an adaptation of the classical amplitude sensing monopulse receiver to infrared systems. A block diagram of an infrared heterodyne monopulse receiver is given in Figure 42. Through passive circuits at the IF frequency this receiver gives three outputs:

- The sum of the four mixer signals,
- The difference between the top pair and the bottom pair of mixers for deviation error, and
- The difference between the left pair and the right pair of mixers for azimuth error.

Historically, the conical-scan receiver was operational in microwave radars for many years when the monopulse receiver was developed by several laboratories to eliminate some of the deficiencies of the conical-scan receiver. In spite of the more complicated electronics, most modern high-performance radar receivers are of the monopulse type. Increased use of the monopulse technique is also being made in communications and telemetry receivers where relative motion occurs between transmitter and receiver, and active tracking is required for pointing. The salient characteristics of monopulse and conical-scan receivers are compared in the following paragraphs.

A. APERTURE UTILIZATION

For a conical-scan tracker the beamwidth is averaged over the scan cycle. The resulting beam is considerably broadened with respect to the diffraction limit of the receiving aperture. In one-way operation, as in a communications link, the resultant antenna gain is about 3 db below the maximum gain (reference 9, page 269, Figure 9-3a). This represents a compromise between:

- The error angle sensitivity needed for tracking, and
- The antenna gain needed for communications.

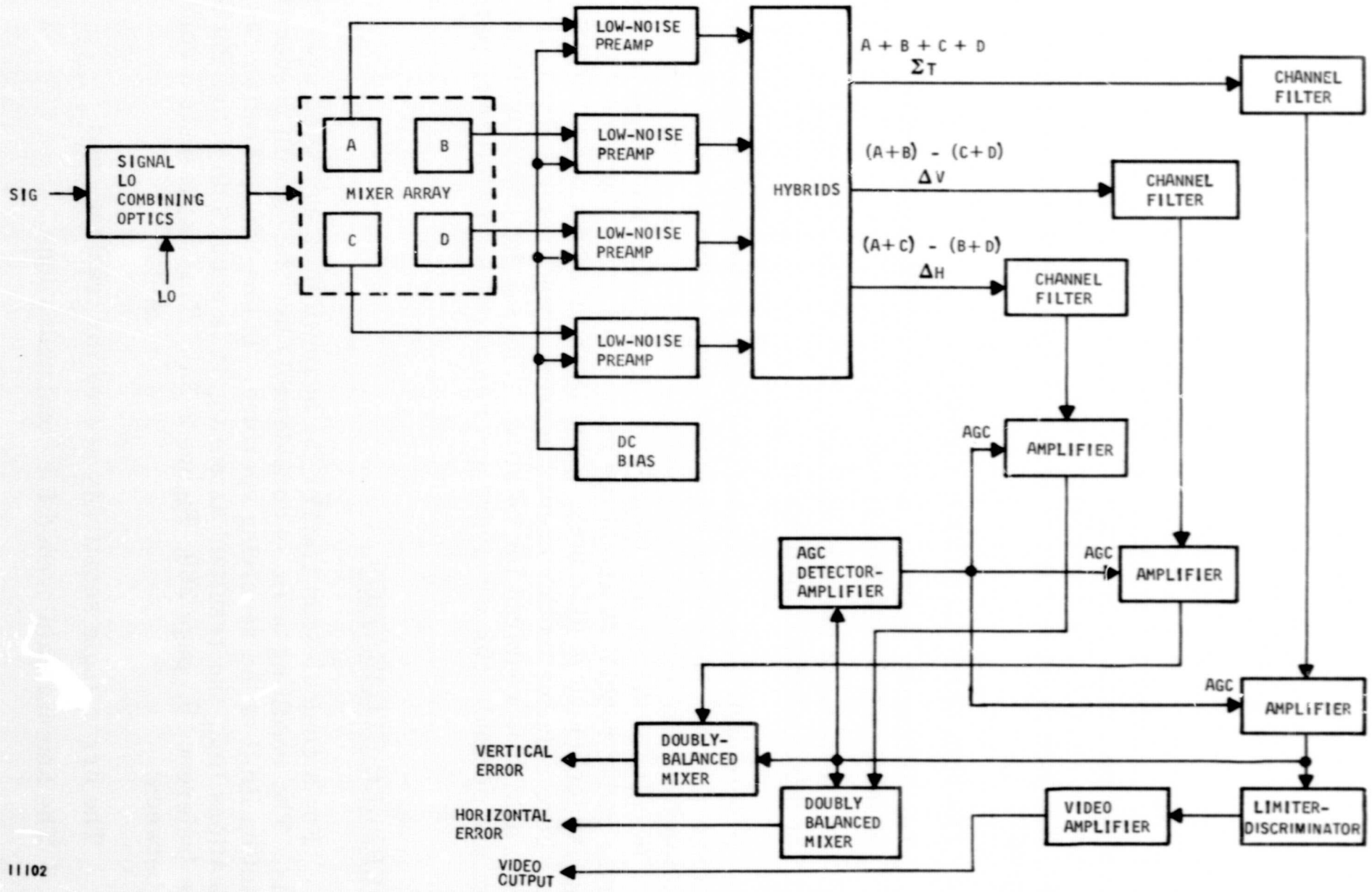

FIGURE 42. QUADRANT-MIXER IF MONOPULSE RECEIVER

Monopulse reception makes full use of the receiving aperture. A 2 x 2 array of mixer elements (equivalent to a four-horn feed in a microwave antenna) can be designed to closely approach the signal capture efficiency of a single receiver element of optimum size (reference 9, page 274). This occurs when the outputs of the four mixers are summed in phase, and the element size and spacing are matched to the effective f-number of the collecting optics.

Under these conditions the sum-signal pattern approximates the optimum pattern, with little loss (0.3 db) being introduced by the sum and difference networks. Furthermore, the energy absorbed in the difference channels is not subtracted from the sum channel since this energy would have resulted in out-of-phase signal cancellations at IF had a single optimum-sized element been used.

B. ANGLE SENSITIVITY

In a comparison of monopulse and conical-scan radars, it has been shown (reference 10) that under strong signal conditions there is no essential difference in angle-error sensitivity, defined here as the normalized slope of the angle-error voltage as it passes through zero (boresight), for equal antenna apertures, antenna gains and basic antenna beamwidths. However, as the noise threshold of the receiver is approached, the monopulse system shows about 70 percent greater angle error sensitivity than the conical-scan receiver.

For the monopulse tracker, it has been shown (reference 9, page 286) that the normalized rms tracking error at the antenna is

$$\frac{\sigma_t}{\theta} = \frac{1}{k_m\left[\left(\frac{S}{N}\right)_{av}\left(\frac{B}{\beta_m}\right)\right]^{1/2}} \qquad (132)$$

where

σ_t = rms tracking error

θ = beamwidth of the sum channel

k_m = error slope factor (≈ 1.57, sum pattern voltage per beamwidth error voltage at boresight)

$\left(\frac{S}{N}\right)_{av}$ = average IF signal-to-noise ratio measured over many modulation periods

B = IF bandwidth

β_m = servo bandwidth

Inserting values assumed for an LCE type of infrared receiver,

$$k_m = 1.57$$

B = 10 megahertz

β_m = 10 kilohertz

$$(S/N)_{av} = 100$$

The above expression gives a normalized rms tracking error of one part in 500 for a 20 db signal-to-noise ratio at IF.

C. AMPLITUDE SCINTILLATION

In a monopulse system the error signals are derived from simultaneous measurements on four channels as ratios of the sums and differences between them. These relative and simultaneous measurements place no requirements of absolute accuracy or absolute stability on the receiver. Therefore, amplitude scintillations induced by atmospheric fluctuations do not affect the monopulse receiver.

On the other hand, for a conical-scan system the error signals are derived from sequential measurements on one channel. If the nutating period of the conical scan is longer than the shortest period of the scintillation spectrum, then amplitude variations will occur before a minimum of one rotation has occurred for an error signal determination. The scintillation-modulated amplitude is then misinterpreted as target motion and pointing errors occur. However, the frequency spectra of atmospherically induced scintillations tend to become insignificant above 100 Hz. Thus, scan rates above 500 rps could remove this effect as a performance limitation.

D. TRACKING

In the conical-scan receiver the error signals appear as a pair of amplitude modulated sidebands on the received carrier. For the monopulse receiver the error signals are derived from the relative magnitudes of the carrier itself in each channel. Therefore, in the conical-scan receiver the thermal (or quantum) noise is accepted from two bandwidths per channel rather than the single bandwidth used with monopulse. Consequently, for a given S/N at IF and the same servo bandwidths, the noise levels in the tracking servo loops for the conical-scan receiver are twice as high as those for the monopulse loops.

It has been shown (reference 9, page 283) that for tracking a continuous wave signal (and if one includes the crossover loss for conical scan) the monopulse receiver has a 6.3-db sensitivity advantage over conical scan. This advantage can represent the difference between link success or failure in a marginal case. Where adequate margins exist, the greater sensitivity can be used for decreasing the acquisition time and increasing the receiver's scintillation tracking bandwidth.

E. FAILURE MODES

For the four-channel monopulse receiver arranged as shown in Figure 42,

$$\Delta V = (A + B) - (C + D)$$
$$\Delta H = (A + C) - (B + D) \qquad (133)$$

The servosystems will drive for a null and achieve it at A = B = C = D. These conditions are met on a sum channel boresight for four balanced channels. Consider the worst case where one channel fails completely, say channel B = 0, then

$$\Delta V = A - (C + D)$$
$$\Delta H = (A + C) - D. \qquad (134)$$

The null condition $\Delta V = \Delta H = O$ is now achieved for C = O, A = D. That is, when channel B fails, the equilibrium position is shifted along the B - C center line toward channel B and away from channel C to the first null of the channel C receiving pattern. Based on typical antenna patterns with 3-db crossovers with respect to each other, it is estimated that the shift away from boresight is about one-half a 3-db beamwidth of a single channel beam. Under these conditions, the sum signal is degraded about 7 db due to the loss of channel B and the shift away from channel C.

For those cases where a degradation but not total failure of performance occurs in one or more channels, boresight error and sum channel loss occur. The magnitude of these changes will be smaller than those estimated for a single channel failure. In addition, small corrections in individual channel performance can be made by adjusting the mixer bias power remotely as necessary.

For the conical receiver, total receiver failure, of course, occurs upon failure of the single mixer element. This situation can be alleviated by incorporating a second mixer element into the receiver if radiation cooler capacity permits. This second mixer can be a nonoperating (standby) element or operating as shown in Figure 43. Similar considerations suggest the use of an extra nutator.

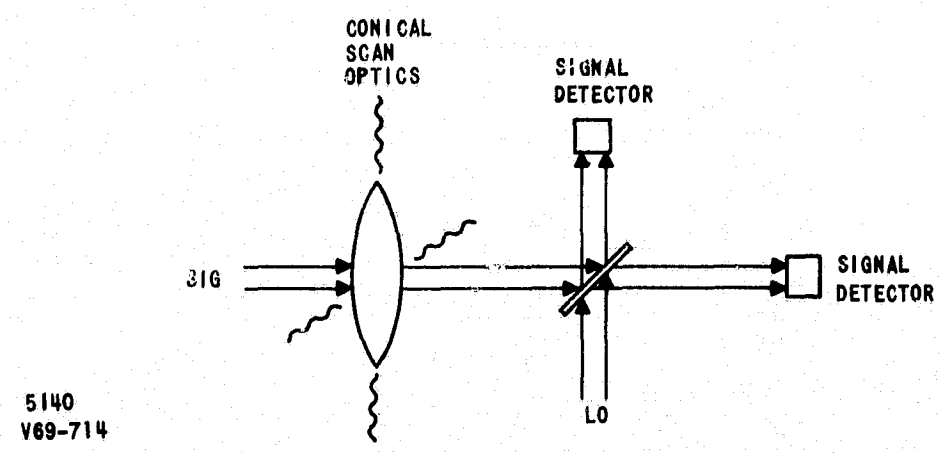

FIGURE 43. TWO-MIXER INFRARED RECEIVER WITH CONICAL SCAN

XI. CONCLUSIONS

The design analysis conclusions are given in the following paragraphs.

A. GENERAL

1. There is an optimum operating region for LO and bias power, representing a compromise between excessive power dissipation and degraded sensitivity (Figure 44). A minimum mixer conversion gain of -8.8 db is required to achieve an overall receiver NEP of 10^{-19} watt/Hz for mixer temperatures up to 120 K, an IF noise factor of 1.5 db and mixer quantum efficiency of 0.50. The required gain is a slow-moving function with noise factor increasing to only -8.0 db for a 2.0 db noise factor.

2. The conversion gain of a photoconductive mixer element operating at a center frequency of 20 MHz goes through a maximum for a lifetime of 8 nsec.

3. A mixer element with a small-signal lifetime of about 3 nsec is required for an IF frequency response flat to 20 MHz within 0.5 db without equalization.

4. The IF amplifier should be designed to operate with a noise factor of approximately 1.5 db with variations in source resistance of greater than 2 to 1. An IF amplifier was breadboarded that essentially met this requirement.

5. The IF amplifier should use transistors with large common-base alpha cutoff frequencies to minimize any variations in IF amplifier noise factor with changes in mixer resistance.

6. One means of minimizing video phase distortion in the IF amplifier is to make its bandwidth larger than required to obtain gain flatness and then use a filter to establish the required passband. This filter also provides RFI reduction due to the LCE transmitter modulator, etc. Data on such a filter is given.

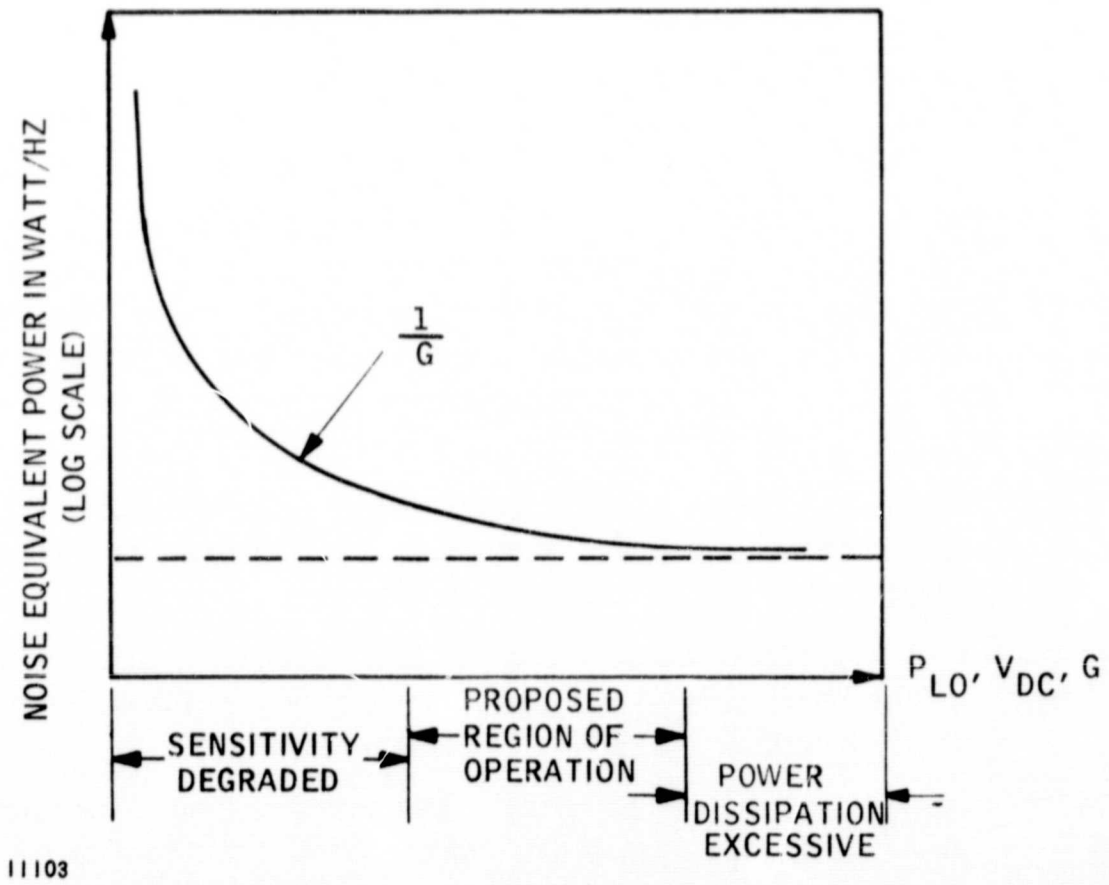

FIGURE 44. REGION OF OPTIMUM MIXER OPERATION

7. For mixer elements with finite dark conductance such as HgCdTe, an equivalent circuit consisting of a dark conductance g_D in parallel with a LO-induced conductance g_o is a useful model.

8. For a fixed power-dissipation budget, there is an optimum ratio of DC bias power to LO power, and g_o/g_D for maximum sensitivity. Also the detector area should be minimized consistent with other considerations.

9. A useful figure of merit in specifying mixer element characteristics (as distinguished from detector elements) is the "specific responsivity in volts/watt per DC bias volt."

10. With mixers, in which lifetime varies with LO power, it is useful to distinguish between:

    - Heterodyne (small-signal) lifetime, τ_{het}
    - Local-oscillator (large-signal) lifetime, τ_{LO} and
    - Dark lifetime τ_D (no LO power applied)

    This modifies the equations for NEP and conversion gain. In the conversion gain, the factor $\frac{\tau}{1+\omega^2\tau^2}$ is replaced by $\frac{\tau_{het}}{\tau_{LO}}\left(\frac{\tau_{het}}{1+\omega^2\tau_{het}^2}\right)$. The frequency response is determined by τ_{het}.

11. The value of τ_{het}/τ_{LO} is smaller than unity, approaching in the limit of large LO powers, one-half for radiative recombination, and one-third for Auger recombination.

12. Effects of degeneracy on the band gap of the mixer must be considered when selecting the fractional mole content x for an $Hg_{1-x}Cd_xTe$ element and 10.6-micron operation.

B. ANALYSIS OF PHOTOCONDUCTIVE n-TYPE HgCdTe MIXER OPERATION WITH AUGER RECOMBINATION

13. The mixer conductance ratio g_o/g_D initially varies linearly and then as the cube-root of applied LO power.

14. If the carrier mobility is assumed to be independent of LO power, then for $\omega\tau_{het} << 1$, the available mixer gain is determined completely by the power ratio P_{DC}/P_{LO}, the conductance ratio g_o/g_D, and the lifetime ratio τ_{het}/τ_{LO}.

15. The mixer conversion gain increases directly with mixer power dissipation.

16. Under certain conditions (values of mixer parameter $\chi \leq 0.237$), there is an optimum value of conductance ratio g_o/g_D which maximizes mixer gain. For $\chi \geq 0.237$, the gain monotonically increases with conductance ratio.

17. For $\chi \leq 0.237$ there is an optimum power ratio $P_{DC}/\eta P_{LO}$ at each value of χ which maximizes the mixer conversion gain.

18. An N_D of 4.68×10^{15} cm^{-3} is calculated to be an optimum concentration of ionized donors in n-type HgCdTe for $g_o/g_D \approx 1$ and $\tau_{het} \approx 3$ nsec at a mixer temperature of 100 K (the mixer volume is taken to be 0.003 inch $\times$ 0.003 inch $\times$ 12 microns).

19. Calculations on the variation of mixer parameters with temperature were carried out for the case where laser LO power and DC bias voltage are both kept constant and the radiation cooler temperature was allowed to vary over the 80 to 120 K temperature range. The results for a temperature variation from 80 to 120 K are as follows:

- τ_{het} varies 1.45 to 1 (2.4 to 3.5 nsec)
- Mixer resistance varies 1.6 to 1 (4.7 to 7.5 ohms)

- Total power dissipation varies from 10.8 mw to 7.4 mw.
- At an IF of 20 MHz, for a quantum efficiency of 0.50, the calculated NEP varies from 9.9×10^{-20} to 1.15×10^{-19} Watt/Hz.

C. PHOTOVOLTAIC HgCdTe MIXER OPERATION

20. The analysis for mixing in PV-HgCdTe indicates that conversion gain varies directly with LO-induced current and inversely with small-signal shunt conductance.

21. Photovoltaic mixers have a theoretical NEP which is lower by a factor of the order of two compared to photoconductive mixers for the same quantum efficiencies. This advantage can be translated into a reduced specfication on quantum efficiency.

22. The analysis indicates that an NEP = 7.8×10^{-20} watt/Hz is obtainable with a current of 0.6 ma generated by absorbed LO power of 0.11 milliwatt for specified conditions including a quantum efficiency of 0.30.

23. The following very encouraging results were obtained for a PV-HgCdTe mixer:

• Frequency Response	Flat to 40 MHz
• Measured Noise Equivalent Power	2.2×10^{-19} watt/Hz at 10 kHz (with 1/f noise subtracted)
• Dissipated LO and Bias Power	Less than 2 mw
• Operating Temperature	77 K
• Measured Quantum Efficiency	0.09 (will increase at high temperatures due to shift in response peak)

D. PHOTOCONDUCTIVE p-TYPE HgCdTe MIXER OPERATION

24. For a given power dissipation budget, the engineering equations for NEP and conversion gain indicate performance in p-type HgCdTe is comparable to n-type HgCdTe under specified conditions. The mixer resistance will be approximately 100 times higher.

25. Analysis for Auger recombination shows that the LO induced conductance initially varies linearly, then as the square root and finally as the cube root of the normalized LO power.

26. Preliminary measurements on a p-type mixer sample (0.016 inch x 0.016 inch) with a dark resistance of 25 ohms resulted in the following results:

- Conductance variation as expected from the analysis
- Frequency response to beyond 20 MHz corresponding to carrier lifetime of approximately 4 nsec
- A relative sensitivity measurement gave $NEP/P_{min} = 2.05$ for a total power (DC bias plus applied LO) of approximately 60 mw. If the mixer area were to be reduced to 0.004 inch x 0.004 inch, the total power would be reduced to 3.8 mw.

E. SYSTEM CONSIDERATIONS

27. A quadrant array of heterodyne mixers followed by phase coherent processing at IF (amplitude-sensing monopulse) gives the best performance as a tracking receiver. However, the added complexity, greater heat load and array procurement problems for this approach may preclude its immediate application.

28. A single-element, conical-scan receiver offers a reasonable compromise between availability of mixer elements, thermal loading of the radiation cooler, and overall receiver performance.

XII. REFERENCES

1. F. Arams, E. Sard, B. Peyton, and F. Pace, "Infrared 10.6 Micron Heterodyne Detection with Gigahertz IF Capability," IEEE Journal of Quantum Electronics, Vol QE-3, p 484-492, November 1967.

2. H. F. Cooke, "Transistor Noise Figure," Solid State Design, p 37-42, February 1963.

3. E. G. Nielsen, "Behavior of Noise Figure in Junction Transistors," Proc. IRE, Vol 45, p 957-962, July 1957.

4. B. Crawford, "Noise in Transistor Amplifier Circuits," Electro-Technology, p 63-70, November 1962.

5. J. S. Blakemore, "Semiconductor Statistics," Pergamon Press, 1962.

6. J. H. McElroy, S. C. Cohen, and H. E. Walker, "First and Second Summary Design Report ATS-F LCE, Infrared Mixer and Radiation Cooler Subsystem," GSFC Report X-524-69-227, April 1969 and July 1969.

7. E. Putley, "Far Infrared Photoconductivity," Phys Stat Sol, Vol 6, p 571-614, 1964.

8. M. DiDomenico and O. Svelto, "Solid-State Photodetection: A Comparison between Photodiodes and Photoconductors," Proc IEEE, 52, p 136-44, 1964

9. D. K. Barton, "Radar Systems Analysis, "Prentice Hall, Inc., p 274, 1964.

10. J. H. Dunn and D. P. Howard, "Precision Tracking with Monopulse Radar," Electronics, p 51-56, 22 April 1960.

APPENDIX I

SPECIFIC RESPONSIVITY AS A FUNCTION OF MIXER PARAMETERS

Parameters such as carrier lifetime, electron carrier concentration, sample thickness, electron mobility and responsivity are interrelated quantities in HgCdTe detectors. This Appendix briefly develops the relationship between the responsivity (a commonly measured detector parameter) and other pertinent mixer parameters by considering a small LO power excitation.

The conductance ratio g_D/g_o caused by the absorbed LO power per unit volume is related to the dark electron concentration and carrier lifetime which are both temperature-dependent quantities (see equation 16). The I-V curve for a HgCdTe photoconductive mixer with and without LO power is shown in Figure I-1. From Figure I-1 we obtain

$$\Delta V = I_D \left(\frac{1}{g_D} - \frac{1}{g_D + g_o} \right) \tag{I-1}$$

$$\Delta V = \left(\frac{I_D}{g_D} \right) \left(\frac{g_o}{g_o + g_D} \right) = \frac{V}{(1 + g_D/g_o)} \tag{I-2}$$

The responsivity is

$$\mathcal{R} = \frac{\Delta V}{\Delta P} = \lim_{P_{LO} \to 0} \frac{V}{P_{LO}\,(1 + g_D/g_o)} \tag{I-3}$$

and substituting equation 17 into equation I-3, the specific responsivity is given by

$$\frac{\mathcal{R}}{V} = \frac{\eta \tau}{\text{Vol}\, n_o\, h\nu} \tag{I-4}$$

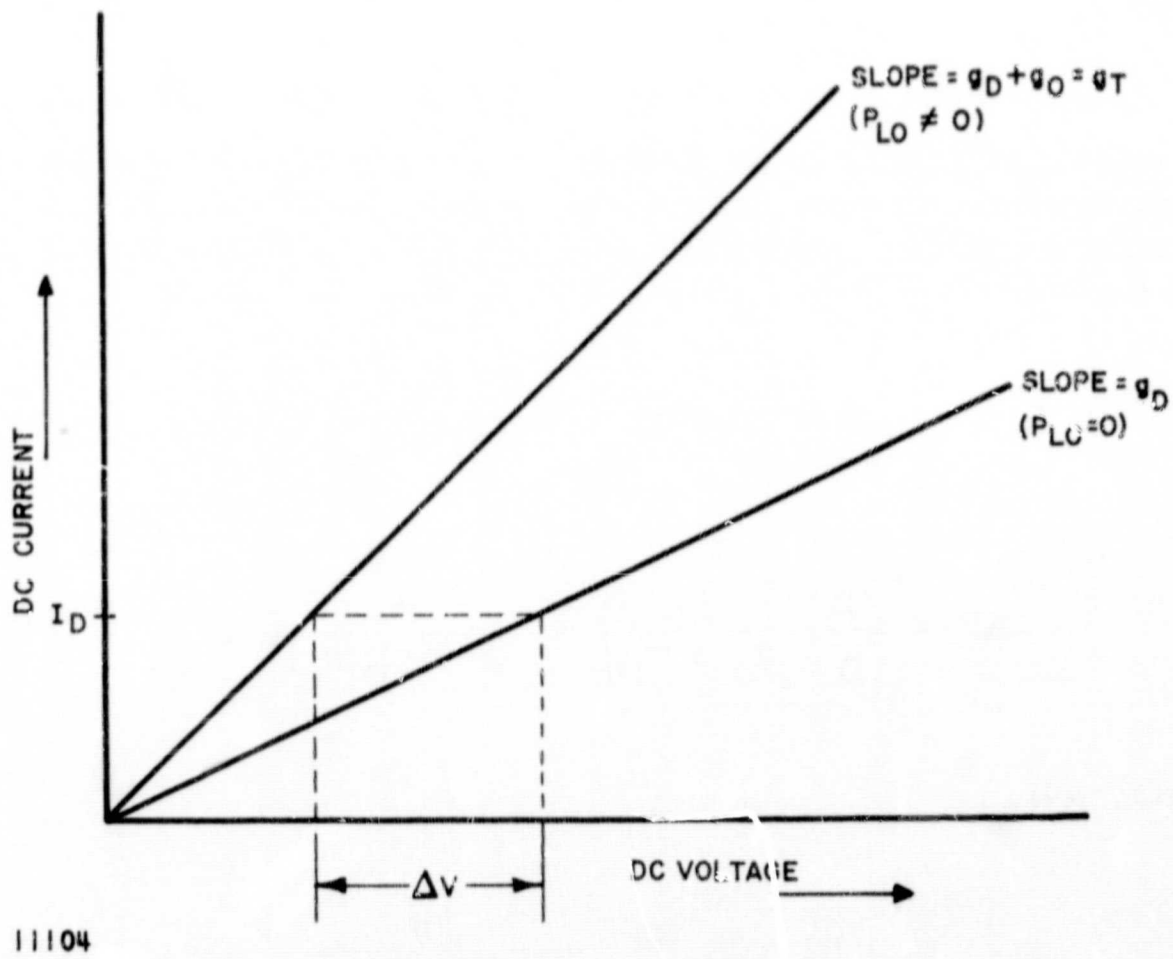

FIGURE I-1. I-V CHARACTERISTIC OF HgCdTe PHOTOCONDUCTIVE MIXER

APPENDIX II

G-R NOISE OF AUGER-LIFETIME-LIMITED PHOTOCONDUCTORS

In this appendix, a general derivation for G-R noise of an intrinsic photoconductor, extrinsic semiconductor, is given for Auger band-to-band recombination dominant. Specific cases of n- and p-type materials are considered. Long* treats radiative recombination similarly.

From equations 8b and 16 of van Vliet,** the spectral power density of the noise current through a photoconductor due to G-R noise is

$$\frac{\overline{i_{GR}^2}}{B} = S_i(\omega) = \left(\frac{I^2}{Vol}\right)\left(\frac{b+1}{bn+p}\right)^2\left(\frac{4r_o\,\tau_{het}^2}{1+\omega^2\tau_{het}^2}\right) \qquad \text{(II-1)}$$

where

B = bandwidth,

I = total DC current (dark plus photoexcited),

Vol = volume of photoconductor,

b = ratio of electron and hole mobilities (>>1),

n, p = total electron and hole concentrations (dark plus photoexcited), respectively,

r_o = average rate of generation of electrons per unit volume (equals average rate of recombination of electrons under steady-state),

τ_{het} = incremental or small-signal Auger lifetime,

ω = angular modulation (IF) frequency.

---

* D. Long, "On Generation-Recombination Noise in Infrared Detection Materials," Infrared Physics, Vol 7, p 169-170, July 1967.

** K. M. van Vliet, "Noise in Semiconductors and Photoconductors," Proceedings of the IRE, Vol 46, No. 6, p 1004-1018, June 1958.

Equation II-1 applies to the excitation and recombination of electron-hole pairs across the band gap, since then $\Delta n = \Delta p$.

To evaluate r_o for Auger processes, from paragraph 6.1.2 of Blakemore,* r_o is

$$r_o = \frac{G_{ee}\, n^2\, p}{n_o^2\, p_o} + \frac{G_{hh}\, p^2\, n}{p_o^2\, n_o} \qquad \text{(II-2)}$$

$$= \frac{n\, p\left(K_{ee}\, n + K_{hh}\, p\right)}{n_i^2}$$

where

G_{ee}, G_{hh} = material constants for Auger recombination (electron-electron and hole-hole processes, respectively),

n_o, p_o = dark electron and hole concentrations, respectively,

$K_{ee} \equiv G_{ee}/n_o$,

$K_{hh} \equiv G_{hh}/p_o$,

n_i = intrinsic carrier concentration $\left(n_i^2 = n_o\, p_o\right)$.

Equation II-2 can be expressed in terms of the large-signal Auger lifetime (Section IV):

$$\tau_{LO} = \frac{n_i^2}{\left(n_o + p_o + n_e\right)\left(K_{ee}\, n + K_{hh}\, p\right)} \qquad \text{(II-3)}$$

---

* J. S. Blakemore, "Semiconductor Statistics," Pergamon Press, New York, Oxford, London, Paris, 1962.

where n_e = excess electron-hole pair concentration due to photoexcitation

$$(n = n_o + n_e,\ p = p_o + n_e)$$

Substitution of equations II-2 and II-3 into equation II-1 then gives

$$\overline{i_{GR}^2} = \left(\frac{I^2}{Vol}\right)\left(\frac{b+1}{bn+p}\right)^2\left[\frac{4\,n\,p\,\tau_{het}^2\,B}{\tau_{LO}\left(n_o + p_o + n_e\right)\left(1+\omega^2\tau_{het}^2\right)}\right] \qquad \text{(II-4)}$$

To relate equation II-4 to equation 68, requires a relation between the total DC current and the photoexcited portion thereof

$$\frac{I}{I_o} = \frac{\sigma}{\sigma - \sigma_D} = \frac{\mu_e\,n\,q + \mu_h\,p\,q}{\mu_e\,n_e\,q + \mu_h\,n_e\,q} \qquad \text{(II-5)}$$

$$= \frac{bn+p}{n_e\,(b+1)}$$

where

σ = total conductivity (dark plus photoexcited),

σ_D = dark conductivity,

μ_e, μ_h = electron and hole mobilities, respectively,

q = electronic charge,

Furthermore, the photocurrent I_o can be expressed in terms of the transit times of electrons and holes by

$$I_o = q\, n_e\, \mathrm{Vol} \left(\frac{1}{T_{r,e}} + \frac{1}{T_{r,h}} \right) \tag{II-6}$$

where $T_{r,e}$, $T_{r,h}$ = transit time of electrons and holes, respectively, $\left(b = T_{r,h} / T_{r,e} \right)$.

Next, substitution of equations II-5 and II-6 into equation II-4 gives

$$\overline{i_{GR}^2} = 4q\tau_{het} \left(\frac{1}{T_{r,e}} + \frac{1}{T_{r,h}} \right) \left(\frac{\tau_{het}}{\tau_{LO}} \right) \left[\frac{np}{n_e \left(n_o + p_o + n_e \right)} \right] \left(\frac{I_o B}{1 + \omega^2 \tau_{het}^2} \right) \tag{II-7}$$

For LO-illuminated n-type material $\left(n_o >> p_o \right)$ where $n_e \sim n_o$, the factor

$$\left[\frac{np}{n_e \left(n_o + p_o + n_e \right)} \right] \approx 1 + \frac{p_o}{n_e} \approx 1, \tag{II-8}$$

For LO-illuminated p-type material $\left(p_o >> n_o,\ n_e \sim p_o / b \right)$, the factor.

$$\left[\frac{np}{n_e \left(n_o + p_o + n_e \right)} \right] \approx 1 + \frac{n_o}{n_e}, \tag{II-9}$$

and in some cases can be significantly greater than unity.

APPENDIX III

EFFECTS OF THE ENERGY OF DEGENERACY ON SELECTING THE EFFECTIVE BAND GAP OF HgCdTe

In selecting the proper material for a photoconductive mixer, one must, of course, be sure that the band gap of the material is at a somewhat longer wavelength than 10.6 microns. Ordinarily, the band gap is the wavelength corresponding to the difference in energy between the bottom of the conduction band and the top of the valence band. However, if the lowest states of the conduction band are all filled; that is, if the conduction band is degenerate, then these states will not be available to receive electrons excited from the valence band. Accordingly the effective band gap is increased by an amount corresponding to the difference in energy between the bottom of the conduction band and the quasi-fermi level of electrons in the conduction band. This difference in energy is called the energy of degeneracy and is related to the electron concentration by the equation:

$$E_{deg} = \frac{h^2}{2q\,m_c}\left(\frac{3\,n}{8\,\pi}\right)^{2/3} \qquad \text{(III-1)}$$

where

h = Planck's constant

q = charge of the electron

n = concentration of electrons

m_c = mass of the electron in the conduction band

This correction to the threshold frequency is necessary if the operating temperature is less than the temperature of degeneracy

$$T_{deg} = \frac{q}{k}\,E_{deg} \qquad \text{(III-2)}$$

where k = Boltzman's constant.

Considerations of degeneracy are important in selecting the value of the compositional parameter x for the $Hg_{1-x}Cd_xTe$ mixer. If there were not degeneracy effects, the value $x = 0.20$ would yield a sufficiently low threshold frequency for excitation by the 10.6 μ local oscillator. However, we require an electron concentration of about 10^{+16}/cc. The corresponding T_{deg} and E_{deg} are 200 K and 0.02 ev respectively. Since the operating temperature is well below 200 K, the degeneracy correction to the threshold frequency is required. Accordingly, we have selected a value of x about 0.18 for our calculations.